Latent structured thermally developed reliefs : principles and applications of photoembossing

Document status and date:
Published: 01/01/2009

Document Version:
Publisher's PDF, also known as Version of Record (includes final page, issue and volume numbers)

Please check the document version of this publication:

• A submitted manuscript is the version of the article upon submission and before peer-review. There can be important differences between the submitted version and the official published version of record. People interested in the research are advised to contact the author for the final version of the publication, or visit the DOI to the publisher's website.
• The final author version and the galley proof are versions of the publication after peer review.
• The final published version features the final layout of the paper including the volume, issue and page numbers.

[Link to publication](#)

Latent Structured Thermally Developed Reliefs

Principles and Applications of Photoembossing

PROEFSCHRIFT

ter verkrijging van de graad van doctor aan de
Technische Universiteit Eindhoven, op gezag van de
Rector Magnificus, prof.dr.ir. C.J. van Duijn, voor een
commissie aangewezen door het College voor
Promoties in het openbaar te verdedigen
op woensdag 29 april 2009 om 16.00 uur

door

Ko Hermans

geboren te Venlo

Dit proefschrift is goedgekeurd door de promotor:

prof.dr. D.J. Broer

Copromotor:
dr.ing. C.W.M. Bastiaansen

Aan Linda

Contents

Summary

Micro sized polymeric relief structures are widely used in various technological fields such as optical data storage, imaging, microfluidics and coatings. With the ongoing trend of miniaturization it can be expected that their importance will only grow. Therefore techniques have to be developed enabling the mass production of new types of structures which are especially designed for specific applications. Photoembossing is such a technique which is particularly interesting due the ease of processing. The technique is based on a solid thin layer of a mixture of polymer, monomer and photoinitiator. This mixture is referred to as the photopolymer. A latent image of the desired relief pattern is created into the photopolymer layer by local exposure to ultraviolet (UV) light and creating radicals into the illuminated areas by activation of the photoinitiator. The relief texture is developed by heating the photopolymer above its glass transition temperature. The increased mobility enhances the radical initiated polymerization of monomer and the resulting local differences in composition of the film causes a diffusion of monomer to the illuminated area. Due to the volume displacement by diffusion, relief structures appear in the illuminated areas. The maximum aspect ratio (the height divided by the width of the structure) which can currently be achieved by photoembossing is low. This limits the number of potential applications. In this thesis several methods are presented to enhance the relief development in photoembossing and new applications are demonstrated.

First, the relief development is investigated by using a numerical model. The model describes the diffusion of monomer due to local changes in chemical potential by the polymerization reaction. The effects of compounds which can interfere with the polymerization reaction by reacting with radicals (e.g. oxygen) are taken into account. The model shows that radical termination, and especially by trapping, is an important factor in the relief development. Molecules which enhance the termination of radicals (e.g. oxygen) are thus observed to have a negative effect on the relief height. Molecules which reinitiate the polymerization after reacting with the radicals (e.g. chain transfer agents) are observed to have a positive effect on the aspect ratio. The transfer/reinitiation reaction results in accumulation of stabilized radicals. These radicals act as "latent initiators", which can reinitiate the polymerization reaction during the heating step.

The modelling results are experimentally investigated by studying the effect of compounds which enhance radical termination (inhibitors/retarders) and compounds which reinitiate the polymerization reaction (chain transfer agents) on the relief

formation in photoembossing. It is demonstrated that inhibition does indeed not improve the aspect ratio of a relief structure. Retardation of the polymerization reaction, however, is observed to increase the relief height by a factor of 7. By investigating the type and stability of the radicals and the kinetic influence it is determined that the increase can be attributed to chain transfer reactions. The effect of chain transfer is further investigated by the addition of reversible addition-fragmentation transfer (RAFT) agents. Also these molecules are capable of enhancing the relief height of the photopolymer system by a factor of 7. The RAFT agents are observed to be non-sensitive towards environmental oxygen which is an important issue for industrial applications. However, their intrinsic color makes these compounds less suitable for use in most of the optical applications.

To improve on the aspect ratio further, new photopolymer systems have been developed. Unlike the conventional polymer/monomer mixtures, these photopolymers do not contain the immobile polymeric binder which normally has to be added in a large amount (up to 50wt.-%) to regulate the diffusional properties of the monomers prior and during heat development. The newly developed photopolymers consists of mobile monomers which are solid at room temperature due to steric or dipole-dipole interactions, and demonstrate therefore a low diffusional mobility of the monomers. However, upon heating during the development step the mobility is extremely high and it is demonstrated that this results in large aspect ratios and consequently large surface modulations.

The increased performance and unique method of development (i.e. by heat) are exploited by investigating new applications for photoembossing. It is demonstrated that the technique can be used to create an antireflection coated microlens array of which the optical characteristics can be easily controlled by tuning the processing parameters. It is also possible to use photoembossing to in-situ seal an array of pre-filled micro-cavities, such as encountered in electrophoretic displays. This method of sealing is demonstrated to be insensitive to small deviations in cavity height, flatness of the cover and thin fluid films remaining between the cover and the top of the cavity walls. Another feature of photoembossing is the low processing and material costs involved. The technique can therefore also be used to create protrusions which are used to increase the viewing angle in liquid crystal displays, or disposable replication mold or stamps.

With photoembossing relief structures are made through diffusion of molecules to pre-specified locations. The opposite effect, relief structures that induce the diffusion of molecules, is used in biosensors. These devices are used to detect biomolecular species (analyte) such as DNA/RNA or proteins in a sample fluid. The current systems either require small volumes of sample fluid or have a high sensitivity. In this thesis, a new type of biosensor which combines small sample volumes with high sensitivity is

designed, manufactured and evaluated. This device is based on a microfluidic channel and can in principle be sealed by using photoembossing.

In conclusion, we show in this thesis that high aspect ratio relief textures can be obtained by photoembossing. The improved performance can be used in range of new applications and broadens the applicability of the technique.

List of symbols

A	-	Network model parameter
A_{exp}	-	Pre-exponential factor
B	-	Network model parameter
c	$mol \cdot l^{-1}$	Concentration
D	$m^2 \cdot s^{-1}$	Diffusion coefficient
D_M	$m^2 \cdot s^{-1}$	Diffusion coefficient in pure polymer
D_s	$m^2 \cdot s^{-1}$	Surface tension driven diffusion coefficient
$D(\varphi_M)$	$m^2 \cdot s^{-1}$	Diffusion coefficient at given monomer conversion
$E_a(k)$	$kJ \cdot mol^{-1}$	Activation energy for reaction constant
$E_a(D)$	$kJ \cdot mol^{-1}$	Activation energy for diffusion constant
$[I]$	$mol \cdot l^{-1}$	Photoinitiator concentration
f	-	Functionality of monomer
G	J	Gibbs free energy
I_a	$Einstein \cdot l^{-1} \cdot s^{-1}$	Effectively absorbed light intensity
I_o	$W \cdot m^{-2}$	Exposure intensity
J	$mol \cdot m^{-2} \cdot s^{-1}$	Diffusion flux
K_0	-	Trapping efficiency
K_1	-	Fitting constant
K_2	-	Fitting constant
k_b	$J \cdot K^{-1}$	Boltzmann constant
k_2	$l \cdot mol^{-1} \cdot s^{-1}$	Propagation rate constant
k_4^{b}	$l \cdot mol^{-1} \cdot s^{-1}$	Biomolecular termination rate constant
k_4^{m}	s^{-1}	Monomolecular termination rate constant
k_5	$l \cdot mol^{-1} \cdot s^{-1}$	Transfer rate constant
$k_{5'}$	$l \cdot mol^{-1} \cdot s^{-1}$	Reinitiation rate constant
k_6	$l \cdot mol^{-1} \cdot s^{-1}$	Termination rate constant
P	$N \cdot m^{-2}$	Pressure
$[M]$	$mol \cdot l^{-1}$	Monomer concentration
M_i	-	Molar weight of species i
m_c	-	Average length of polymer chain between two crosslinks
N	-	Total number of molecules
n_i	-	Number of molecules of species i
R	$J \cdot K^{-1} \cdot mol^{-1}$	Ideal gas constant
$[R\cdot]$	$mol \cdot l^{-1}$	Propagating radical concentration

t	s	time
T	K	Temperature
$[T\cdot]$	$mol \cdot l^{-1}$	Trapped radical concentration
W_I	$mol \cdot s^{-1}$	Rate of initiation
X_{gel}	-	Monomer conversion at gelpoint
x	-	Polymer conversion
$[ZX]$	$mol \cdot l^{-1}$	Kinetic inferring compound concentration
$[Z\cdot]$	$mol \cdot l^{-1}$	Stabilized radical concentration

Greek characters

α	-	Monomer conversion
ε	-	Efficiency factor
ε_I	$l \cdot mol^{-1} \cdot m^{-1}$	Molar extinction coefficient photoinitiator
ϕ_i	-	Volume fraction of species i
Φ_P	-	Total polymer volume fraction at moment of crosslinking
Φ	-	Initiation quantum yield
μ	$J \cdot mol^{-1}$	Chemical potential
κ	-	Curvature of surface
γ	$J \cdot m^{-2}$	Surface energy
χ	-	Interaction parameter
v	$m^3 \cdot mol$	Molar volume
ρ_i	$kg \cdot m^3$	Density of species i

Chapter 1

Introduction

1.1 Micro relief structures

The presence of micro sized polymeric relief structures in today's world is often overlooked. Their size makes them hardly visible to the eye and almost impossible to feel by touch. It is therefore the more surprising that their significance is truly immense! Originally the production of microelectronic chips has been the main area of interest for micro patterning techniques.[1] A patterned polymer is used to implement and integrate functional components in a microchip. Over the last decades microstructures have also found their way in a variety of other technological fields such as optical data storage, imaging, microfluidics and coatings.[2-6] Typical examples of their use are in liquid crystal displays (LCD), digital video discs (DVD), video projection systems, micro-electromechanical systems (MEMS) and biosensors. With the ongoing trend of miniaturization it can only be expected that in the future their importance will grow even further. To keep up this trend, new technologies are required that can be used to create new types of relief structures on a large scale. In this thesis the possibilities of a newly developed surface relief texturing technology, called photoembossing, are explored.

1.2 Conventional processing techniques

A variety of techniques are currently used to create micro relief structures in polymers.[7] Each method varies with respect to the size and shape of the relief and the production speeds at which they are obtained. For example, in laser ablation a high intensity pulsed laser beam is used to selective remove material from a polymeric substrate.[8] The obtained structures have the shape of the laser beam spot and are therefore usually spherical with a diameter of several μm or larger. Although complicated patterns can be created by connecting multiple spherical structures, the technique lacks controllability over the geometry of created relief structures. This disadvantage is also encountered in other surface texturing techniques such as ink jet printing. With this technique a drop of liquid material (ink) is propelled to a substrate.[9] At the surface of the substrate the drop solidifies and, typically, the obtained relief structures are spherical with a size of at minimum 50 μm. Also here it is possible to connect several spherical structures and create patterns, but the controllability over the geometry remains poor. Although quite a variety of techniques can be used to sculpture

the surface of a polymer (e.g. micro cutting, soft lithography, ion-beam etching, proton beam writing, molecular self-assembly), their mass production is predominantly based on two techniques: replication and photolithography.[10-13]

Replication is by far the most common method for creating surface relief structures in polymers (Figure 1.1).[14,15] This technique uses a mold with an inverse imprint of the required texture. The basic principle is that the imprint of the relief in the mold is transferred into a polymer or its precursor by mechanical contact. Several varieties of this technique are currently used on an industrial scale. In hot-embossing an unstructured polymer substrate is softened by raising its temperature above the glass transition.[15] At this temperature the mold is pressed into the substrate. The shape of the relief structure is fixed by lowering the temperature until the polymer solidifies. During this cooling process the mold remains into firm contact with the polymer to ensure that an exact copy of the relief is obtained. Due to its simplicity hot-embossing is used to produce a large variety of products ranging from precise microfluidic devices to aesthetic textures on shower curtains.[16] A similar concept as hot-embossing is injection molding.[17] Here a polymer is liquefied, by raising its temperature above the glass transition or melting temperature, and injected under high pressure into a closed mold. After cooling, the mold opens and a replicate of the mold is obtained. This technique is for example used in the manufacturing of compact discs (CD) and digital video discs (DVD). Instead of using a polymer it is also possible to use a mixture of a photoinitiator and polymer precursor.[18] This mixture is applied as a liquid thin layer onto a substrate. When the mold is pressed into the thin layer, the imprint is fixed by applying an ultraviolet (UV) exposure upon which the photoinitiator is activated and the polymer precursor is polymerized. This process is commonly used to manufacture micro-optical components.

Due to its simplicity, replication via structured masters or molds is the most frequently used technique to create micro sized relief structures. Thousands or even millions of replications can be produced by using a single mold and the processing times are usually within the order of seconds or minutes. This makes replication a fast and cost effective technique when large quantities of the same product are required. When only a few products are required this technique is less suitable since the mold is quite expensive. Also replication cannot be used for all materials. Some materials cannot be liquefied or degrade at elevated temperature. Others lose their functional surface properties due to the mechanical contact with the mold. In addition, also the height of structures is limited to avoid problems upon releasing of the product from the mold.
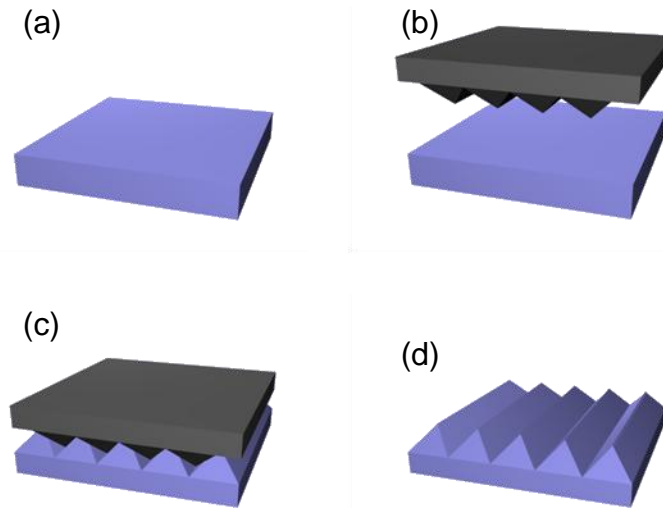
Figure 1.1: Schematic representation of a replication process, which consists of (a) substrate and (b) a mold, which are (c) brought in mechanical contact to (d) transfer the imprint of the mold into the substrate.

Another frequently used technique for manufacturing surface relief structures is photolithography (Figure 1.2).[19] This technique makes use of electromagnetic radiation to transfer a pattern of light into a photo sensitive layer (photoresist) on a substrate. The electromagnetic radiation can be ultraviolet (UV), deep ultraviolet (DUV), extreme ultraviolet (EUV), e-beam, ion beam or X-ray photons. In the principle the minimum size of the features which can be transferred into the photoresist depends on the wavelength of the electromagnetic radiation. The image to be transferred as a pattern of light is located on a lithographic mask, which is positioned between the photosensitive layer and the light source. It is also possible that the pattern is created by the interference of two (laser) light sources as is done in holography. In all photolithographic patterning methods a chemical reaction is initiated in the exposed areas, due to which a difference in solubility between the exposed and non-exposed areas is obtained. In case of a positive tone photoresist the exposed areas undergo a change in chemical structure and become soluble in a, often alkaline, developing solution. A negative tone photoresist behaves in an opposite manner. Here, the exposed areas become polymerized which makes them insoluble and it is thus the unexposed areas which are removed upon contact with a developing solution. Photolithography is often used in the semi-conductor industry, where the obtained polymeric relief structures are used to partially protect an underlying layer (e.g. silicon) such that the unprotected areas can be engraved or removed via an etching procedure.

Due to its accuracy, photolithography is particularly useful for creating very small sized structures. By using complicated optical systems it is possible to obtain structures with sizes in the range of ±30nm.[20] This is only a fraction of that of the wavelength (±193 nm) with which they are produced. Also extremely high structures, relative to their lateral dimensions, can be manufactured by using a highly collimated light source such as a laser and anisotropic developing methodologies.[21] The downside of photolithography is that many (batch-wise) processing steps are needed in the process. This makes photolithography an elaborate and thus expensive process. In addition the technique is based on inefficient use of materials. The substrate is fully covered with photoresist, while most of it is removed during the development step. Photolithography is therefore mainly used in more sophisticated products such as microelectronics for e.g. computer chips, liquid crystal display or biosensors.
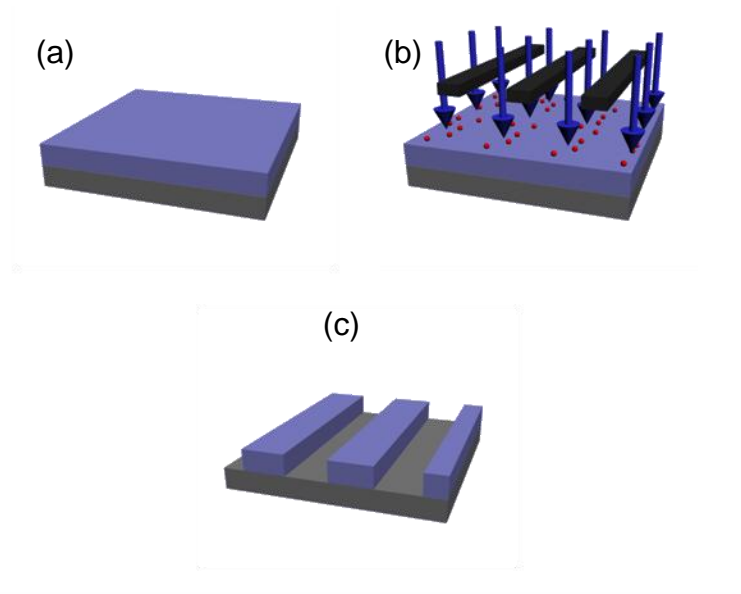
Figure 1.2:   Schematic representation of a photolithographic process, which consists of (a) sample preparation, (b) a patterned exposure and (c) removing soluble areas with solvent.

1.3   Photoembossing

A promising new technique for creating surface relief structures is photoembossing.[22-25] This technique is based on a self-developing photopolymer that in its most simple form consists of a polymeric binder, a multi-functional monomer and a photoinitiator.[26,27] This mixture is processed from solution to form a solid thin film on a substrate. A relief structure is created into the photopolymer layer by a simple two step procedure (Figure 1.3). First, a patterned UV exposure is applied to the photopolymer to create a latent image. This exposure is usually performed by exposing through a lithographic mask, but in principle also other patterning techniques like

holography can be used. During the patterned exposure, the photoinitiator in the photopolymer layer is locally activated and as a result the monomer starts to polymerize. The polymerization reaction is, however, limited due to a low mobility of reactive species within the solid photopolymer layer at room temperature and, consequently, a latent image is initially obtained. In a second step, the sample is heated to a temperature around 100ºC. The molecular mobility increases within the photopolymer which enhances the polymerization reaction and the diffusion of reactive species to the exposed areas. This mass transport of material from the non-exposed to the exposed areas originates from the local difference in photopolymer composition due to the polymerization reaction. The diffusion causes a local increase of the volume in the exposed areas which manifests itself as a surface relief structure.[28,29] Since the relief structures appear during the heating of the photopolymer, this step is referred to as the "developing step". After the developing step the photopolymer layer is fully cured via a flood exposure or thermal baking step, to avoid any reactions from non-reacted materials.
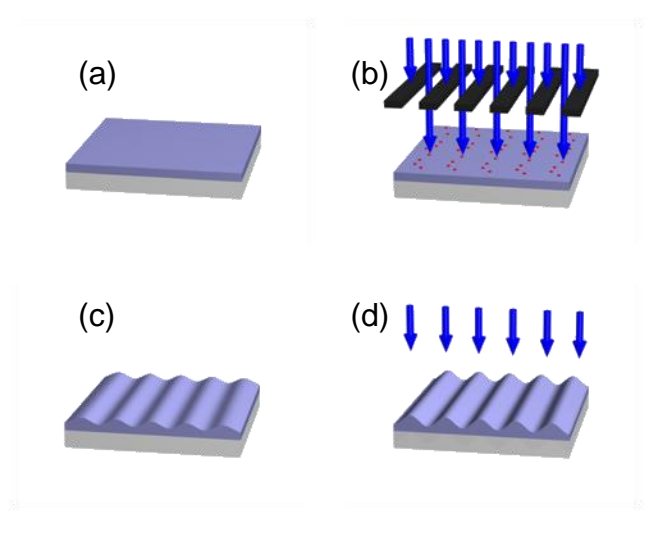
Figure 1.3:   Schematic representation of the photoembossing process, which consists of (a) sample preparation, (b) patterned UV exposure, (c) developing step and (d) flood exposure.

Photoembossing is not only a simple, but also a very efficient technique for creating micro relief structures. Instead of removing material from the substrate, as in photolithography, the technique is based on moving material on the substrate. In addition, the technique is capable of creating complex textures since it uses a latent image and it is thus possible to apply multiple exposures before development.[1] Hereby benefiting from the fact that the surface remains relatively flat until the temperature is raised, thus not altering the optical path of the second exposure. A unique feature of the process is the non-contact development (i.e. by heat) of the relief structures. Unlike the

conventional patterning techniques, photoembossing does not require contact with molds or solvents, but uses heat instead. Overall it can be said that the technique is ideal for creating microstructures when photolithography is too expensive and mechanical replication with structured masters and/or molds is not possible.

In the past, photoembossing was proposed for the formation of diffusive reflectors in reflective displays. These diffuse reflectors can redirect ambient light efficiently to a viewer.[30] In this particular case, photoembossing is used (and not lithography or mechanical embossing), because of its ease of processing. The structures needed for this application are relatively shallow and relatively easy to realize. However in order to broaden the application potential of photoembossing, it necessary to improve on its performance. One particular disadvantage is that the height of the obtained relief structures is rather low. To express the height of a relief structure it is common to use the term aspect ratio (AR) which equals h/w, where h is the height of a structure and w its width. The required aspect ratio depends on the function of the relief structure. For example, the focal length of a microlens depends on its curvature and thus lenses that are designed for light collimation, imaging or outcoupling require a different aspect ratio.[31] Currently with photoembossing only very low aspect ratios are obtained with an aspect ratio of less than 0.05. Typically these structures are in the range of 2.5-20 μm wide and less than respectively 0.1-1 micron high.

It has been shown by Sanchez et al. that the aspect ratio of photoembossed relief structures can be improved by using thicker photopolymer layers, and thus having in absolute value more material to diffuse.[32] Nevertheless, the aspect ratio remains low. Especially when taking into account that approximately half of the photopolymer consists of reactive species and thus the maximum obtainable height of a structure is roughly equal to the layer thickness. In other words: aspect ratios of approximately 0.15 - 1 should be possible in case of a periodic structure with equal exposed and dark areas.

1.3.1 Reaction kinetics

The relief formation in photoembossing is based on the diffusion of reactive species to UV exposed areas of the photopolymer layer. The extent of diffusion depends on the difference in chemical potential of the reactive components between the exposed and non-exposed areas. Besides the interaction parameters between monomer and polymer, reactivity, size and crosslinkability of the reactive species, network elasticity and surface tension, the main contribution to the chemical potential is the consumption of monomer in the exposed areas.[33-35] It can thus be expected that the performance of a photopolymer is to a large extent controlled by the reaction kinetics of the reactive species.

In photo-induced processes of similar nature it is often reported that compounds that interfere with the reactions kinetics have a significant influence on the performance of a photopolymer. The reported effects, however, differ and depend on the type of compound, the type of reactive species and the processing environment.[36-38] For instance, oxygen has been demonstrated to have a negative effect on surface relief formation upon the holographic exposure of photopolymers.[39,40] Oxygen is an effective inhibitor for radical mediated reactions by reacting with propagating radicals to form relatively non-reactive peroxide radicals. These radicals are terminated by reacting with themselves or other propagating radicals. As a result, the radical concentration in the activated areas is reduced and thereby the driving force for polymerization induced diffusion. Consequently, the presence of oxygen reduces the height of the obtained modulation and overall performance of a photopolymer. To reduce the effects of oxygen inhibition tertiary amines can be added to the photopolymer composition.[41] The oxygen reacts first with the amine and forms an unstable intermediate, which is most likely to be a hydroperoxide. After consumption of the oxygen, free radicals are produced by the decomposition of the photochemical unstable intermediate upon UV radiation. This reduces the loss of radicals present in the reaction mixture, causing a higher polymerization rate, but a lower molecular weight of the polymers. It has been suggested that inhibitors could also have a positive effect on photopolymers by controlling the undesired reaction of reactive species in the non-exposed areas.[23] These undesired reactions, which can occur due to scattering of UV light or diffusion of reactive species within the photopolymer film, reduce the difference in chemical potential between the exposed and non-exposed areas and hinder the diffusion of reactive species. However, tests performed by adding well-known inhibitors such as 4-ethoxyphenol and p-benzoquinone did not result in the expected increase in performance. In a similar approach, it has been tried to control the movement of reactive species to undesired areas via polymer chain growth by the addition of sodium formate as a chain transfer agents in a polyvinylalcohol/acrylamide based photopolymer.[42] This approach results in an increased performance of the photopolymer.

The influences of a variety of compounds that interfere with the reaction kinetics in photopolymers have thus been reported. The results vary per system and it is difficult to compare and translate the obtained results to photoembossing. Especially, since photoembossing is based on penta/hexa functional monomers which create a densely crosslinked network. This will have a large influence on the diffusion of monomer and radical termination.[43,44] The effect of the kinetic interfering compounds can thus not be deduced from their behavior reported on mono- or di-functionalized reactive species.

1.4   Aim of the thesis

In the previous sections it was explained that polymeric surface structures are widely used in various technological fields. Originally the microelectronic chips have been the main area of interest for micro patterning techniques. Nowadays, microstructures have also found their way in a variety of other technological fields and with the ongoing trend of miniaturization it can be expected that their importance will only grow. Therefore techniques have to be developed for the mass production of new types of structures especially designed for specific applications. Photoembossing is such a technique which is especially interesting due its ease of processing and non-contact developing method. This makes this technique ideal to create surface textures in case conventional techniques like photolithography are too expensive and replication techniques are not possible.

To increase the range of potential applications for photoembossing, the performance of the process needs to be increased. The aspect ratio which can currently be obtained is often too low. The first aim of this thesis is therefore to improve the aspect ratio of photoembossed relief structures. Since relief formation is based on a reaction driven diffusion within the photopolymer it is investigated if this objective can be achieved via altering the reaction kinetics by using additives. Also new types of photopolymers will be investigated. A second objective of this thesis is to explore potential applications for photoembossing. It is especially the unique non-contact method of development (i.e. by heat) which will be of prime interest.

1.5   Outline of the thesis

To improve the aspect ratio of photoembossed relief structures, its relief forming process is first investigated by a mathematical model (**Chapter 2**). The model is based on the Flory-Huggins theory of mixing of polymers and monomers. A dynamic model is created by calculating for a certain time interval the monomer concentrations, the chemical potential and monomer displacement to re-establish a thermodynamic equilibrium. This calculation is repeated over several time intervals until a certain reaction-time has lapsed. In the model the reaction kinetics are treated such that effects of kinetic interfering compounds, such as oxygen, can modeled and predicted. In general these compounds can be classified as either inhibitors, which terminate radical species, or chain transfer agents, which reinitiate polymerization.

To experimentally verify the results from the model the effect of *tert*-butyl hydroquinone (TBHQ), a well known inhibitor/retarder, on the performance of the photopolymer is investigated (**Chapter 3**). The research is performed under both inert and oxygen containing atmospheres since it is known that oxygen can have a synergetic inhibition effect with hydroquinones. The type of radical species formed by the transfer

reaction and the stability of these species is determined by electron spin resonance (ESR) spectroscopy. The resulting change in kinetics is monitored by real time Fourier transform infra-red (FT-IR) spectroscopy. The performance of the photopolymer upon the addition of TBHQ is assessed by measuring the obtained aspect ratio with a confocal microscope.

By using similar methods also the effect of chain transfer agents is investigated (**Chapter 4**) and these results are compared to those obtained from the addition of inhibitors to the photopolymer composition.

To further enhance the performance of the photopolymer, new photopolymer systems are explored (**Chapter 5**) which are mainly based on monomers. The conventional photopolymer composition is based on a mixture of a polymer binder and multifunctional monomer. The polymeric binder is used for processing reasons, but it is immobile and cannot contribute to the height of the developing structure. The new photopolymers are based on monomers which are solid at room temperature such that no polymeric binder is required. The absence of a polymeric binder in these systems allows higher structures to be developed.

Next, potential applications for photoembossing are investigated (**Chapter 6**). The dry development step makes it an ideal technique for creating relief structures in case contact between a polymer and a mold (replication) or etching fluid (photolithography) is not possible. It is shown that this feature makes photoembossing an ideal technique for sealing an electrophoretic display (or a microfluidic device), creating antireflection coated micro optical elements and creating protrusions for vertically aligned liquid crystal displays.

Surface relief structures can be manufactured by the diffusion of molecules. It is also possible that a surface relief structure induces the diffusion of molecules. This concept is used in a newly developed protein sensor (**Chapter 7**). This type of sensor is based on microfluidic chip which could potentially also be sealed by using photoembossing.

1.6 References

[1] C. Witz, C. Sanchez, C. W. M. Bastiaansen, D. J. Broer, *Handbook of Polymer Reaction Engineering*, Vol. 2 (Eds. T. Meyer, J. Keurentjes), Wiley-VCH, Weinheim, Germany **2005**, Ch.19.

[2] G. Kampf. D. Freitag, W. Witt, *Die Angewandte Makromolekulare Chemie* **1990**, *183*, 243.

[3] H. Yoshida, A. Takeda, Y. Taniguchi, Y. Tasaka, S. Kataoka, Y. Nakanishi, Y. Koike, K. Okamoto, *Mol. Cryst. Liq. Cryst.* **2004**, *410*, 255.

[4] F. T. O'Neill, J. T. Sheridan, *Optik (Jena)* **2002**, *113*, 391.

[5]   Y-T. Cheng, D. E. Rodak, *Appl. Phys. Lett.* **2005**, *86*, 144101.

[6]   T. Koener, L. Brown, R. Xie, R. D. Oleschuk, *Sensors and Actuators B* **2005**, *107*, 632.

[7]   O. Rötting, W. Röpke, H. Becker, C. Gärtner, *Microsyst. Technol.* **2002**, *8*, 32.

[8]   P. E. Dyer, *Appl. Phys. A* **2003**, 77, 167.

[9]   S. Roy, *J. Phys. D: Appl. Phys.* **2007**, *40*, 413.

[10]   J. A. van Kan, P. G. Shao, K. Ansari A. A. Bettiol, T. Osipowicz, F. Watt, *Microsyst. Technol.* **2007**, *13*, 431.

[11]   Y. Suzuki, *Nucl. Instr. and Meth. in Phys. Res. B* **2003**, *206*, 501.

[12]   B. Serrano, *Formation of 3D micro- and nanostructures*, Technische Universiteit Eindhoven, Eindhoven, The Netherlands, **2008**, Ch. 1-7.

[13]   S. Gowri, P. Ranjith Kumar, R. Vijayaraj, A. S. S. Balan, *Int. J. Materials and Structural Integrity* **2007**, *1*, 161.

[14]   H. Becker, C. Gärtner, *Anal. Bioanal. Chem.* **2008**, *390*, 89.

[15]   M.T. Gale, *Microelect. Eng.* **1997**, *34*, 321.

[16]   S. Y. Chou, P. R. Krauss, P. J. Renstrom, *Appl. Phys. Lett.* **1995**, *67*, 3114.

[17]   J. Giboz, T. Copponnex, P. Mélé, *J. Micromech. Microeng.* **2007**,*17*, 96.

[18]   B. K. Long, B. K. Keitz, C. G. Willson, *J. Mater. Chem.* **2007**, *17*, 3575.

[19]   E. Koukharenko, M. Kraft, G. J. Ensell, N. Hollinshead, J. Materials Sci. Mater. Electron. **2005**, 16, 741.

[20]   M. Totzeck, W. Ulrich, A. Göhnermeier, W. Kaiser, *Nat. Photonics* **2007**, *1*, 629.

[21]   A. del Campo, C. Greiner, *J. Micromech. Microeng.* **2007**, *17*, 81.

[22]   O. V. Sakhno, T. N. Smirnova, *Optik* **2002**, *113*, 130.

[23]   J. R. Lawrence, F. T. O'Neill, J. T. Sheridan, *Optik (Jena)* **2001**, *112*, 449.

[24]   T. F. O'Neil, I. C. Rowsome, A. J. Carr, S. M. Daniels, M. R. Gleeson, J. V. Kelly, J. R. Lawrence, J. T. Sheridan, *Proc. of SPIE* **2005**, *5827*, 445.

[25]   C. de Witz, D. J. Broer, *Polym. Preprints*, **2003**, *44*, 236.

[26]   N. Adams, B-J. De Gans, D. Kozodaev, C. Sànchez, C. W. M. Bastiaansen, D. J. Broer, U. S. Schubert, *J. comb. Chem.* **2006**, *8*, 184.

[27]   B. J. De Gans, C. Sanchez, D. Kozodaev, D. Wouters, A. Alexeev, M. Escuti, C. Bastiaansen, D. Broer, U. Schubert, *J. Comb. Chem.* **2006**, *8*, 228.

[28]   C. M. Leewis, A. M. De Jong, L. J. van IJzendoorn, D. J. Broer, *J. Appl. Phys.* **2004**, 95, 4125.

[29]   C. M. Leewis, A. M. De Jong, L. J. van IJzendoorn, D. J. Broer, *J. Appl. Phys.* **2004**, *95*, 8352.

[30]   D. J. Broer, C. M. R. Witz, T. van Bommel, WO 2005/008321, **2005**.

[31]   E. Hecht, *Optics*, 4th edition, Addison Wesly, San Francisco, USA, **2002**, (149-233).

[32]   C. Sánchez, B.-J. de Gans, D. Kozodaev, D. Wouters, A. Alexeev, M. J. Escutti, C. Van Heesch, T. Bel, U. S. Schubert , C. W. M. Bastiaansen, D. J. Broer, *Adv. Mater* **2005**, *17*, 2567.

[33]   C. M. Leewis, A. M. De Jong, L. J. van IJzendoorn, D. J. Broer, *J. Appl. Phys.* **2004**, 95, 4125.

[34]   C. M. Leewis, P. H. A. Mutsaers, A. M. de Jong, L. J. van IJzendoorn, D. J. Broer, M. J. A. de Voigt, *Nucl. Instr. Meth. B* **2001**, *181*, 367.

[35]   M. R. Gleeson, J. V. Kelly, D. Sabol, C.E. Close, S.Liu, J.T. Sheridan, *J. Appl. Phys.* **2007**, *102*, 023108.

[36]   G. Odian, *Principles of Polymeriztion*, 4th edition, Wiley Interscience, New Jersey, USA, **2004,** (255-264).

[37]   G. Moad, D. H. Solomon, *The Chemistry of Free Radical Polymerization*, Elsevier Science Ltd, Great Britain, **1995**, (260-266).

[38]   J. Brandrup, E. H. Immergut, *Polymer Handbook*, 4th edition, Wiley Interscience, New York, **1999** (II-53 –II-55).

[39]   A. Fimia, N. López, F. Mateos, R. Sastre, J. Pineda, F. Amat-Guerri, *J. Modern Optics*, **1993**, *40*, 699.

[40]   A. K. O'Brien, C. N. Bowman, *Macromol. Theory Simul.* **2006**, *15*, 176.

[41]   R. Sato, T. Kurihara, M. Takeishi, *Polymer International* **1998**, *47*, 159.

[42]   M. R. Gleeson, D. Sabol, S. Liu, C. E. Close, J. V. Kelly, J. T. Sheridan, *J. Opt. Soc. Am. B* **2008**, *25*, 396.

[43]   K. Dušek, M. Dušková-Smrčková, *Prog. Polym. Sci.* **2000**, *25*, 1215.

[44]   E. Selli, C. Oliva, *Macromol. Chem. Phys.* **1995**, *196*, 4129.

Chapter 2

Photoembossing model

The objective of this chapter is to investigate the effect of a kinetic interfering compound (Z) on the relief formation by means of photoembossing via using a numerical model. Diffusion of monomer to the relief forming areas is driven by the polymerization reaction in the illuminated areas. Rather than a difference in monomer concentration between the illuminated and non-illuminated areas, it is the difference in chemical potential which is the actual driving force for diffusion. To calculate the chemical potential, the model uses the Flory-Huggins theory of mixing polymer and monomers. Also the contribution of the network elasticity and surface tension are taken into account. The polymerization reaction kinetics in the presence of Z and the diffusion are inserted into the model to create a dynamic system. Z interferes by accepting propagating radicals and subsequently terminating the radicals (inhibition) or reinitiating the polymerization reaction (chain transfer). The model consists of two simulation cycles of which the first simulates the patterned light exposure and the second the heating step. The simulations are performed to get quantitative results and the input parameters are therefore based on order of magnitude estimations. The model shows that an inhibition reaction has a negative effect on the aspect ratio. Propagating radicals are required for the conversion of monomer and their termination thus reduces the driving force for diffusion. The effect of inhibition can be overcome by increasing the exposure dose and consequently increasing the initial concentration of propagating radicals. A chain transfer reaction is observed to have a positive effect on the aspect ratio. The transfer/reinitiation reaction results in accumulation of stabilized radicals during the patterned light exposure. These radicals act as "latent initiators", which can reinitiate the polymerization reaction during the heating step. Also the initial polymerization during the patterned illumination is reduced by the transfer reaction. The low polymer content at the onset of the thermal development enhances the diffusion of monomer.

2.1   Introduction

Rather than describing the diffusion of monomeric species between the illuminated and non-illuminated areas in terms of a concentration difference alone, it is better quantified by the difference in chemical potential. To model the relief development it is thus necessary to find an expression for the chemical potential that considers the thermodynamics of mixing polymers and monomers. Leewis used the Flory-Huggins theory of mixing as a basis for modeling the development of relief or volume gratings in a photopolymer based on a blend of two monomers.[1] A dynamic model was created by calculating for a certain time interval the monomer concentrations, the chemical potential and monomer displacement to re-establish a thermodynamic equilibrium. This calculation is repeated over several time intervals until a certain reaction-time has elapsed. Also Kjellander and Penterman used a similar model for modeling polymerization induced phase separation and photo-enforced stratification of liquid crystal/monomer mixtures, respectively.[2,3]

   The main contribution to a difference in chemical potential is the local conversion of monomer to polymer. To create a dynamic model it thus necessary to take into account the polymerization kinetics. These depend not only on the characteristics (e.g. functionality and reactivity) of the monomers. Also compounds which are added to stabilize the photopolymer by inducing threshold values (e.g. polymerization inhibitors), environmental oxygen or compounds added to overcome the effects of environmental oxygen (e.g. tertiary amines) are known to influence the reaction kinetics.[4-6] The reported effects of these compounds differ and depend on the type of compound and system in which it is used.[7-9] It is thus not possible to simply translate the obtained results to photoembossing. The fundamental mechanism by which these compounds interfere with the kinetics is, however, similar.[10] It is based on a transfer reaction of propagating radicals to stabilized species. In a subsequent reaction step the stabilized species either reinitiate the polymerization reaction or are terminated via recombination with other radical species. The reinitiation reaction is known from literature as a "chain transfer" reaction and the termination reaction is known as "inhibition".[7] The influence of these compounds can be predicted by incorporating these fundamental reactions into the model to describe the relief development in photoembossing.

   In this chapter the relief formation in photoembossing is investigated by using a dynamic reaction/diffusion model. As a base, the model developed by Leewis has been taken. This model is adjusted such that it takes into account a monomer/polymer system (instead of a two monomer system) and complex reaction kinetics. Also the single step procedure (i.e. only exposure) is replaced by a two step procedure which consists of an exposure and thermal development step. The contributions to the chemical potential in

the illuminated and non-illuminated areas are discussed in paragraph 2.2. To create a dynamic model it is necessary to incorporate the reaction kinetics and diffusion into the model. These processes are discussed in paragraph 2.3. After a discussion of the input parameter in paragraph 2.4, the model is used to predict the relief development in the photopolymer during photoembossing. Also the effect of chain transfer and inhibition reactions on the surface relief development is discussed in paragraph 2.5.

2.2 Chemical potential

As a result of the polymerization reaction in the illuminated areas, the systems energy changes locally with respect to the non-illuminated areas. The amount by which the Gibbs free energy (ΔG) of a system would change if an additional particle (n) is introduced, at constant temperature (T) and pressure (p), is known as the chemical potential ($\Delta\mu$).

$$\Delta\mu = \left(\frac{\partial \Delta G}{\partial n_i}\right)_{T,p,nj(j\neq i)} \tag{2.1}$$

For two phases (illuminated and non-illuminated) in equilibrium to coexist in a single system the chemical potential of each component in the system must be equal:

$$\Delta\mu \text{ (illuminated)} = \Delta\mu \text{ (non-illuminated)} \tag{2.2}$$

In the case of the photopolymer, which consists of a blend of polymer and monomer, it is the chemical potential of the monomer which needs to be considered. The chemical potential of the polymer does not need to be considered since the polymer is immobile. The main contribution to the chemical potential is attributed due to mixing of polymer and monomer, but also network elasticity and surface tension should be taken into account when creating a dynamic model. In the next section these contribution to the chemical potential are discussed.

2.2.1 Mixing

The main contribution to the chemical potential arises from the interaction between monomer and polymer. Already before the polymerization starts, the photopolymer consists of a homogenous mixture of a polymeric binder and a multifunctional monomer. Both the binder and monomer are usually based on (meth)acrylates and can be mixed in a wide range of concentrations.[11-13] In our model it is assumed that the interaction of the monomer with the polymeric binder can be considered equal to the

interaction between monomer and polymer formed in-situ by the conversion of monomer. This is justified by the fact that for most of our formulation both polymers are chemically quite similar and differ mainly in their state of crosslinking. Since the monomer does not distinguish between the type of polymer, the volume of polymerized monomer and the volume of polymeric binder can be considered as one overall polymer volume (ϕ_P). Based on this assumption and the Flory-Huggins lattice model, the effect of local changes in composition on the Gibbs free energy can be expressed by the following equation:[14]

$$\frac{\Delta G^{mix}}{N k_b T} = n_M \ln \phi_M + n_P \ln \phi_P + n_M \varphi_P \chi_{M-P} \tag{2.3}$$

In this expression N is the number of molecules, k_b is the Boltzmann constant (1.380 J · K^{-1}), and T is the temperature. ϕ_M and ϕ_P are the volume fractions of the monomer and polymer, n_M and n_P are the number of molecules of these components. χ_{M-P} is the Flory-Huggins interaction parameter between the monomer and polymer. The interaction parameter χ takes into account the energy of interdispersing polymer and monomer. The chemical potential is equal to:

$$\frac{\Delta \mu^{mix}}{k_B T} = \ln \phi_M + (1 - \phi_M) - \phi_P \frac{N_M}{N_P} + \chi_{M-P} \phi_P^2 N_M \tag{2.4}$$

where N_M and N_P are the amount of unit cells taken by respectively the monomer and polymer. For reasons of simplification, the size of the monomer and monomer repeat units in the polymer are considered to be unity. The size of a polymer is to be considered as significantly larger than the size of a monomer. The difference in chemical potential for the monomer and polymer can then be calculated by:

$$\frac{\Delta \mu^{mix}}{k_B T} = \ln \phi_M + (1 - \phi_M) + \chi_{M-P} \phi_P^2 \tag{2.5}$$

2.2.2 Network elasticity

A network is formed by crosslinking of multifunctional monomer in the illuminated areas. The elasticity of this network resists swelling, giving a second contribution to the chemical potential. It has been shown in phase separation models that the contribution of network elasticity to the chemical potential is of significant importance.[2,3] The

following equation can be used to describe the contribution of the network deformation by swelling:

$$\frac{\Delta G^{el}}{Nk_BT} = \frac{\phi_P}{m_c}\left[\frac{3}{2}A\Phi_P^{2/3}\left(\phi_P^{-2/3}-1\right)+B\ln\phi_P\right]$$ (2.6)

Here Φ_P is the total polymer fraction at the moment of crosslinking and m_c is the average length of polymeric chain between two crosslinks. Assuming that the polymeric binder will either via physical or chemical crosslinking form a part of the crosslinked network and contribute to its elasticity $\Phi_P = \phi_P$. A and B are network model parameters and are equal to:

$$A=1 \qquad ; \qquad B=2/f$$ (2.7)

where f is the functionality of the monomer (one double bond has a functionality of 2) and is equal to 12 for our mostly used monomer. This network model assumes a ring free network and that the lengths of the polymer chains between the crosslinks have a Gaussian distribution. However, in chain reactions it is often observed that densely crosslinked microgel particles are formed. Upon further reaction these particles connect together and form a gel.[10] The microgel particles contain many closed rings that do not contribute to the elasticity. In addition, m_c will not have a Gaussian distribution. Therefore a rough estimation of m_c is obtained by using the mean field approximation, which is applied to describe the polymerization for di-vinyl monomers.[15,16] This approximation assumes that all double bonds are equally likely to react. It further assumes that the double bond and monomer conversion proceed to completion. The monomer conversion (α) relates to the double bond conversion (x) by:

$$\alpha = 1-(1-x)^{f/2}$$ (2.8)

The average chain length between two crosslinks is than given by:

$$m_c^{-1} = \frac{x^2}{\alpha} = \frac{\left[1-(1-\alpha)^{1/6}\right]^2}{\alpha}$$ (2.9)

Here x^2 the probability for a unit to be crosslinked. To correct for cyclization and overall efficiency factor ($\varepsilon \leq 1$) is introduced. Differentiation of equation 2.6, combined with 2.7 gives the elastic contribution to the chemical potential:

$$\frac{\Delta\mu^{el}}{k_B T} = \varepsilon m_c^{-1}\left[1-\frac{2}{f}\right]\phi_P \tag{2.10}$$

2.2.3 Surface energy

The diffusion of monomer deforms the surface of the photopolymer film and thus leads to an increased surface area. A driving force counteracting diffusion is the surface tension of the film. To describe the chemical potential of a surface, a concept is used from the surface diffusion of solids. [1,17] The chemical potential of a surface is given by:

$$\mu^s = -\kappa\gamma\nu = -\gamma\nu\frac{\dfrac{\partial^2 h}{\partial x^2}}{\left(1+\left(\dfrac{\partial h}{\partial x}\right)^2\right)^{3/2}} \tag{2.11}$$

Here, κ is the curvature of the surface, γ is the surface energy and ν the molar volume of the migrating species. The bulk migration of a number (n) of migrating species per unit length in the x-direction it then given by:

$$\frac{\partial n}{\partial t} = \frac{\partial}{\partial x}\left[\frac{D_s n}{kT}\frac{\partial\mu_s}{\partial x}\right] = \frac{\partial}{\partial x}\left[\frac{D_s n\gamma\nu}{kT}\frac{\partial}{\partial x}\left(\frac{\dfrac{\partial^2 h}{\partial x^2}}{\left(1+\left(\dfrac{\partial h}{\partial x}\right)^2\right)^{3/2}}\right)\right] \tag{2.12}$$

Here, D_s is a surface tension driven diffusion coefficient relating to movement of particles at the surface.

2.3 Reaction / diffusion mechanisms

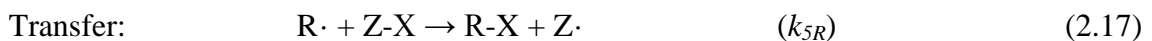The polymerization of monomer in the illuminated areas causes the chemical potential to change within these areas. For the illuminated and non-illuminated areas to coexist in equilibrium, the chemical potential is re-established by diffusion. To develop a dynamic reaction/diffusion model it is necessary to derive equations which describe the polymerization reaction kinetics and the resulting diffusion of monomer.

2.3.1 Radical polymerization

Under inert conditions the radical polymerization of a monomer in a photopolymer can be described by basic initiation, propagation and termination reactions. Upon the patterned illumination of the photopolymer with ultraviolet (UV) light, the photoinitiator (I) is locally activated and free radicals (R·) are formed. These radicals add to a monomer (M) forming a reactive center which continues to propagate by adding more monomer. In this simplified reaction scheme it assumed that the reactivity of the photoinitiated radicals and the propagating radicals is equal. The propagating radicals are terminated via recombination/disproportionation or trapped with the growing polymer network.[18,19] The latter reaction is often observed upon polymerization of multifunctional monomers such as used in the photopolymer composition.[20] Trapping of radicals becomes increasingly important when the polymer chains become crosslinked and the segmental diffusion of radicals is suppressed. Although highly reactive, these radicals are known to be extremely stable for up to days and more.[21,22] After the patterned UV illumination step the sample is heated. This enhances the mobility of the system and allows some of the trapped propagating radicals to continue the reaction with monomer. In the model bimolecular termination is assumed to be the dominant termination reaction below the gel point and monomolecular termination above.

Initiation: $\quad\quad\quad$ I → 2R· $\quad\quad\quad\quad\quad\quad\quad\quad$ (k_1) $\quad\quad\quad\quad$ (2.13)

Propagation: $\quad\quad$ R· + M → R· $\quad\quad\quad\quad\quad\quad\quad$ (k_2) $\quad\quad\quad\quad$ (2.14)

Termination: $\quad\quad$ R· + R· → polymer $\quad\quad\quad\quad$ (k_4^b) $\quad\quad\quad\quad$ (2.15)

$\quad\quad\quad\quad\quad\quad\quad$ R· → trapped radicals (T·) $\quad$ (k_4^m) $\quad\quad\quad\quad$ (2.16)

Upon the addition of a compound (ZX or Z) that can participate in the radical reaction, the propagating radical can be transferred to this compound either via a transfer or addition reaction to form an intermediate radical Z· or RZ·.[12]

Transfer: $\quad\quad\quad$ R· + Z-X → R-X + Z· $\quad\quad\quad\quad$ (k_{5R}) $\quad\quad\quad\quad$ (2.17)

Addition: $\quad\quad\quad$ R· + Z → RZ· $\quad\quad\quad\quad\quad\quad\quad$ (k_{5R}) $\quad\quad\quad\quad$ (2.18)

It is possible that ZX (or Z) can also react with the trapped radicals (T·). The reaction of the relatively large monomer molecules with T· is sterically hindered. Molecules which are small enough might, however, have enough mobility to react with these radicals. Stabilized radicals can thus also be formed by a transfer from trapped radicals:

| Trapped transfer: | T· + Z-X → T-X + Z· | (k_{5T}) | (2.19) |
| Trapped addition: | T· + Z → RZ· | (k_{5T}) | (2.20) |
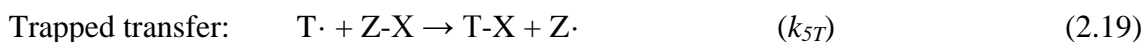
Although it is possible that this mechanism can release some of the trapped radicals, it is unlikely that all can be released. The radicals which cannot be released can be considered as non-reactive and thus terminated. To describe this effect, an efficiency factor (K_0) is introduced in the model. K_0 is the fraction of propagating radicals which are trapped and can react according to equation 2.19 or 2.20. Thus, if $K_0=0$ all trapped radicals are terminated and if $K_0=1$ all trapped radicals can react. The reaction rate constants for the reaction of Z-X (or Z) with R· and T· are considered to be equal ($k_{5R} = k_{5T} = k_5$).

The reactive properties of the intermediate radicals (Z· or RZ·) are different from the propagating radicals. Depending on the reactivity of the intermediate radical and the environment, the intermediate radical can reinitiate polymerization. The overall transfer/reinitiation reaction is known in literature as chain transfer.[7]

| Reinitiation | Z· + M → Z + M· (or ZM·) | $(k_5,)$ | (2.21) |
| or | RZ· + M → RZ + M· (or ZM·) | $(k_5,)$ | (2.22) |
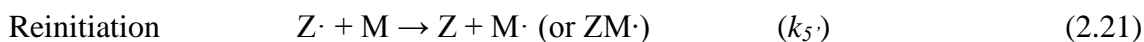
It can be assumed that the reaction products have approximatly the same reactivity as the primary propagating radicals. If the rate of equation 2.21 to 2.22 is low or does not take place at all, the concentration of intermediate radicals strongly increases. These radicals are likely to terminate via crossrecombination with propagating radicals or its own species. The probability of the latter reaction is for chemical reasons usually much lower.[12] The stabilized radicals are less likely to terminate via trapping. Often the reinitiating species are not bound to the polymer network. Even if the stabilized radicals are bound the polymer network, as with some types of Z like for example RAFT agents, this does not neccesarily mean the reinitiating species are trapped.[23] In these cases the reinitiating radicals can become separated from the stabilized species. The overal transfer/termination reaction is known in literature as inhibition.[7]

| Termination: | Z· + R· → polymer | (k_6) | (2.23) |
| or | RZ· + R· → polymer | (k_6) | (2.24) |

Based on equation 2.13 to 2.24 a general equation can be derived for the monomer conversion rate:

$$-\frac{[\text{M}]}{dt} = k_2[\text{R·}][\text{M}] + k_{5'}[\text{Z·}][\text{M}] \tag{2.25}$$

Here, the equations for the transfer (reaction equation 2.17/2.19) instead of the addition reaction (reaction equation 2.18/2.20) were used. In principle the use of both types of reactions will arrive at the same rate equations. The rate equations for compound Z, the propagating radicals, stabilized radicals and trapped radicals are given by:

$$-\frac{[\text{ZX}]}{dt} = k_5[\text{R·}][\text{ZX}] + k_5[\text{T·}][\text{ZX}] \tag{2.26}$$

$$\frac{[\text{R·}]}{dt} = W_1 + k_{5'}[\text{Z·}][\text{M}] - k_4^b[\text{R·}]^2 - k_4^m[\text{R·}] - k_5[\text{R·}][\text{ZX}] - k_6[\text{Z·}][\text{R·}] \tag{2.27}$$

$$\frac{[\text{Z·}]}{dt} = k_5[\text{R·}][\text{Z}] - k_{5'}[\text{Z·}][\text{M}] - k_6[\text{Z·}][\text{R·}] + k_5[\text{T·}][\text{Z}] \tag{2.28}$$

$$\frac{[\text{T·}]}{dt} = K_0 k_4^m[\text{R·}] - k_5[\text{T·}][\text{Z}] \tag{2.29}$$

$$W_1 = 2\Phi I_a = 2\Phi \cdot 2.3 I_0 \varepsilon_I[\text{I}]z = \text{constant} \tag{2.30}$$

Here W_1 is the rate of initiation and depends on the initiation quantum yield Φ of the photoinitiator at the irradiation wavelength and I_a, which is the light intensity that is effectively absorbed by the initiator. A factor of 2 is used to indicate that two radicals are formed per initiator molecule. Assuming that only the initiator molecules absorb light, the absorbed intensity can be derived from Beer's law. The factor 2.3 is the natural logarithm, I_0 is the intensity with which the film is exposed, ε_I is the molar extinction coefficient of the photoinitiator, [I] is the initiator concentration and z is the layer thickness. Since only a small fraction of the initiator will be activated during the exposure, the rate of initiation can be assumed to be constant.

The above equations are valid for reaction mixtures creating linear polymers. For crosslinked reactions, the equations need to be corrected. The main reason is that crosslinking monomers have multiple reactive groups (C=C) of which in principle all can participate during the reaction. The monomer conversion is thus not equal to the conversion of reactive groups. A way to describe this relation is by using the mean field approximation which was already discussed in paragraph 2.2.2.

2.3.2 Diffusion

Diffusion processes can be described with Fick's well known second law. Fick's first law describes how a flux of particles moves from a region of high concentration to a low concentration. This occurs with a magnitude proportional to the concentration gradient and, limiting ourselves to one spatial dimension, is given by:

$$J = -D\frac{\partial c}{\partial x} \tag{2.31}$$

Here, J is the diffusion flux, D is the diffusion coefficient, c is the concentration and x the position in length. During photoembossing the composition within the volume changes with time and in this case Fick's second law of diffusion applies:

$$\frac{\partial c}{\partial t} = \frac{\partial}{\partial x}\left(D\frac{\partial c}{\partial x}\right) \tag{2.32}$$

In compliance with our model we need to convert the concentration gradient to a gradient in chemical potential. For ideal gaseous mixtures of non-interacting hard spheres, the chemical potential is given by $\mu = k\,T\,ln\,c$. The flux of particles is then given by:

$$J = -\frac{Dc}{kT}\frac{\partial \mu}{\partial x} \tag{2.33}$$

The polymer/monomer mixture of the photopolymer cannot be considered as ideal spheres therefore the more general equation 2.35 should be applied. The concentration can also be expressed in terms of density ρ_i, volume fraction ϕ_i and the molar weight M_i of the component:

$$c = \frac{\phi_i \rho_i}{M_i} \tag{2.34}$$

This gives the general diffusion equation of:

$$\frac{\partial \phi}{\partial t} = \frac{\partial}{\partial x}\left(\frac{D\phi}{kT}\frac{\partial \mu}{\partial x}\right) \tag{2.35}$$

The diffusion coefficient is not constant during the polymerization, but instead it reduces with increasing formation of a polymer network. The denser the network gets,

the more difficult diffusion becomes. From the free volume theory, which treats the looseness of a polymer solution by means of an extra available volume, the following expression for the diffusion coefficient can be obtained:[24,25]

$$D(\varphi_M) = D_M \cdot e^{\dfrac{1}{K_1\left(\dfrac{1}{\varphi_M}+K_2\right)}} \tag{2.36}$$

Here D_M is the monomer diffusion coefficient in the pure polymer and K_1 and K_2 are positive constants described in the free volume theory.[25] These parameters are usually treated as fitting parameters.

2.3.3 Temperature

The surface relief development in photoembossing consists of a two step procedure of which the first step is performed at room temperature and the second at an elevated temperature. The heating step is used to enhance both monomer conversion and diffusion. Several previously discussed parameters do depend on the temperature. The main parameters which are influenced are the diffusion and reaction coefficients. The temperature dependency of the reaction constants can be described by the Arrhenius equation:

$$k = A_{\exp} \cdot e^{\dfrac{-E_a(k)}{RT}} \tag{2.37}$$

, where A_{exp} is the pre-exponential factor, R is ideal gas constant ($8.314 \text{ J} \cdot \text{K}^{-1} \cdot \text{mol}^{-1}$) and $E_a(k)$ is the activation energy. Assuming that the pre-exponential factor and activation energy do not depend on the temperature it is possible to calculate the reaction constant at different temperature by using:

$$\frac{k_{T1}}{k_{T2}} = e^{\dfrac{E_a(k)}{R}\left(\dfrac{1}{T_2}-\dfrac{1}{T_1}\right)} \tag{2.38}$$

Also the diffusion coefficient depends on the temperature according to an Arrhenius equation:[26]

$$\frac{D_{T1}}{D_{T2}} = e^{\dfrac{E_a(D)}{R}\left(\dfrac{1}{T_2}-\dfrac{1}{T_1}\right)} \tag{2.39}$$

, where $E_a(D)$ is the activation energy of diffusion.

2.3.4 Dynamic simulation procedure

The surface relief development is modeled by using a numerical approach (Figure 2.1). The two-dimensional photopolymer layer is divided into N discrete volumes of which the height is equal to the layer thickness (h) and the length is equal to Δx. It is assumed that there is no gradient absorption of light within the photopolymer film. The polymerization reactions occur homogenously throughout each discrete volume and it thus not necessary to subdivide the height. The model consists of a cycle of calculations which are repeated until a certain reaction time has elapsed. First, the initial volume fraction of each component within each volume is calculated. Due to the polymerization reaction in the illuminated areas the concentration of monomer and polymer changes in each discrete volume. From these concentrations the chemical potentials of mixing, network elasticity and surface tension can be calculated. The chemical potential of the network elasticity, mixing and surface tension are used to calculate the diffusion by using equation 2.35 and equation 2.12. After the diffusion step, the local concentrations are re-calculated and the next reaction step can be performed.
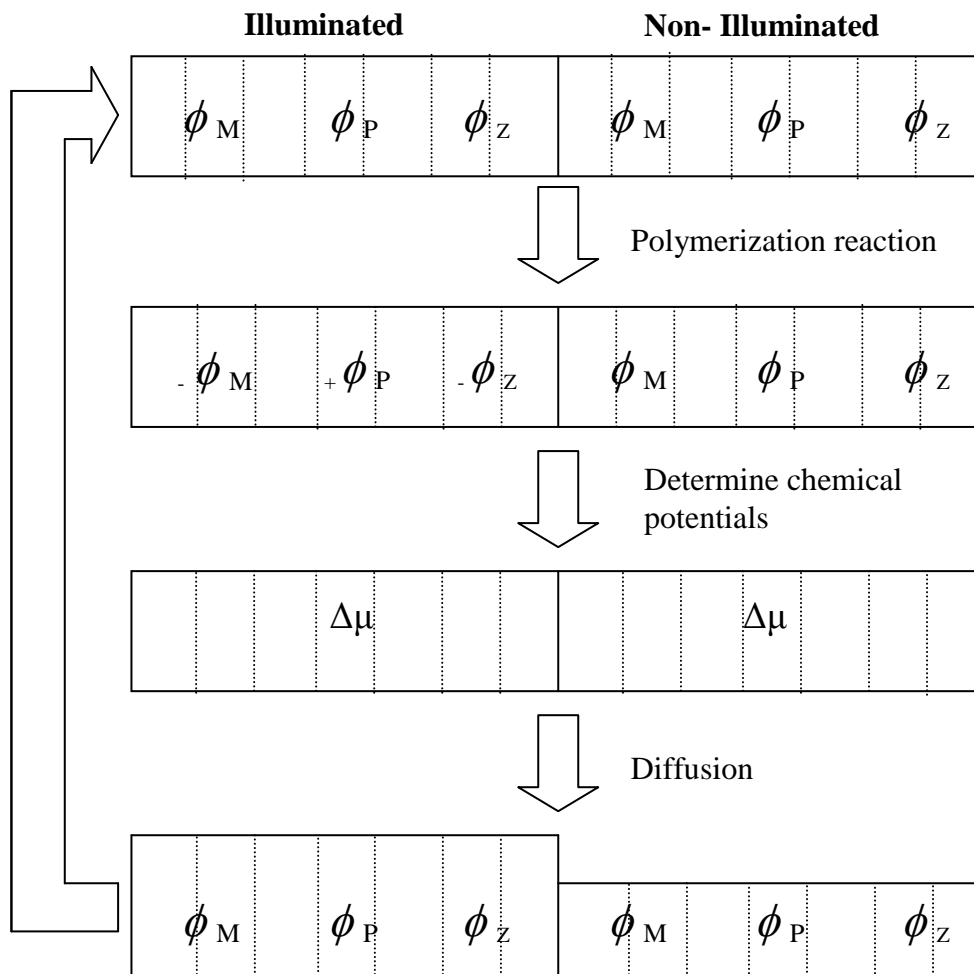

Figure 2.1: Schematic representation of dynamic reaction/diffusion model.

Photoembossing consists of a two step procedure: a patterned illumination and a heating step. In the model these two steps are incorporated as separate cycles. In the first cycle, the reaction driven diffusion during the patterned illumination step is calculated by using reaction and diffusion constants based on room temperature values. In the heating cycle, the initiation reaction is stopped and reaction/diffusion constants are correct for an elevated temperature. In the model it is assumed that the temperature of the photopolymer layer changes instantaneously to the set temperature. In reality it can be expected that the temperature of the photopolymer gradually increases upon heating. The ramping time will depend on the method of heating.

2.4 Model parameters

In this paragraph the input parameters for the model are discussed. The goal of the model is to get quantitative information of the effect of inhibition and chain transfer reactions on the performance of a photopolymer. Most of the parameters are taken from literature.

2.4.1 Photopolymer composition & photoembossing procedure

The composition of the photopolymer is based on the optimized composition found in literature.[11-13] The photopolymer consist of 47.5 wt.-% of polybenzyl methacrylate (M_w = 70.000 gram · mol^{-1}) as a polymeric binder, 47,5 wt.-% of dipentaerythritol hexacrylate (M_w = 578 gram · mol^{-1}) as a monomer and 5 wt.-% of Irgacure 819 (M_w = 418 gram · mol^{-1}) as a photoinitiator. The chemical structures are given in Figure 2.2. In principle, the kinetic interfering compound Z can be all kind of compounds in a wide range of concentrations. For example oxygen, which is a typical inhibiting compound, has only a limited solubility in most organic materials and is usually present in the range of several ppm. Other compounds such as a reversible addition-fragmentation transfer (RAFT) agent, which is a typical reinitiating compound, is commonly used in concentrations equal to the initiator. In the model Z is assumed to be a molecule with molecular weight of 150 gram · mol^{-1} and a concentration of 1 wt.-%. The patterned illumination cycle is carried out at 293 K while using a 40 μm periodicity with equal size of illuminated and non-illuminated areas. The heating step was carried out at 383 K. All parameters relating to the photopolymer composition and the photoembossing procedure are given in Table 2.1.

Photopolymer composition		
ϕ_M *(initial)*	Initial volume fraction of monomer [-]	0.470* - 0.475 [11-13]
ϕ_P *(initial)*	Initial volume fraction of polymer [-]	0.470* - 0.475 [11-13]
ϕ_I *(initial)*	Initial volume fraction of initiator [-]	0.05 [11-13]
ϕ_Z *(initial)*	Initial volume fraction of Z [-]	0.01
ρ	Density photopolymer [kg · m^{-3}]	1000
M_{wM}	Molecular weight monomer [gram · mol^{-1}]	578
M_{wP}	Molecular weight monomer [gram · mol^{-1}]	70.000
M_{wI}	Molecular weight monomer [gram · mol^{-1}]	418
M_{wZ}	Molecular weight monomer [gram · mol^{-1}]	150
Photoembossing procedure		
t_{exp}	Exposure time [s]	5
t_{heat}	Heating time [s]	60
T_1	Temperature during patterned illumination [K]	293 [11-13]
T_2	Temperature during thermal development [K]	383 [11-13]
Λ	Grating periodicity [μm]	40 [12-14]
h	Layer thickness [μm]	16 [12-14]

Table 2.1: Model parameters relating to the photopolymer composition and photoembossing procedure. *This monomer and polymer volume fraction is used when Z is added to the photopolymer composition.
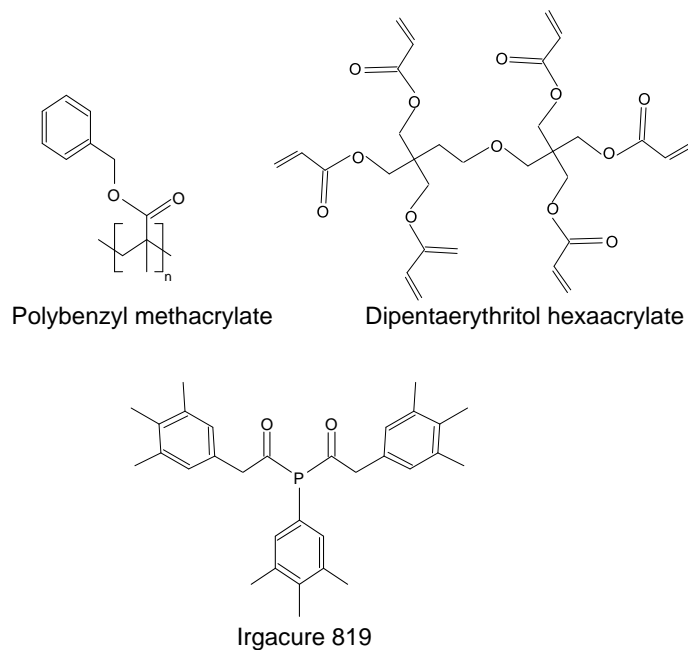

Polybenzyl methacrylate   Dipentaerythritol hexaacrylate

Irgacure 819

Figure 2.2: Chemical structures of the polymeric binder, monomer and photoinitiator.

2.4.2 Chemical potential

The polymeric binder, the monomer and its polymerized counterpart are all based on similar (meth)acrylate units. It can therefore be expected that the Hildebrand solubility parameters are approximately equal and there is little energetic interaction between the polymer and the monomer.[27] To calculate the chemical potential of mixing a value of 0 was therefore taken for χ. This assumption might be an underestimation of the actual value. To calculate the contribution of the network elasticity, it is assumed that crosslinking occurs homogenously throughout the photopolymer. It is likely that already at low conversions the micro-gel particles crosslink into a network. Therefore an efficiency factor of 1 was used. The surface tension for various acrylates is between 0.030-0.040 J $\cdot$ m^{-2}.[28] For the model a value of 0.035 J $\cdot$ m^{-2} was used. A rough estimation of the surface diffusion coefficient based on fluid dynamics shows that its value is in the order of 10^{-6} m^2 $\cdot$ s^{-1}.[1]

Mixing		
χ	Interaction parameter [-]	0 [1-3]
Network elasticity		
ε	Network efficiency factor [-]	1
m_c	Network chain length [-]	Eq. 2.9
f	Monomer functionality [-]	12
Surface tension		
γ	Surface energy [J $\cdot$ m^{-2}]	0.035 [28]
v	Molar volume of monomer [m^3 $\cdot$ mol^{-1}]	578*10^{-6}
D_s	Surface tension diffusion coefficient [m^2 $\cdot$ s^{-1}]	10^{-6} [1]

Table 2.2:   Model parameters relating to the chemical potential.

2.4.3 Kinetics

To determine the rate of initiation (W_I) from equation 2.30, the absorption spectrum of a photopolymer layer was measured by using UV-VIS spectrophotometer (Figure 2.3). The molar extinction coefficient at 365 nm was calculated by using Lambert-Beer law ($\varepsilon = 1.3*10^5$ liter $\cdot$ mol^{-1} m^{-1}). When using equation 2.30, the intensity with which a film is exposed (I_0) should be calculated in Einstein $\cdot$ liter^{-1} s^{-1}. Generally the intensity is, however, given in energy per area (mW $\cdot$ cm^{-1}). To convert the intensity in mW $\cdot$cm^{-1} it should be divided by the layer thickness and by the energy of one mole of photons at the irradiation wavelength. The quantum efficiency of most photoinitiators is around 0.5.[2] The simulations were performed at different exposure doses (exposure time multiplied by intensity) by varying the intensity of the light source.
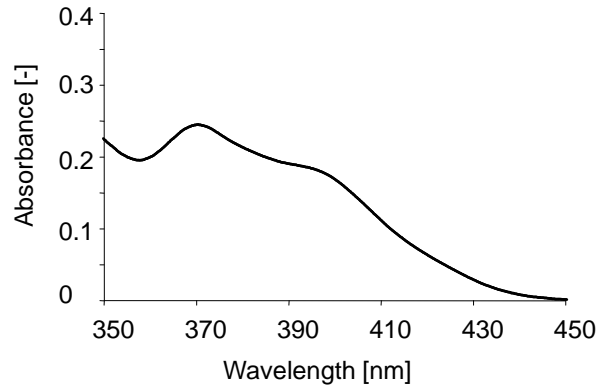
Figure 2.3:   Absorption spectrum of a 16 μm layer of photopolymer containing 5 wt.-% of photoinitiator.

The propagation and termination reaction constants for the polymerization of multi-functional acrylates depend on the conversion.[29] At the onset of polymerization the values are several orders of magnitude higher than at the end of the reaction. In the model averaged values for the reaction constants are used. The propagation reaction constant (k_2) for acrylates is typically in the order of 10^4 liter · mol^{-1} · s^{-1}. The rate constant for bimolecular radical termination ($k_2{}^b$) is typically in the order of 10^4 to 10^7 liter · mol^{-1} · s^{-1}. These values are corrected in the thermal development cycle by using equation 2.38 and assuming an activation energy ($E_a(k)$) of both termination and propagation in the order of 20 kJ · mol^{-1}.[7] Once the gel point is reached the bimolecular termination changes to monomolecular termination. The gel point for multifunctional monomers can occur at a conversion of the functional groups as low as a few percent.[30] The gel point reduces with increasing functionalities of the monomer and for the model it is assumed to occur at 15% monomer conversion. For monomer molecular termination the rate coefficient ($k_4{}^m$) of (meth)acrylates is in the order of 0.01-1 mol^{-1}.[31] In the model a value of 0.01-0.5 mol^{-1} has been used. Monomolecular termination depends on physical trapping of radicals. Its known that at elevated temperatures trapped radicals can escape their traps and continue polymerization.[22] The rate at which this occurs is low. The process of trapping does not appear to be completely passive since (low) activation energies for this process are reported.[32] The effect of temperature on the monomolecular termination constant it is thus ambiguous. The effect is any case small and it has therefore not been corrected for temperature during the heating cycles.

A wide range of values for the radical transfer constant (k_5) of Z can be found in literature.[9] Both with inhibition and chain transfer the value of k_5 is usually expressed in terms of k_2 (respectively z or $c = k_5/k_2$). Typical values of k_5 for inhibitors in acrylates range from 1 for phenols to 10^8 for oxygen.[7,33] Typical values for chain transfer

compounds in acrylates range from 10^{-5} to 10^5.[34] In the model k_5 is varied between 50 and 5000 liter $\cdot$ mol^{-1} $\cdot$ s^{-1}. The termination rate constant (k_6) is often fast and assumed to be of the same order of magnitude as the propagation constant. The reinitiation rate constant ($k_{5'}$) is usually low compared to the transfer constant.[34] This results in accumulation of stabilized radicals or other types of dormant species. These species are slowly released to reinitiate the polymerization. Typically these values are 10^4 to 10^9 lower than the transfer rate constant. In the model $k_{5'}$ was varied between 0.01-0.001 liter $\cdot$ mol^{-1} $\cdot$ s^{-1}. In the heating cycle, the rate constants were corrected by using an $E_a(k)$ of 20 kJ $\cdot$ mol^{-1}. An overview of the model parameters which relate to the reaction kinetics is given in Table 2.3.

Polymerization kinetics		
W_1	Rate of initiation	*
k_2	Propagation rate constant [liter $\cdot$ mol^{-1} $\cdot$ s^{-1}]	10^4 [29]
k_4^b	Bimolecular termination rate constant [liter $\cdot$ mol^{-1} $\cdot$ s^{-1}]	10^4 [29]
k_4^m	Monomolecular termination rate constant [s^{-1}]	0.1[31]
$E_a(k)$	Activation energy [kJ $\cdot$ mol^{-1}]	20 [7]
k_5	Transfer rate constant [liter $\cdot$ mol^{-1} $\cdot$ s^{-1}]	50-5000 [33,34]
k_5'	Reinitiation rate constant [liter $\cdot$ mol^{-1} $\cdot$ s^{-1}]	10^{-2}-10^{-3} [34]
k_6	Termination rate constant [liter $\cdot$ mol^{-1} $\cdot$ s^{-1}]	10^4
X_{gel}	Monomer conversion at gel point [-]	0.15
K_0	Efficiency reaction trapped radicals with Z	0-1

Table 2.3: Model parameters relating to the polymerization kinetics. *Depends on the intensity of the light source and is varied in the simulations.

2.4.4 Diffusion

Typical values for the diffusion coefficient of monomer in the pure polymer (D_M) are in the order of 10^{-11} to 10^{-12}.[3] For the model a value of 10^{-12} has been used and corrected for temperature by using an activation energy of 30 kJ $\cdot$ mol^{-1}.[26] It is reasonable to assume that during the polymerization of a multifunctional acrylate the diffusion coefficient decreases several orders magnitude. The used values for K_1 and K_2 are respectively 0.21 and 0.[1,26] It is assumed that the contribution of the polymeric binder to the diffusion coefficient of the acrylate monomer in the photopolymer will be similar to effect of polymerized monomer. An overview of all the parameters for the reference model is given in Table 2.4.

Diffusion		
D_M	Monomer diffusion coefficient [$m^2 \cdot s^{-1}$]	10^{-12} [1]
K_1	Constant free volume theory [-]	0.21 [1]
K_2	Constant free volume theory [-]	0 [1]
$E_a(D)$	Activation energy of diffusion [$kJ \cdot mol^{-1}$]	30 [26]

Table 2.4:   Model parameters relating to diffusion.

2.5   Results and Discussion

The in the previous section discussed parameters are inserted into the model. First, the relief formation of a reference photopolymer (without Z) is studied. Compared to the model by Leewis, the above discussed model consists of two simulation cycles (i.e. a patterned illumination and a heating cycle) and contains complex reaction kinetics.[1] It is especially these features which are evaluated. Next, the effect of inhibition and chain transfer on the relief profile formation is studied.

2.5.1 Reference photopolymer

The relief profiles of a reference sample (without Z) after the illumination cycle and after the subsequent heating cycle are given in Figure 2.4. After the illumination cycle the modulation in the photopolymer layer is small and the structure height is minimal (12 nm). During this cycle the polymerization of monomer is initiated, which provides a driving force for diffusion. However, diffusion is limited and the modulation in layer thickness is consequently low. After the heating cycle, the modulation in the photopolymer layer has increased and the aspect ratio of the obtained relief structure is 0.04 (780 nm).
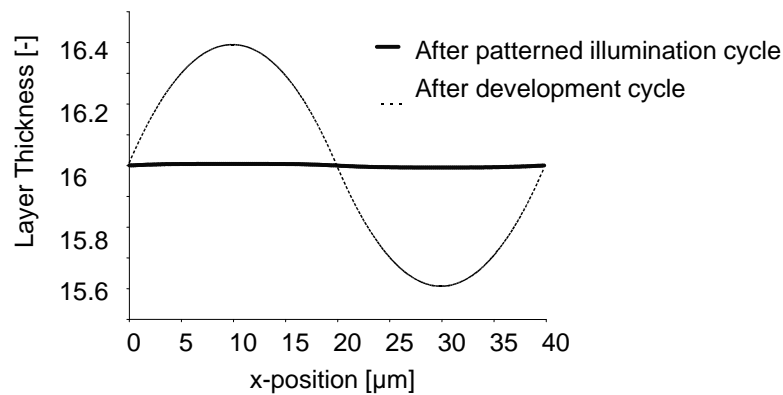

Figure 2.4:   Relief profile after exposure cycle (Exposure dose = 16.5 mJ · cm^{-2}) and after development cycle.

The increase in modulation is partially attributed due to continuation of the polymerization reaction upon the thermal treatment and partially to an increase in diffusion. In the technique of photoembossing this low modulation during the patterned illumination is used to perform multiple exposure steps, which allows creating complex multi-level surface textures.[35]
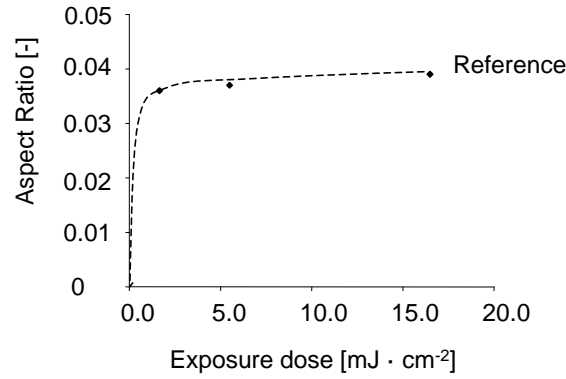

Figure 2.5: Aspect ratio for different exposure doses with a reference photopolymer.

The effect of the exposure dose during the patterned illumination cycle on the aspect ratio of the relief structures is given in Figure 2.5. Only a small exposure dose is required to initiate the polymerization reaction. The conversion of monomer continues until the propagating radicals are terminated via bimolecular or monomolecular termination (trapping). By increasing the monomolecular termination constant (k_4^m) from 0.1 to 1 s^{-1} it is found that trapping of radicals is the main limitation to the aspect ratio of relief structures (Table 2.5). Also the conversion at which monomolecular termination becomes dominant above bimolecular termination (X_{gel}) thus has a large influence. This is demonstrated by reducing X_{gel} from 0.15 to 0.1, which results in a significant reduction in the aspect ratio of the relief structures. On the other hand increasing the bimolecular termination constant (k_4^b) from 10^4 to 10^6 mol · liter · s^{-1} results only in a minimal change in aspect ratio. The results show that the relief development in photoembossing is to a large extent controlled by the termination of propagating radicals. These radicals are required to continue the polymerization reaction of monomer in the exposed areas and provide a driving force for diffusion.

Exposure dose [mJ · cm^{-2}]	Reference	$k_4^b = 10^7$ [mol · liter · s^{-1}]	$k_4^m = 1$ [s^{-1}]	$X_{gel} = 0.1$ [-]
1.6	0.036	0.036	0.036	0.027
5.5	0.037	0.037	0.036	0.028
16.5	0.039	0.039	0.036	0.030

Table 2.5: Aspect ratio of relief structures for varying values of k_4^b, k_4^m and X_{gel}.

2.5.2 Inhibition

The effect of inhibition on the relief development was investigated by adding compound Z into the model and varying the transfer rate constant (k_5). Here it is assumed that trapped radicals (T·) are terminated and cannot react with Z. This is valid since also the transfer of T· to Z would result in radical termination via Z. The aspect ratios of structures (after the development cycle) for different exposure doses are in given Figure 2.6. It can be observed that inhibition reduces the aspect ratio of the relief structures. A fast inhibition reaction, when using a transfer constant (k_5) of 5000 liter · mol^{-1} · s^{-1}, reduces the aspect ratio such that almost no structure is developed. A slow inhibition reaction, when using a k_5 of 50 liter · mol^{-1} · s^{-1}, also results in a reduction of the aspect ratio, but the extent of which depends on the exposure dose. The reduced aspect ratio is caused by a reduction of the propagating radical concentration via the inhibition reaction. These radicals are transferred to compound Z and subsequently terminated via cross-recombination with propagating radicals. As a result the monomer conversion in the illuminated areas is less and thus also the driving force for diffusion. The reduced concentration of propagating radicals can be overcome by increasing the exposure dose. The exposure dose required to overcome inhibition does depend on the rate of the inhibition reaction and the concentration of Z. In principle, the more inhibition occurs, the higher the required exposure dose to overcome the negative effect of radical termination.
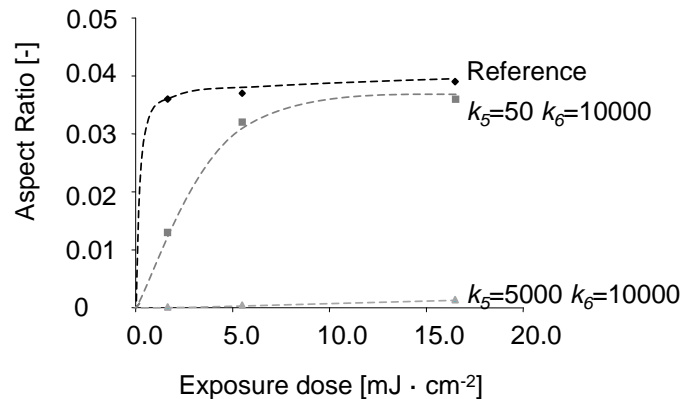

Figure 2.6: Aspect ratio at different exposure doses for a reference sample without Z and in the presence of Z in the case of slow inhibition ($k_5 = 50$ liter · mol^{-1} · s^{-1}) and fast inhibition ($k_5 = 5000$ liter · mol^{-1} · s^{-1})

2.5.3 Chain transfer

The effect of chain transfer was investigated by adding compound Z into the model and varying the transfer rate constant (k_5) and the reinitiation rate constant (k_5'). Initially it is

assumed that trapped radicals (T·) cannot be reinitiated by compound Z. The aspect ratios of structures (after the development cycle) for different exposure doses are in given Figure 2.7a. It can be observed that chain transfer can increase the aspect ratio of the relief structures. The increase in aspect ratio is attributed to an accumulation of stable radicals during the patterned illumination by the transfer of propagating radicals to Z. These stable radicals act as "latent initiators" and can reinitiate the polymerization reaction during the thermal development. This results in a higher conversion of monomer and thus a larger driving force for diffusion. In the absence of Z, the polymerization during the thermal development is limited. In this case, the radical concentration reduces since there is no initiation via the photodecomposition of the initiator. Especially after the gel point, the propagating radical concentration is rapidly reduced by trapping.

Besides affecting the total monomer conversion, the chain transfer reaction also reduces the degree of polymerization in the illumination step. As can be deduced from equation 2.36, this affects the diffusion during the thermal development. In this step the diffusion coefficient is at its highest. When the polymer content at the onset of the thermal development is low, the diffusion of monomer is less restricted. Also this effect will attribute to an increase in aspect ratio by the chain transfer reaction.
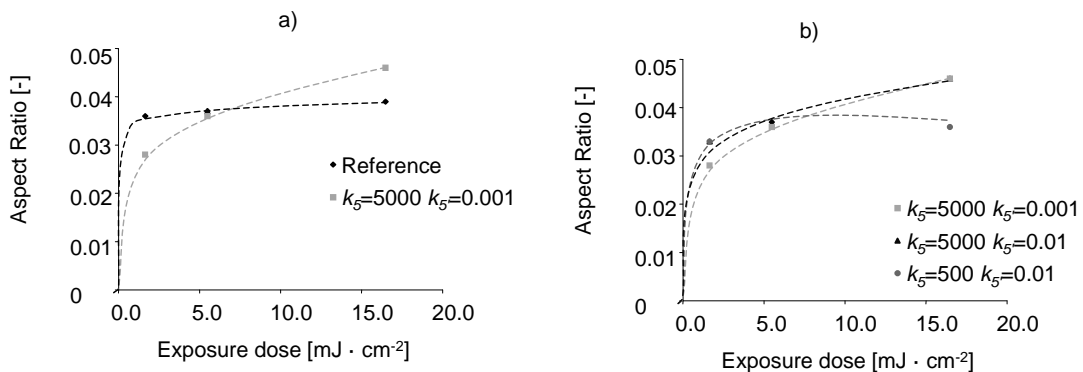

Figure 2.7: Aspect ratio at different exposure doses for a) a reference sample without Z and in the presence of Z and b) for different values of k_5 and $k_{5'}$.

Whether an increase in aspect ratio is obtained depends on a balance between the exposure dose, the rate of transfer and reinitiation. It can be observed from Figure 2.7b that low values for k_5 and/or a high value for $k_{5'}$ are preferred when using a low exposure dose. The exposure dose sets the initial concentration of propagating radicals. These species are the prime radicals for converting monomer into polymer and providing a driving force for diffusion. The values of k_5 and $k_{5'}$ determine the amount of propagating radicals which are transferred to stabilized species. The stabilized species are a secondary type of reactive species for the polymerization of monomer. As

concluded before, these species are essential for continuation of the polymerization reaction in the heating step, especially when propagating radicals are becoming trapped into the crosslinked network. When the exposure dose is low, it is not possible to create a crosslinked network. Hence there is less or even no benefit from the accumulation of stabilized species. A low value for k_5 and/or a high value $k_{5'}$ are thus preferred. At a high exposure dose, the opposite effect is observed. Here, the effect of the stabilized species becomes more pronounced since a dense network is quickly formed.

The results from Figure 2.7 were obtained without taking into account that it is possible that trapped radicals can be reinitiated by Z. When investigating this effect, it is observed that the reactivation of trapped radicals increased the aspect ratio relief structures significantly (Figure 2.8). Especially at higher exposure doses the structure development clearly benefits. This observation is explained by the fact that, as previously mentioned, stabilized radicals act as latent initiator. The obtained aspect ratio depends on the value of K_0. This parameter determines the amount of radicals which are terminated by trapping. When $K_0=1$ it can be observed that there is a maximum aspect ratio at a certain exposure dose. In the absence of radical trapping a densely crosslinked network is formed by the continuous reinitiation. This hinders diffusion into these areas and limits the aspect ratio of the relief structures.
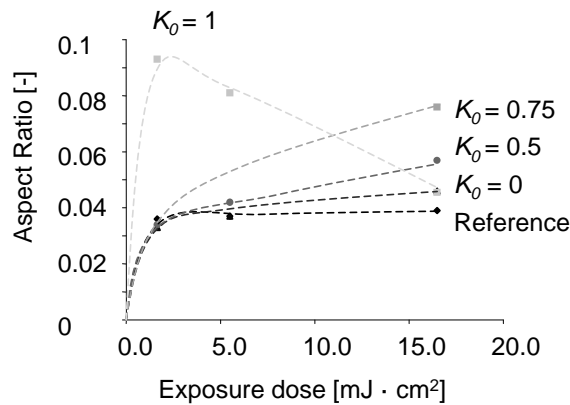

Figure 2.8:   Aspect ratio at different exposure doses for a reference sample without chain transfer compound and with a chain transfer compound ($k_5 = 5000$ mol $\cdot$ liter^{-1} $\cdot$ s^{-1} and $k_{5'} =$ 0.01 mol $\cdot$ liter^{-1} $\cdot$ s^{-1}) for different values of K_0.

2.6   Conclusion

The relief development in photoembossing was simulated by using a numerical model. The model is based on the diffusion of monomer due to a change in chemical potential by the polymerization reaction in the illuminated areas. To calculate the chemical

potential, the model uses the Flory-Huggins theory of mixing polymer and monomers. Also the contribution of the network elasticity and the surface tension are taken into account. The polymerization kinetics were described such that it incorporated the presence of a kinetic interfering compound (Z). Z is capable of interfering with polymerization reaction kinetics by accepting propagating radicals and subsequently terminating (inhibition) or reinitiating (chain transfer) the polymerization reaction. The model showed that the aspect ratio of photoembossed structures can be increased by chain transfer inducing compound.

An inhibition reaction was observed to have a negative effect on the aspect ratio. The conversion of monomer depends on the concentration of propagating radicals. A reduction in the concentration thus reduces the driving force for diffusion. The inhibiting effect of Z could be overcome by increasing the exposure dose and increasing the initiator concentration.

A chain transfer reaction was observed to have a positive effect on the aspect ratio. The transfer/reinitiation reaction resulted in the accumulation of stabilized radicals in the illuminated areas. These radicals act as "latent initiators", which can reinitiate the polymerization reaction during the heating step. The transfer reaction also reduces the monomer conversion in the illuminated areas. The low polymer content at the onset of the thermal development increases the diffusion of monomer.

The model is based on simplified assumptions and it is well possible that in practice also other effects contribute to the relief development. In addition the extent to which K_0 (fraction of trapped radicals which can be transferred to Z) affects the polymerization reaction is not known from literature. To confirm the findings of the model it is thus necessary to experimentally investigate the effect of compound Z on the relief development in photoembossing.

2.7   References

[1]   C. M. Leewis, *Formation of Mesoscopic Polymer Structures for Optical Devices*, Technische Universiteit Eindhoven, Eindhoven, The Netherlands, **2002**, Chapter 4.

[2]   C. Kjellander, *Multilayer optical switches by photopolymerization-induced phase separation*, Technische Universiteit Eindhoven, Eindhoven, The Netherlands, **2006**, Chapter 2.

[3]   R. Penterman, *Photo-enforced stratification of liquid crystal / monomer mixtures*, Technische Universiteit Eindhoven, Eindhoven, The Netherlands, **2005**, Chapter 4.

[4]   A. Fimia, N. López, F. Mateos, R. Sastre, J. Pineda, F. Amat-Guerri, *J. Modern Optics*, **1993**, *40*, 699.

[5] A. K. O'Brien, C. N. Bowman, *Macromol. Theory Simul.* **2006**, *15*, 176.

[6] R. Sato, T. Kurihara, M. Takeishi, *Polymer International* **1998**, *47*, 159.

[7] G. Odian, *Principles of Polymeriztion*, 4th edition, Wiley Interscience, New Jersey, USA, **2004,** (255-264).

[8] G. Moad, D. H. Solomon, *The Chemistry of Free Radical Polymerization*, Elsevier Science Ltd, Great Britain, **1995**, (260-266).

[9] J. Brandrup, E. H. Immergut, *Polymer Handbook*, 4th edition, Wiley Interscience, New York, **1999** (II-53 –II-55).

[10] F. Tudős, T. Foldes-Berezsnich, *Prog. Polym. Sci.* **1989**, *14*, 717.

[11] C. Sánchez, B.-J. de Gans, D. Kozodaev, D. Wouters, A. Alexeev, M. J. Escutti, C. Van Heesch, T. Bel, U. S. Schubert , C. W. M. Bastiaansen, D. J. Broer, *Adv. Mater* **2005**, *17*, 2567.

[12] N. Adams, B-J. De Gans, D. Kozodaev, C. Sànchez, C. W. M. Bastiaansen, D. J. Broer, U. S. Schubert, *J. comb. Chem.* **2006**, *8*, 184.

[13] B.J. De Gans, C. Sanchez, D. Kozodaev, D. Wouters, A. Alexeev, M. Escuti, C. Bastiaansen, D. Broer, U. Schubert, *J. Comb. Chem.* **2006**, *8*, 228.

[14] Flory, P.J., *J. Chem. Phys.* **1941**, *9*, 660; Huggins, M.L., *J. Chem. Phys.*, **1941,** 9, 440.

[15] H. M. J. Boots, J. G. Kloosterboer, C. Serbutoviez, F. J. Touwslager, *Macromol.* **1996**, *29*, 7683.

[16] J. G. Kloosterboer, G. M. M. van de Hei, H. M. J. Boots, *J. Polym. Commun.* **1984**, *25*, 354.

[17] L. B. Freund, *Int. J. Solids Structures* **1995**, *32*, 911.

[18] H. Fischer, *Chem. Rev.* **2001,** *101,* 3581.

[19] C. Oliva, I. R. Bellobono, R. Morelli, *Phys. Chem. Chem. Phys.*, **1999**, *1*, 215.

[20] E. Selli, C. Oliva, *Macromol. Chem. Phys.* **1995**, *196*, 4129.

[21] C. Decker, K. Moussa, *J. Polym. Sci. Polym. Chem. Ed* **1987**, *25*, 739.

[22] J. Pavlinec, N. Moszner, J. Plaček, *Macromol. Chem. Phys.* **2001**, *202*, 2387.

[23] E. L. Madruga, *Prog. Polym. Sci.* **2002**, *27*, 1879.

[24] H. Fujita, A. Kishimoto, *J. Chem. Phys.* **1961**, *34*, 393.

[25] V. L. Colvin, R. G. Larson, A. L. Harris, M. L. Schilling, *J. Appl. Phys.* **1997**, *81*, 5913.

[26] J. Xia, C.H. Wang, *J. Pol. Sci. Part B. Pol. Phys.* **1995**, *33*, 899.

[27] Y. S. Choi, I. J. Chung, *Macromol. Research.* **2003**, *11*, 425.

[28] www.sartomer.com

[29] C. Decker, *Macromol. Rapid Commun.* **2003**, *23*, 1067.

[30] K. Dušek, M. Dušková-Smrčková, *Prog. Polym. Sci.* **2000**, *25*, 1215.

[31] E. Andrzejewska, *Prog. Polym. Sci.* **2001**, *26*, 605.

[32]   Y. G. Medvedevskikh, A. R. Kytsya, L. I. Bazylyak, A. M. Bratus, A. A. Turovski, G. E. Zaikov, *J. Appl. Polym. Sci.* **2003**, *91*, 2376.

[33]   M. Simonyi, F. Tudős, S. Holly, J. Pospišil, *Eur. Polym. J.* **1967**, *3*, 559.

[34]   W. A. Braunecker, K. Matyjaszewski, *Prog. Polym. Sci. 32* **2007**, *32*, 93.

[35]   C. Witz, C. Sanchez, C. W. M. Bastiaansen, D. J. Broer, *Handbook of Polymer Reaction Engineering*, Vol. 2 (Eds. T. Meyer, J. Keurentjes), Wiley-VCH, Weinheim, Germany **2005**, Ch.19.

Chapter 3

Inhibition / retardation

It is the objective of this chapter to experimentally investigate the effect of compounds which terminate propagating radicals on the relief formation in photoembossing. Depending on their efficiency, these compounds are typically known as inhibitors (efficient) or retarders (less efficient). It is demonstrated by the addition of tert-butyl hydroquinone (TBHQ) to the photopolymer that inhibition does not improve the aspect ratio of a relief structure. Inhibition of the polymerization reaction occurs when a TBHQ containing photopolymer is processed under an oxygen containing environment (e.g. air). The polymerization is halted until the TBHQ is consumed, after which the reaction proceeds as normal. The performance of the photopolymer, expressed in the maximum obtainable aspect ratio of the structures formed, is not improved, but the relief formation is merely delayed. These results support the model in Chapter 2. A different effect is observed when the photopolymer is processed under an inert nitrogen atmosphere. Under these conditions TBHQ acts as a retarder and the aspect ratio of the relief structures is increased by up to a factor 7. This is somewhat surprising since it was concluded in Chapter 2 that radical termination cannot improve the aspect ratio. By investigating the type and stability of the radicals and the kinetic influence it is believed that the increase can be attributed to chain transfer reactions. The chain transfer reactions improve the mobility of both the radicals and monomeric species in the exposed areas and thus enhance relief development. Although the addition of TBHQ results in some chain transfer, these molecules are not designed for this type of reaction. When comparing the performance of TBHQ to other hydroquinone derivatives it is found that electron withdrawing groups such as fluor, reduce the exposure dose required for obtaining a certain aspect ratio. Most likely the presence of electron withdrawing groups reduces radical termination due to a slow transfer of propagating radicals to a fluoro-hydroquinone.

3.1 Introduction

It was shown in the Chapter 2 that the performance of a photopolymer depends to a large extent on the reaction kinetics.[1-5] Molecules that interfere with the reaction kinetics can have a significant influence on the performance of a photopolymer. Upon the addition of a compound (Z) that can participate in the radical reaction, the propagating radical can be transferred to Z via a transfer (or addition) reaction to form an intermediate radical RZ·, or Z·.[6] Depending on the stability of the intermediate radical and its environment, RZ· or Z· can reinitiate polymerization or terminate. In this chapter it is experimentally investigated what the effect of molecules that are known to favor termination of radical species is on the performance of the photopolymer. These molecules are typically known as inhibitors. In the case of a slow transfer reaction, these molecules are also known as retarders. The difference between inhibition and retardation is a matter of the degree of slowing down or hindering the reaction and often there is no sharp distinction. In principle inhibitors stop every radical, and completely halt the polymerization until they are consumed. Hereafter, polymerization continues as normal. Retarders are less efficient and stop only a portion of the propagating radicals. Hence, polymerization occurs, but at a reduced rate (Figure 3.1). Therefore the transition between inhibition and retardation is often somewhat vague and depends on experimental parameters, such as the type of monomers or processing conditions.
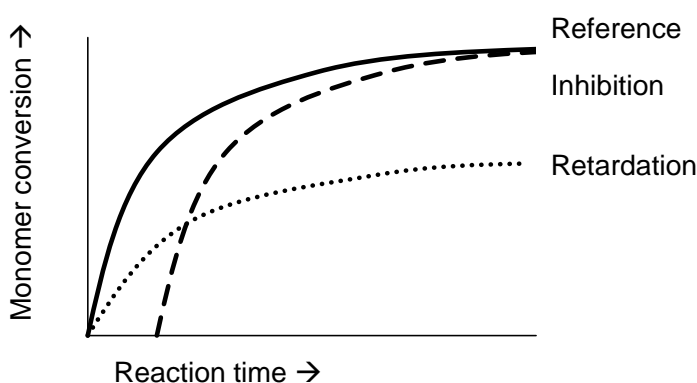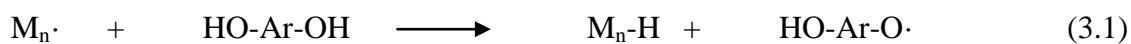

Figure 3.1: Schematic representation of inhibition and retardation.

3.1.1 Reactions of hydroquinone

A well known inhibitor/retarder is hydroquinone. This molecule is often used to stabilize monomer during storage or processing and prevent premature polymerization reactions. In general the transfer from a propagating radical to hydroquinone involves a two step procedure. First, a hydrogen atom is transferred to a propagating radical. Second, a radical is transferred to the hydroquinone: [7,8]

$$M_n\cdot \quad + \quad HO\text{-}Ar\text{-}OH \quad \longrightarrow \quad M_n\text{-}H \quad + \quad HO\text{-}Ar\text{-}O\cdot \qquad (3.1)$$

$$HO\text{-}Ar\text{-}O\cdot \quad + \quad M_n\cdot \quad \longrightarrow \quad \text{p-benzoquinone} \quad + \quad M_n\text{-}H \qquad (3.2)$$

Also, the hydrogen transfer occurs in a two step procedure. First, there is a transfer of a proton to the radical and then there is a transfer of the electron. Due to the acidic nature of a phenolic compound it is expected that the latter reaction will be rate determining. Substituents on the phenyl group that influence the stability of the phenolate ion will therefore have a significant influence on the overall rate of this reaction.[9] Electron withdrawing groups, such as halogens, typically stabilize the phenolate ion and thus reduce the rate of transfer. On the other hand electron donating groups, such as methyl, destabilize the phenolate ion and therefore increase the rate of transfer. Due to the presence of two hydroxide groups, hydroquinone is able to react with at least two propagating radicals. It can be expected that the amount of radicals terminated by hydroquinone is much larger since the reaction product, p-benzoquinone, is also known to be a very effective inhibitor. The transfer reactions for p-benzoquinone are quite complex. However, two major reaction products can be obtained. Depending if the reaction occurs at the C or O atom, a quinone or respectively ether may be formed (Figure 3.2).
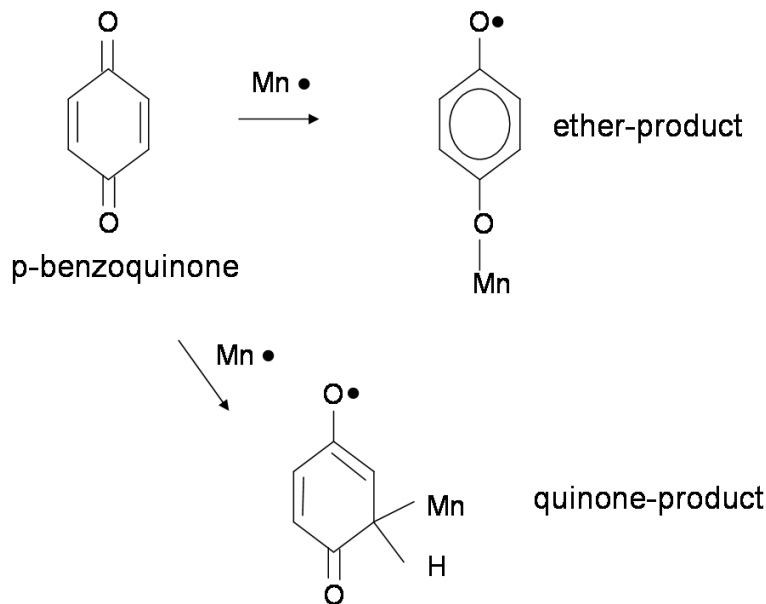

Figure 3.2: Proposed inhibition/retardation pathways of p-benzoquinone.[7]

In the presence of oxygen the radical terminating effect of hydroquinone is known to be increased dramatically.[10,11] This phenomenon is not just attributed to radical

terminating effect of oxygen itself, which reacts with propagating radicals to form relatively un-reactive peroxide radicals.

$$M_n \cdot \quad + \quad O_2 \quad \longrightarrow \quad M_n\text{-O-O} \cdot \qquad\qquad (3.3)$$
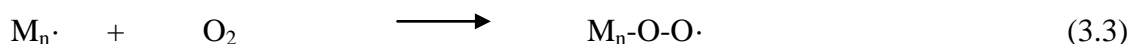
It is believed that in the presence of hydroquinone the increased termination is a consequence of the transfer reaction (4) towards peroxy radicals being faster than towards alkyl radicals.

$$M_n\text{-O-O} \cdot \quad + \quad HO\text{-Ar-OH} \quad \longrightarrow \quad M_n\text{-O-O-H} \quad + \quad ArO \cdot \quad (3.4)$$

The effectivity of a hydroquinone may be further enhanced by the oxidation of the hydroquinone into p-benzoquinone.[12]

In this chapter it is investigated if the addition of *tert*-butyl hydroquinone (TBHQ) improves the performance of a photopolymer. The effect of a hydroquinone depends highly on the environment and processing condition.[13] Therefore, it is first investigated via Electron Spin Resonance (ESR) spectroscopy which radical species are dominantly formed in a reacting photopolymer the presence or absence of a hydroquinone(paragraph 3.3.1). Also the stability of these radicals was investigated. Since oxygen is known to influence the activity of a hydroquinone, the measurements are performed under both inert and oxygen containing conditions. The effect on the polymerization kinetics of the multifunctional monomer is investigated by gel content measurements and attenuated total reflection infra-red (ATR-IR) spectroscopy (paragraph 3.3.2). The performance of the photopolymer is evaluated by measuring the aspect ratio of the developed relief structures (paragraph 3.3.3) for different periodicities (paragraph 3.3.4). In paragraph (paragraph 3.3.5) the effect of *t*-butyl hydroquinone (TBHQ) is compared to other hydroquinones to determine which substituents to the phenyl group give the best performance. Finally the experimental results are compared to the model (paragraph 3.3.6).

3.2 Experimental section

3.2.1 Materials

For the photopolymer polybenzylmethacrylate (M_w 70 kg mol^{-1}; Scientific Polymer Products) was used as a polymeric binder, dipentaerythritol penta/hexa-acrylate (Sigma Aldrich) as a multifunctional monomer and Irgacure 819 (CIBA, Specialty Chemicals) as a photoinitiator. As a solvent a 50/50 wt.-% mixture of ethoxypropylacetate (Avocado Research Chemicals) and propyleneglycol-methyletheracetate (Aldrich) was

used. To prepare the photopolymer solutions the multifunctional monomer and the solvent were mixed in a weight ratio of 1:2 and the 500 ppm of 4-methoxyphenol present in the monomer was removed by using a silica packed inhibitor removing column (Aldrich). The monomer/solvent mixture was mixed with the polymer and photoinitiator in a weight ratio of respectively 30:10:1. The inhibitors were added to this solution in different weight ratio. As an inhibitor either tert-butyl hydroquinone (TBHQ), tertra-fluorohydroquinone (TFHQ) or trimethyl hydroquinone (TMHQ) was used (see Figure 3.3). All inhibitors were purchased from Sigma Aldrich.
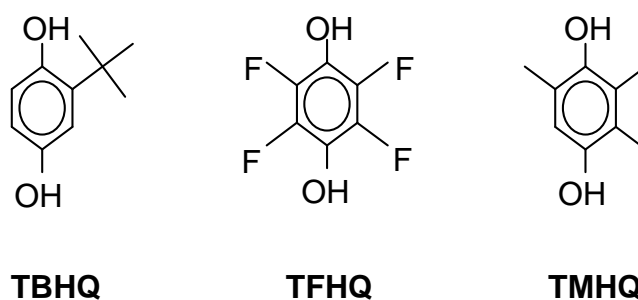

Figure 3.3:   Molecular structures of the investigated hydroquinone derivatives.

3.2.2 Sample preparation

The D263 glass substrates (5 × 5 cm) were cleaned by rubbing with a sodium hydroxide solution, flushed with demineralized water, rubbed with acetone, rubbed and flushed with ethanol and finally dried with nitrogen. Directly after cleaning the photopolymer solution was spincoated on top of the glass substrates at 800 rpm with a Karl Suss RC8 spincoater. To remove the solvent the samples were dried at 80 °C for 20 minutes after which they were cooled to room temperature, resulting in dry films with a thickness of approximately 16 μm. The samples were exposed with an Oriel arc lamp housing (66902) fitted with USHIO (UXM-502) deep UV lamp exposing system having an intensity of 5 mW · cm^{-2} (λ = 320-390 nm). During exposure a rectangular lithographic mask (28 mm × 31 mm) that consists of five parallel sectors (4 mm × 31 mm) was placed onto the sample. Each sector has a line grating with a periodicity of 40, 30, 20, 15 and 10 μm, respectively (dark and transparent areas of the same size). Unless stated otherwise only the results of the 40 μm periodicity are given. On top and perpendicular to the line mask a lithographic optical density (OD) mask was placed in order to change the intensity of the light that reaches the sample. The OD mask also consists of seven parallel sectors, absorbing 10, 49, 79, 89, 95, 98 and 99% of the light, respectively. After exposure the masks were removed and the sample was gradually heated to a temperature of 110 °C and kept for 10 minutes at this temperature. Finally, a flood exposure was applied for 5 minutes at a temperature of 110 °C. To study the effect of

environmental oxygen during exposure, development and flood exposure, the samples were placed under a protective atmosphere by constant nitrogen blanketing using a custom build hot plate. This hot plate was built into an aluminum box that could be flushed with nitrogen and contained a quartz glass window through which the samples could be exposed to UV light. In case the experiments were performed under ambient conditions, the box was flushed with air. To vary the oxygen content of the environment, the box was flushed with a mixture of pure nitrogen and pure oxygen. The flows of the oxygen and nitrogen stream were monitored and adjusted to obtain a mixture with desired oxygen content.

3.2.3 Characterization

Confocal microscopy: The height of the photoembossed relief structures was investigated using a confocal microscope (Sensofar, PLμ2300) with a 50x objective.

Electron spin resonance (ESR) spectroscopy: The ESR spectra were measured with a Bruker ESP300 spectrometer. A dry photopolymer layer was prepared on cleaned D263 glass substrates as described above. The films were removed with a razor blade and positioned in a quartz glass tube. During measurements the tubes were placed under vacuum and exposed to laser light source (λ = 351 nm, I = 10 mW $\cdot$ cm^{-2}). The obtained results were fitted using WINEPR simulation software.

Attenuated Total Reflection Infra-red (ATR-IR) spectroscopy: The IR measurements were performed on an Excalibur ATR-IR (FTS 3000 MX), which was equipped with a Specac Golden Gate diamond ATR. An Oriel light source housing (69054) which was equipped with a USHIO deep UV lamp (USH-200DP) was used for exposure of the sample. The samples were applied from solution and dried for 10 minutes at 80 °C after which they were cooled to 30 °C before the measurement was started. A continuous UV exposure (λ = 365 nm, I = 2.5 mW $\cdot$ cm^{-2}) was initiated 10 seconds after starting the experiment. The acrylate conversion was determined by measuring the absorbance at 1635 cm^{-1} (C=C stretching) and 1407 cm^{-1} (C-H bending). Only the results obtained at 1635 cm^{-1} are shown in the figures.

Gel content: A dry photopolymer layer was prepared on cleaned D263 glass substrates as described above. The photopolymer layer was flood exposed using an Oriel arc lamp housing (66902) fitted with USHIO deep UV lamp (UXM-502) exposing system. After exposure, the photopolymer layer was removed from the substrate with a razor blade and the soluble components were extracted by using a 50/50 mixture of ethoxypropylacetate (Avocado Research Chemicals) and propyleneglycol-

methyletheracetate (Aldrich) in which the photopolymer dissolved by stirring for 4 hours and soaking overnight. The mixture was filtered and the filtrate was dried in a vacuum oven at 80º for 1 hour. The gel content was determined by the difference in sample weight before and after dissolving the soluble components. Negative values in the absence of a gel are most likely caused by moisture in the filter before use. It is possible that at very high gel contents some physically trapped monomer is not extracted.

Scanning Electron Miscopy (SEM): SEM images were taken with an XL30 ESEM from Philips. Photoembossed samples prepared and broken parallel to the relief. The samples were coated with a thin gold layer by vapor deposition. The images were taken under angle of 30º from horizontal.

3.3   Results and discussion

3.3.1 Type and stability of radical species

The inhibitory effect of hydroquinones depends on the transfer of propagating radicals to phenolic radicals and the subsequent termination of these species via cross-recombination. Since the effect of hydroquinones depends highly on the environment and processing condition it was first investigated by ESR which radical species are dominant upon addition of TBHQ to the photopolymer mixture.[7,8,13] Measurements (Figure 3.4a) show that upon continuous exposure of a reference sample, free of hydroquinone, under an inert atmosphere the ESR signal consisted of a complex line pattern. This suggests the presence of multiple radicals or radicals in different conformations. The main contribution, however, is ascribed to a mid-chain acrylate radical, exhibiting hyperfine coupling to two of the four methylene protons, giving rise to a three-line ESR spectrum. This mid-chain radical species is the dominant species found for most multi-functional acrylates.[14] Although being highly reactive these radicals were found to have an extreme longlivity (Figure 3.4b). Even 5 minutes after the UV exposure was stopped, the ESR signal did not show any relevant change in intensity. This extremely longlivity is caused by the highly crosslinked polymer network formed by the polymerization of the multifunctional monomers. The network can trap radicals and prevents any further reaction at room temperature.[15-17] This is supported by measurements of the gel content of exposed samples (Figure 3.5). The measurements show that even after applying a very low exposure dose of 10 mJ $\cdot$ cm^{-2} to the photopolymer almost 50% of the monomer has been converted into an insoluble network.

The ESR signal (Figure 3.4c) for a photopolymer containing 7wt.-% of TBHQ exposed under an inert atmosphere was found to be clearly different. The single line spectrum fits the expected signature of a phenol radical under conditions of reduced spectral resolution as present in a solid polymer film.[18] These radicals were also found to be exceptionally stable (Figure 3.4d). This indicates that radical termination is minimal and that also these radicals were at least partially stabilized by trapping. Gel content measurements support this and show that in the presence of a hydroquinone an insoluble network can be formed upon the exposure of a photopolymer; however, a higher exposure dose is required. The intensity of the ESR spectrum, though relatively stable, decreased faster than the spectrum of the mid-chain radicals measured in the absence of a hydroquinone. The reduced gel content at equal exposure dose and higher mobility explains the faster reduction of the ESR signal of the phenoxy radicals compared to the mid-main radicals.
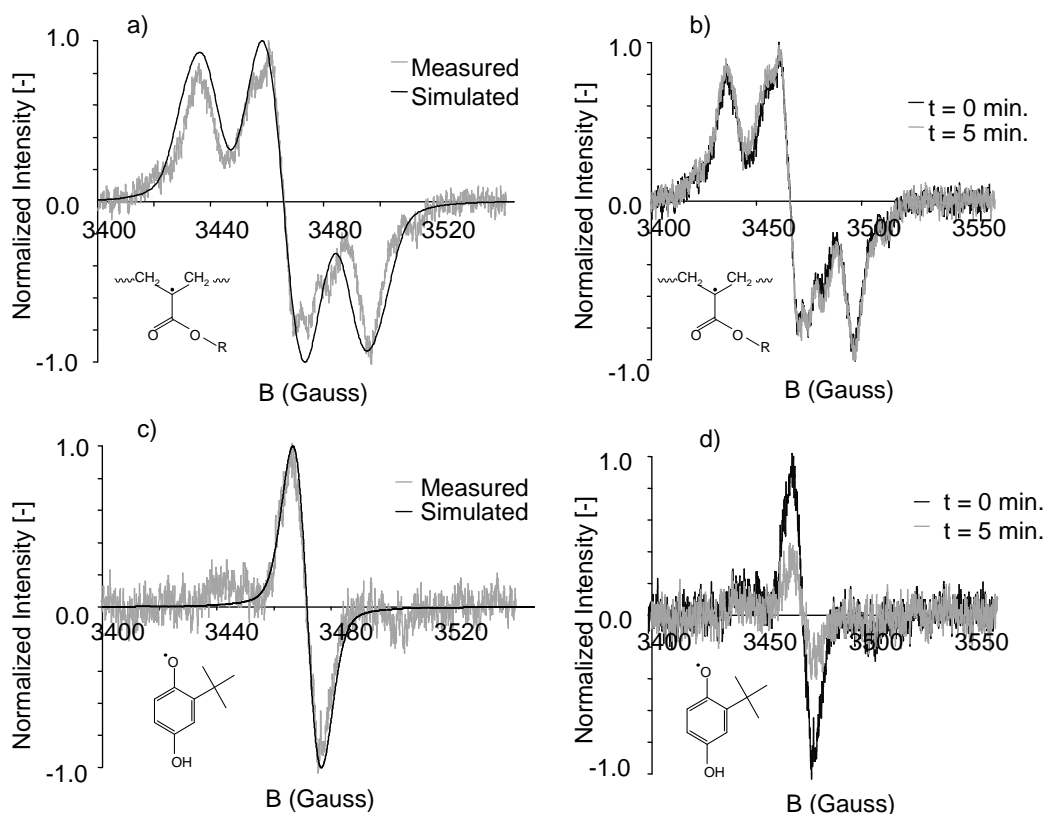

Figure 3.4:   ESR spectra of a reference sample (a) upon continuous exposure and (b) after exposure. ESR spectra of a sample containing 7 wt.-% TBHQ (c) upon continuous exposure and (d) after exposure.

When samples containing 7 wt.-% of TBHQ were exposed under an oxygen containing atmosphere (air), no ESR signal was found (data not shown). It is known that in the presence of oxygen, which itself is a strong inhibitor/retarder, the effect of a

hydroquinone is increased dramatically. This is a consequence of the efficient transfer reaction between oxygen and the free radicals. The effectiveness of the hydroquinone is further enhanced by the oxidative formation of quinone that is also known to be a strong inhibitor. The presence of radicals in samples measured under inert conditions was shown to depend on trapping. This suggests that the absence of an ESR signal for hydroquinone containing samples is caused by termination of these radical before trapping due the formation of crosslinked network could occur.
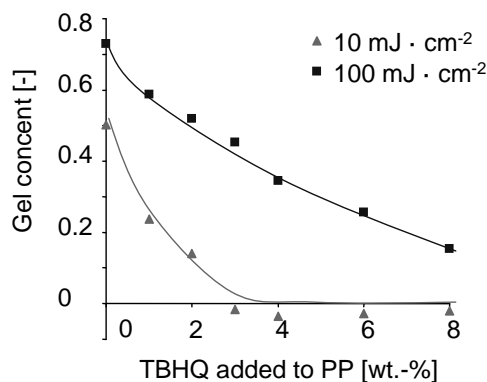

Figure 3.5: Gel content after UV exposure of a photopolymer layer containing different concentrations of TBHQ.

3.3.2 Polymerization kinetics

The ESR measurements have shown the presence of stable phenoxy radicals upon the addition of TBHQ to the photopolymer. Although this proves that a transfer of propagating radicals to the hydroquinone occurs, it does not show the influence of this transfer reaction on the polymerization kinetics. Therefore real time ATR-IR measurements were performed. The results (Figure 3.6) show that under inert conditions the addition of TBHQ reduces the rate of acrylate conversion. The extent of this reduction can be controlled by the TBHQ content. This behavior is classified as retardation and occurs due to a relatively slow transfer of propagating radicals to stabilized species. From this result it can be concluded that the reduced gel-content, observed in Figure 3.5, is at least partially caused by a reduction in the rate of polymerization. The time it takes to obtain a certain conversion is simply delayed. It would also be possible to obtain a reduction in gel content due to chain transfer effects. This effect is however expected to small, at least at room temperature, in the case of inhibitors/retarders.
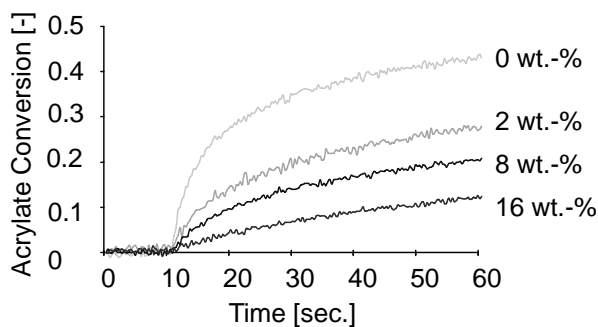
Figure 3.6: Acrylate conversion under inert conditions upon continuous UV exposure (initiated after 10 seconds) for photopolymers containing different concentration of TBHQ.

In the presence of an oxygen containing atmosphere (air) the polymerization kinetics were found (Figure 3.7) to be different for both the reference and hydroquinone containing samples. The rate of polymerization in a reference sample was reduced by the presence of oxygen. The observed retardation by the presence of TBHQ is similar to polymerization under inert conditions This is quite surprising since oxygen is usually a far more powerful inhibitor/retarder than TBHQ. However, as stated before, the effect of all inhibitors/retarders depends on the system in which they are used. In addition the inhibiting effect of environmental oxygen is controlled by the diffusion of oxygen into the photopolymer. Therefore the intensity of the UV light source during the exposure has a significant effect as well as it affects the ratio between free radical formed and the actual local oxygen concentration.

Polymerization of a hydroquinone containing sample during exposure in air was characterized by an induction period at the onset of the exposure. During this period no polymerization occurs. The length of the induction period was found to depend on the concentration of hydroquinone present in the photopolymer and oxygen content of the environment. This observation concurs with the absence of a signal in the ESR measurements reported in paragraph 3.3.1. This was explained by the synergetic effect between oxygen and the hydroquinone. Due to this, the radical formation and the resulting polymerization reaction are halted until one of the compounds is consumed. When processing under air the limiting compound is hydroquinone. It can thus be concluded that under these conditions TBHQ behaves as an inhibitor in the photopolymer.
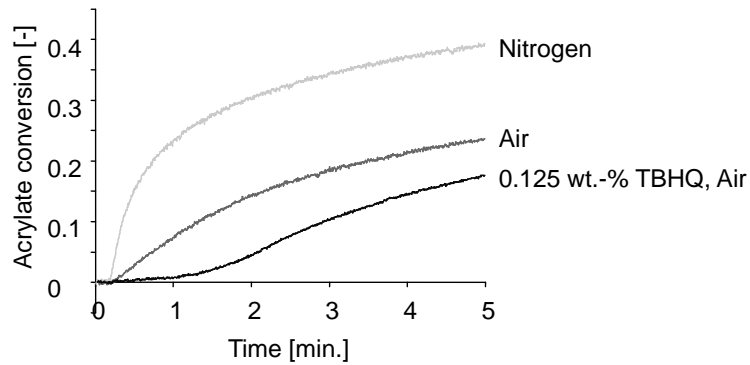
Figure 3.7: Acrylate conversion under different atmospheric conditions upon continuous UV exposure (initiated after 10 seconds) of a photopolymer under different atmospheric conditions.

3.3.3 Aspect ratio

The ESR and IR measurements have shown that depending on atmospheric conditions different characteristics (retardation and inhibition) can be observed in a photopolymer. To investigate the effect of retardation on the performance of a photopolymer, samples containing different concentration of TBHQ were photoembossed under an inert atmosphere and the resulting relief structures were investigated by confocal microscopy. The results are given in Figure 3.8. First of all, it can be observed that the addition of TBHQ results in a significantly higher aspect ratio. SEM images of cross-sectional profiles of some of the relief structures were taken to emphasize the extent of the observed increase in aspect ratio (Figure 3.9). The increase is mainly ascribed to the reactivation of mid-chain radicals by transfer to phenoxy radicals as observed by the ESR measurements. The mid-chain species are, although intrinsically still reactive, trapped within a crosslinked network. The crosslinked network not only makes the radicals inaccessible, but also restricts the diffusion of monomer. The phenoxy radicals, although less reactive at room temperature, enable the reactive species to escape from the traps. In addition they are confined within a less dense network due to retardation of the polymerization reaction. Continuation of the polymerization as well as the diffusional mobility of the reactive species during thermal development is therefore enhanced. Other effects that might affect the diffusion of monomer positively during the heating step, but are considered to be less dominant, are the reduction in kinetic chain length due to the chain transfer function of the TBHQ thus postponing gel point. Also, especially at high concentrations, the TBHQ may act to some extent as a plasticizer, thus reducing the modulus and glass transition temperature and enhancing diffusional monomer mobility. Moreover, the hydroquinone may prevent unwanted early polymerization in the unexposed areas during the development step.
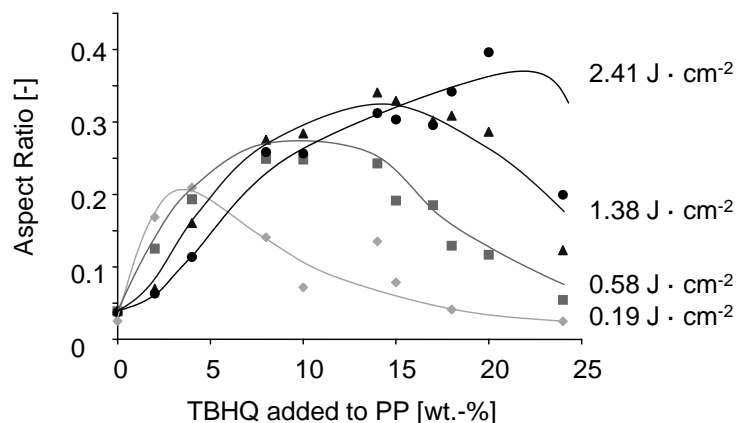
Figure 3.8:   Aspect ratio of photoembossed relief structures (40 μm periodicity) of samples containing different concentration of (a) TBHQ compared to (b) TMHQ and TFHQ.

It is also observed in Figure 3.8 that at too high TBHQ concentrations the aspect ratio decreases again. It was observed in Figure 3.6 that at these concentrations a strong retarding and nearly inhibiting effect occurs, which leads to termination of the polymerization reaction. Since the conversion of monomer is one of the main contributions to a difference in chemical potential between the exposed and non-exposed areas this thus leads to a reduction in the aspect ratio of the relief structures. The effect can be postponed by choosing a higher exposure dose, increasing the concentration of the initially created reactive species.
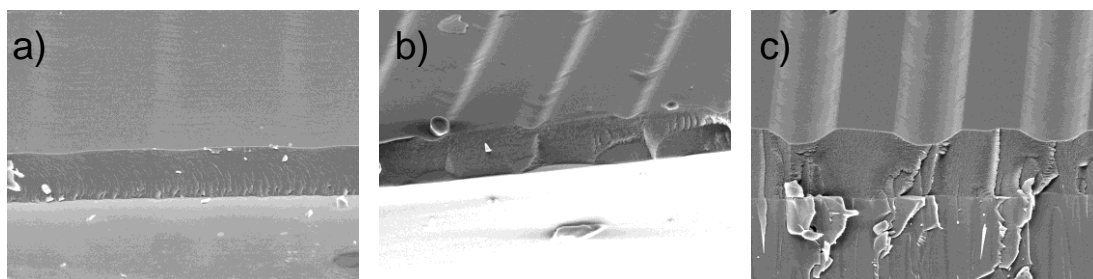

Figure 3.9:   SEM pictures of photoembossed structures from samples with b) 0 wt.-%, c) 4 wt.-%, d) 20 wt.-% of TBHQ added to the photopolymer and exposed to 2.4 J · cm^{-2}.

In the previous paragraphs it was concluded that the retardation effect observed for TBHQ, when processed under inert conditions, becomes inhibition once the processing was performed in the presence of oxygen. Before investigating the effect of inhibition on the performance of a photopolymer, we first have a look at the effect of oxygen itself.
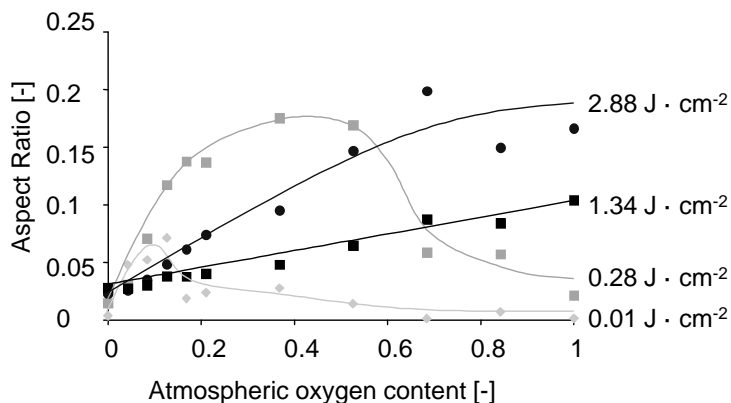
Figure 3.10: Aspect ratio of photoembossed relief structures (40 μm periodicity) of reference samples processed under a variable oxygen containing atmosphere (pressure 1 atm.).

Reference samples, containing no TBHQ, were photoembossed under atmospheres containing different ratios of oxygen/nitrogen. The results are given in Figure 3.10. It can be observed that oxygen increases the aspect ratio of photoembossed relief structures. Similar to the conclusion from Figure 3.10, the increase is mainly ascribed to the transfer of mid-chain radicals to more easily accessible species, which are in this case peroxide radicals. When comparing the results obtained with Figure 3.10, it is observed that the maximum obtained aspect ratio in the presence of oxygen is significantly lower. A possible explanation for this observation might be that the transfer of alkyl radicals to oxygen is in general faster than to hydroquinones.[12] This enhances the termination of radical species. In addition, unlike TBHQ, oxygen is not distributed homogeneously within the photopolymer layer. Instead it diffuses continuously from its surrounding into the photopolymer while it is reacting, thus most likely providing a gradient over the film thickness depending on its diffusion rate in relation to its consumption rate. As a result the extent of the reaction between the alkyl radicals and oxygen depend on the light intensity upon exposure. It is thus possible that a different intensity of the light source can result in higher/lower aspect ratios.

To investigate the effect of inhibition on the performance of a photopolymer, TBHQ containing samples were processed under air. The results are given in Figure 3.11. It is observed that the addition of TBHQ does not result in an increase in aspect ratio. Independently of its concentration the same maximum aspect ratio of 0.15 is obtained, however the required exposure dose differs. This effect is attributed to a macroscopic manifestation of the polymerization induction period observed in the ATR-IR measurements (Figure 3.7). During the induction period the atmospheric oxygen reacts with propagating radicals forming peroxide radicals, which rapidly react with TBHQ (Reaction 3 and 4). Both oxygen and TBHQ are consumed by this reaction.

However, since the former is available in excess, the reaction continuous until TBHQ is consumed. Hereafter it proceeds as normal under air atmosphere and as result the maximum obtainable aspect ratio is the same independent of the concentration of TBHQ. It simply requires a higher exposure dose to overcome the effect of the induction period.
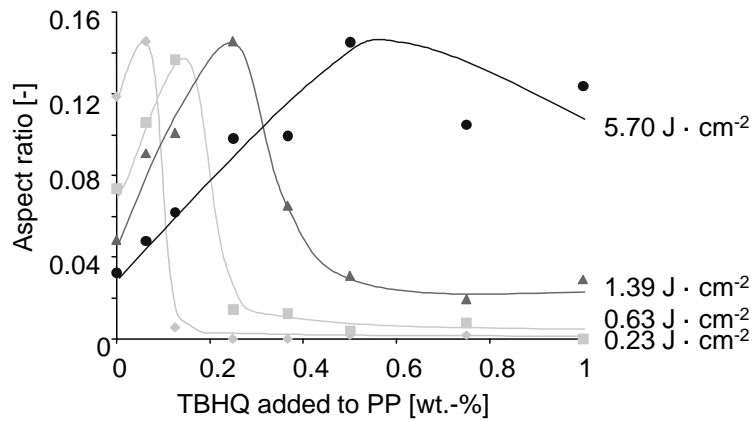

Figure 3.11: Aspect ratio of photoembossed relief structures (40 μm periodicity) of samples containing different concentration of TBHQ and processed under air.

3.3.4 Aspect ratio dependency of the periodicity

Photoembossing is based on the diffusion of a multifunctional monomer. It can thus be expected that the performance of a photopolymer depends on the size and distance between the relief structures. Therefore the aspect ratios of relief structures of different periodicities have been investigated. The samples were photoembossed under inert conditions. The results are given in Figure 3.12. It can be observed (Figure 3.12a) that for a reference sample the maximum aspect ratio is obtained at a periodicity of 20 μm. The occurrence of a maximum is explained in terms of surface tension at small periodicities and limited monomer diffusion lengths at higher periodicity. For samples containing TBHQ (Figure 3.12b and c) the maximum obtained aspect ratio shift to approximately 30 μm. This shift occurs due to an extension of the monomer diffusion lengths by a reduced network density. It thus depends also on the exposure dose at which periodicity a maximum aspect ratio is obtained.
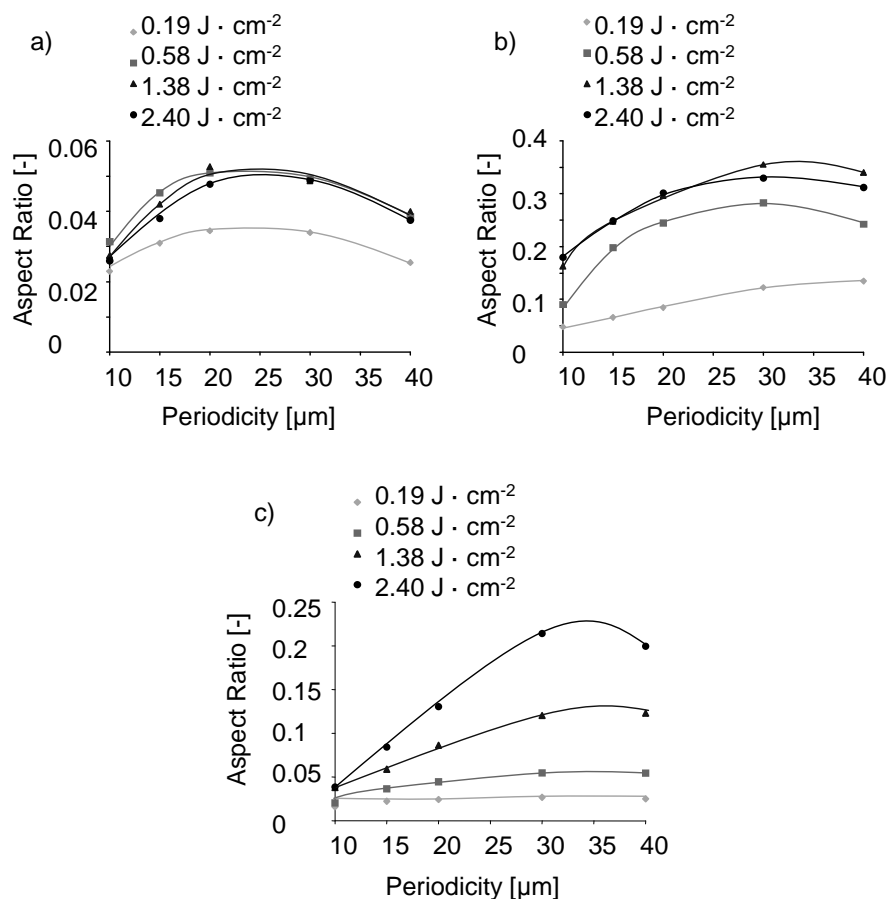
Figure 3.12: Aspect ratio of photoembossed relief structures with different periodicity for (a) reference samples, (b) samples containing 7wt.-% of TBHQ and (c) samples containing 12wt.-% of TBHQ.

3.3.5 Substituents on phenyl group of hydroquinones

In previous paragraphs it has been shown that under inert conditions TBHQ can effectively increase the performance of a photopolymer. In principle, a large variety of hydroquinone derivatives can be used. These derivatives mainly vary with respect to the substituent present at the phenyl group. In this paragraph it is investigated what the effect of these substituents on the performance of the photopolymer are. It is known from literature that especially electron withdrawing and donating groups have a large influence on the rate of transfer to a hydroquinone. Therefore two other derivatives, which contain fluoro (electron withdrawing) and methyl (electron donating) groups, have been tested and compared to TBHQ. First, the polymerization kinetics was investigated by measuring the acrylate conversion upon UV exposure, which is initiated after 10 seconds starting the measurement. The experiments were performed at a molar ratio of 0.56:1 (Inhibitor:Initiator). The results are given in Figure 3.13. The results show that the rate of acrylate conversion is the most reduced by TMHQ and TBHQ.

TFHQ only has a small influence on the rate of polymerization. As mentioned in the introduction paragraph of this chapter, substituents that influence the stability of the phenolate ion, which is an intermediate compound during the transfer reaction, have a significant influence on the overall rate of this reaction. Electron withdrawing groups, such as fluor, typically stabilize the phenolate ion and thus reduce the rate of transfer. On the other hand electron donating groups, such as methyl, destabilize the phenolate ion and therefore increase the rate of transfer. The small difference in effect between TBHQ and TMHQ could in addition also arise from steric effects from the bulky *tert.-*butyl group, which could hinder the reaction.
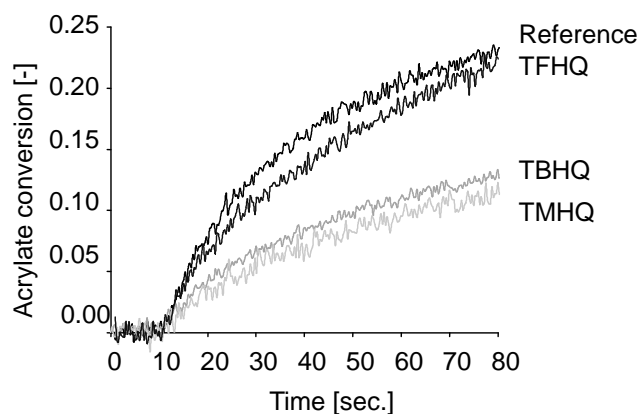

Figure 3.13: Acrylate conversion upon continuous UV exposure (initiated after 10 seconds) for photopolymers containing an equal molar concentration of TBHQ, TMHQ and TFHQ.

When comparing the aspect ratios of relief structures made via photoembossing in photopolymers containing (initiator to inhibitor concentration of 0.56:1) TBHQ, TMHQ and TFHQ, it can noticed that all can obtain the same maximum aspect ratio (See Figure 3.14). The exposure dose required to obtain this maximum aspect ratio is however different. In the presence of TFHQ the maximum aspect ratio is obtained at an exposure dose of approximately $0.15 \; J \cdot cm^{-2}$, for TBHQ this is $0.3 \; J \cdot cm^{-2}$ and for TMHQ this is $0.6 \; J \cdot cm^{-2}$. Due to the strong retardation caused by TMHQ, radical termination is likely to occur. This can be overcome by using a higher exposure dose to increase the initial concentration of radical species. TFHQ is a poor retarder and thus the termination of radicals is low and the required exposure is thus significantly less.
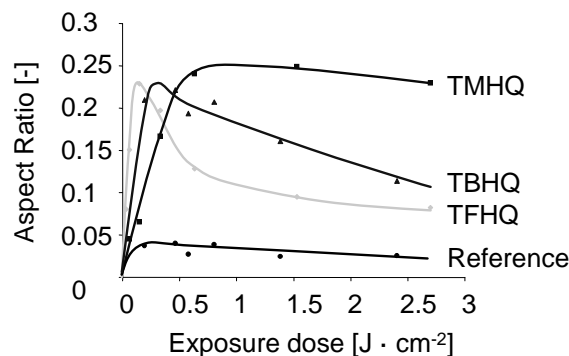
Figure 3.14:   Aspect ratio of photoembossed relief structures (40 μm periodicity) of samples containing equal molar concentrations of TBHQ, TMHQ and TFHQ.

3.3.6 Comparison experimental and modeling results

From the model in Chapter 2 it was concluded that an inhibition reaction cannot increase the aspect ratio of photoembossed relief structures. These predictions were tested experimentally by adding TBHQ to the photopolymer composition. It was verified that the addition of TBHQ resulted in inhibition of the polymerization reaction when the photopolymer was processed under an oxygen containing atmosphere (air). Under these condition the aspect ratio did, as predicted by the model, indeed not increase. A different effect was observed when a TBHQ containing photopolymer was processed under inert conditions. Under these conditions, retardation occurred rather than inhibition. It was observed that under these conditions the stabilized radicals were trapped in the forming polymer network. The network restricts termination of the stabilized radicals. Instead of being terminated, the trapped radicals can reinitiate the polymerization during the thermal development step. The retardation by TBHQ can under these conditions thus best be described by chain transfer rather than inhibition.

Although the addition of TBHQ resulted under certain processing conditions in chain transfer, hydroquinones are not designed for this type of reaction. In Chapter 4 this reaction is further investigated by using molecules which are designed for chain transfer reactions. At the end of Chapter 4 the theoretical chain transfer model is compared to the experimental results and the differences are discussed.

3.4   Conclusion

In this chapter the effect of compounds which terminate propagating radicals on the relief formation in photoembossing was investigated. Depending on their efficiency, these compounds are typically known as inhibitors (efficient) or retarders (less efficient). It is demonstrated by the addition of tert-butyl hydroquinone (TBHQ) to the photopolymer that inhibition does not improve the aspect ratio of a relief structure

This reaction was observed when TBHQ containing photopolymers were processed under an oxygen containing atmosphere (air). The combined effect of hydroquinone and oxygen resulted in inhibition of the polymerization reaction due a fast transfer and termination of propagating radicals. This reaction continues until either the hydroquinone or oxygen is fully consumed; in the here presented experiments the excess compound is oxygen in air. Hereafter the polymerization reaction starts as normal when processing under air conditions. Hence no improvement over normal processing under air, in the absence of a hydroquinone, is obtained. This observation concurs with the results from Chapter 2 in which it was shown that radical termination does not improve the aspect ratio.

An improved performance by the addition of TBHQ was observed when the photoembossing procedure was performed under an inert atmosphere. The mid-chain radicals, which were found to be dominant species in the absence of hydroquinone, were transferred to phenoxy radical species. Both radical species were demonstrated to be particularly stable. This stability is caused by trapping of the radicals in the crosslinked network formed by polymerization of the multifunctional monomer. However, due to the transfer of radical species the rate of polymerization is reduced as well as the network density. As a result, the mobility of both the radicals and monomeric species in the exposed areas of the photopolymer are improved leading to higher relief structures. This effect also occurs when a photopolymer, without added inhibitor, is processed under an oxygen containing atmosphere. The environmental oxygen diffuses into the photopolymer layer where it reacts with alkyl radicals to form peroxide radicals. The retardation by TBHQ or oxygen can be best described by the chain transfer rather than the inhibition model from Chapter 2. This effect is further investigated in Chapter 4.

The positive effect of TBHQ under inert conditions can in principle be obtained in a large variety of hydroquinone derivatives. Particularly interesting are hydroquinones with electron withdrawing substituents (e.g. fluor) on the phenyl group. These substituents stabilize the phenolate ion intermediate, which results in a slow transfer of propagating radicals and less termination. As a consequence the exposure dose required for obtaining a maximum aspect ratio is reduced.

3.5   References

[1]   M. R. Gleeson, J. V. Kelly, D. Sabol, C. E. Close, S. Liu, J. T. Sheridan, *J. Appl. Phys.* **2007**, *102*, 023108.

[2]   C. M. Leewis, D. P. L. Simons, A. M. de Jong, D. J. Broer, M. J. A. de Voigt, *Nucl. Instr.Meth B* **2000**, *161-163*, 651.

[3]   C. M. Leewis, P. H. A. Mutsaers, A. M. de Jong, L. J. van IJzendoorn, D. J. Broer, M. J. A. de Voigt, *Nucl. Instr. Meth. B* **2001**, *181*, 367.

[4]   C. M. Leewis, A. M. De Jong, L. J. van IJzendoorn, D.J. Broer, *J. Appl. Phys.* **2004**, 95, 4125.

[5]   C. M. Leewis, A. M. De Jong, L. J. van IJzendoorn, D. J. Broer*, J. Appl. Phys.* **2004**, *95*, 8352.

[6]   F. Tudős, T. Foldes-Berezsnich, *Prog. Polym. Sci*. **1989**, *14*, 717.

[7]   G. Odian, *Principles of Polymeriztion*, 4th edition, Wiley Interscience, New Jersey, USA, **2004**,(255-264).

[8]   G. Moad, D. H. Solomon, *The Chemistry of Free Radical Polymerization*, Elsevier Science Ltd, Great Britain, **1995**, (260-266).

[9]   M. Simonyi, F. Tudős, J. Pospišil, *european polymer journal* **1967**, *3*, 101.

[10]   A. Fimia, N. López, F. Mateos, R. Sastre, J. Pineda, F. Amat-Guerri, *J. Modern Optics*, **1993**, *40*, 699.

[11]   A. K. O'Brien, C. N. Bowman, *Macromol. Theory Simul.* **2006**, *15*, 176.

[12]   M. S. Kharasch, F. Kawahara, W. Nudenberg, *J. Org. Chem.* **1954**, *19* ,1977.

[13]   J. Brandrup, E. H. Immergut, *Polymer Handbook*, 4th edition, Wiley Interscience, New York, **1999** (II-53 –II-55).

[14]   E. Selli, C. Oliva, *Macromol. Chem. Phys*. **1995**, *196*, 4129.

[15]   H. Fischer, *Chem. Rev.* **2001,** *101,* 3581.

[16]   C. Oliva, I. R. Bellobono, R. Morelli, *Phys. Chem. Chem. Phys*., **1999**, *1*, 215.

[17]   K. Dušek, M. Dušková-Smrčková, *Prog. Polym.* Sc.i **2000**, *25*, 1215.

[18]   J. Zhu, W.J. Johnson, C.L. Sevilla, J. W. Herrington, M. D. Sevilla, *J. Phys. Chem.* **1990**, *94*, 7185.

Chapter 4

Chain transfer

It is the objective of this chapter to investigate the effect of compounds which reinitiate propagating radicals on the relief formation in photoembossing. Typical compounds which are known for this effect are radical addition-fragmentation transfer (RAFT) agents. The efficiency of these molecules depends on the activating and leaving group and the system in which they are used. Therefore the reaction kinetics of photopolymers containing different RAFT agents are investigated. It is found that a phenyl activating group gives a fast transfer of propagating radicals to the RAFT agents. As a consequence the rate of polymerization is reduced. Both methoxycarbonyl propyl and cyanobutyl leaving groups are shown to be able to reinitiate the polymerization reaction. When measuring the aspect ratio of photoembossed relief structures it is observed that the addition of RAFT agents results in an increase. The increase is subscribed to improved mobility of both the radicals and monomeric species in the exposed areas due to the chain transfer reaction. The results concur with the expectation from Chapter 2 and 3. Although both RAFT and retarders (Chapter 3) can improve the aspect ratio, they each behave differently in the photopolymer. Photopolymers containing RAFT agents show significant dark reaction after exposure to ultraviolet (UV) light. This dark reaction, caused by the continuous reinitiation and the absence of radical termination by the RAFT agent, is sustained until the forming crosslinked network prevents further reaction. The main advantage of RAFT agents is the non-sensitivity towards environmental oxygen which is an important issue in industrial applications. Their intrinsic color makes these compounds however less suitable for use in most of the optical applications.

4.1   Introduction

In the previous chapters it has been demonstrated that compounds which interfere with the polymerization reaction by transfer of propagating radicals to stabilized species can improve the aspect ratio of photoembossed relief structures. Whether or not an increased aspect ratio was obtained depended on the reaction succeeding the transfer of the propagating radical. This can be either termination of the radial species or reinitiation of the polymerization reaction. By investigating the effect of inhibitors, it was demonstrated (Chapter 2 and 3) that termination does not improve the performance of the photopolymer. However, an increase in performance is expected when the intermediate radicals reinitiate the polymerization reaction. Encouraged by the findings of the model (Chapter 2) and the results obtained with retarder molecules (Chapter 3), this effect is further investigated in this chapter by using compounds which are known to stabilize a propagating radical and subsequently reinitiate the polymerization reaction. This reaction is known in literature as chain transfer.[1-3] It can be caused unintentionally by certain monomers, initiators or solvents, but it can also be induced via the addition of so-called transfer agents to the reactive mixture. These molecules are added to a monomer to control the molecular weight upon polymerization and create polymers with a very narrow polydispersity.[4] Since the polymerization is reinitiated rather than terminated, the "living" character of this type of polymerization makes it also possible to create polymer products that can be reactivated for chain extension or block synthesis.[5] A few types of living polymerizations are known: Atom transfer radical polymerization (ATRP) is based on an organic halide undergoing a reversible redox process catalyzed by a transition metal compound such a cuprous halide.[6] Stable Free-Radical Polymerization (SFRP) uses thermal decomposition to create stable radicals such as nitroxide, triazolinyl, trityl, and dithiocarbamate.[7] Both ATRP and SFRP rely on reversible termination and obviate the use of a conventional initiator since the radicals are created by the transfer agents themselves. Therefore these techniques are not suitable for investigating the transfer of radical species originating from photo activation. To avoid this problem we have used radical addition-fragmentation transfer (RAFT) agents.

4.2   Chain transfer by RAFT agent

RAFT polymerization controls the chain growth of a polymer through reversible chain transfer.[8,9] The mechanism is based on an equilibrium between intermediate stabilized radicals and dormant species with a dithioester moiety (Figure 4.1). After photoinitiation, a propagating radical is transferred via an intermediate stabilized radical to the leaving group of the RAFT agent (R). The transfer constant is thus a composite term which depends on the rate constant for addition to the dithioester and the

partitioning of the intermediate between starting materials and products.[10] The kinetics of a RAFT agent depends on the leaving group and the activating group (Z) attached to the dithioester moiety and the type of monomer. The leaving group is one of the key factors during the initialization period of the RAFT polymerization. It should be capable of forming a free radical which can rapidly reinitiate polymerization. The effectiveness depends on steric factors, radical stability and polar factors. In general it can be stated that the more stable, the more electrophilic and the bulkier the radicals the better the leaving group.[11] A typical effective leaving group is for example cyanoisopropyl. The activating group determines the activity of the RAFT agent. Its effect is based on the enhancement of the reactivity of the C=S bond. One of the most active leaving groups is phenyl.
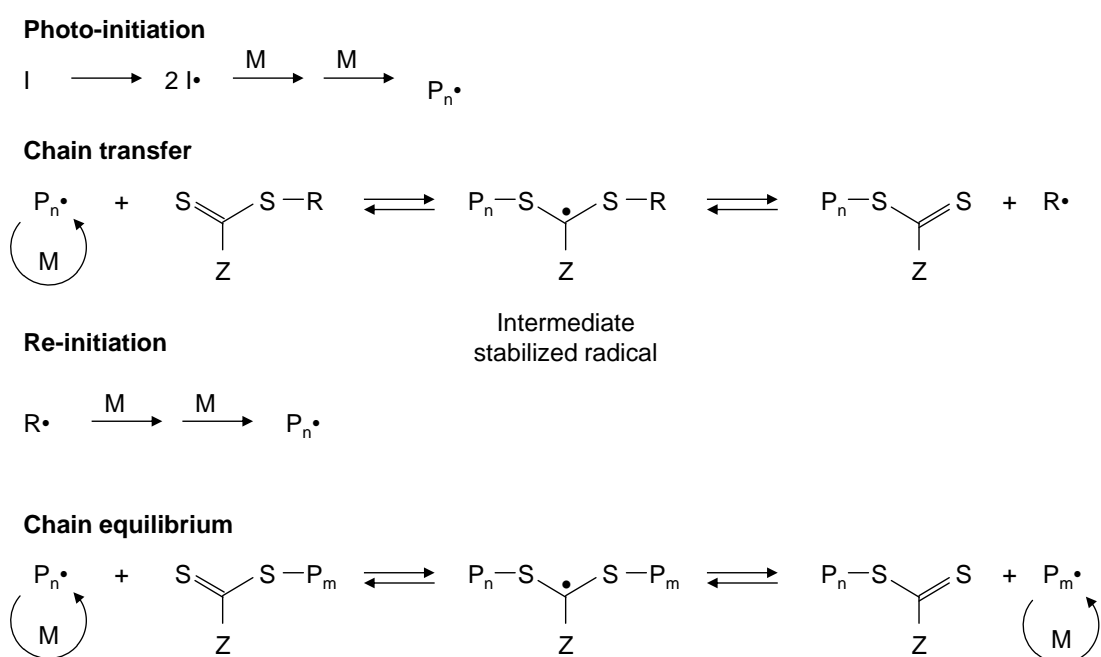

Figure 4.1: Schematic presentation of the reversible addition-fragmentation chain transfer (RAFT) polymerization.

In this chapter it is investigated whether the addition of a RAFT agent can improve the performance of a photopolymer. The influence on the polymerization kinetics of several RAFT agents is studied by real time attenuated total reflection infra-red (ATR-IR) spectroscopy upon the exposure to ultraviolet (UV) light and during the subsequent dark reaction (paragraph 4.4.1). The aspect ratio of photoembossed relief structures in the presence of the RAFT agents is monitored by confocal microscopy and compared for different periodicities (paragraph 4.4.2). To establish a clear difference between retarders/inhibitors discussed in previous paragraph and RAFT agents, the different techniques are compared in paragraph 4.4.3.

4.3 Experimental section

4.3.1 Materials

For the photopolymer polybenzylmethacrylate (M_w 70 kg mol^{-1}; Scientific Polymer Products) was used as a polymeric binder, dipentaerythritol penta/hexa-acrylate (Sigma Aldrich) as a multifunctional monomer and Irgacure 819 (CIBA, Specialty Chemicals) as a photoinitiator. As a solvent a 50/50 wt.-% mixture of ethoxypropylacetate (Avocado Research Chemicals) and propyleneglycol-methyletheracetate (Aldrich) was used. To prepare the photopolymer solutions the multifunctional monomer and the solvent were mixed in a weight ratio of 1:2 and the 500 ppm of 4-methoxyphenol present in the monomer was removed by using a silica packed inhibitor removing column (Aldrich). The monomer/solvent mixture was mixed with the polymer and photoinitiator in a weight ratio of respectively 30:10:1. The RAFT agents were added to this solution in different weight ratio. As a RAFT agent 2-cyanobut-2-yl dithiobenzoate (C-DB), 2-(methoxycarbonyl)prop-2-yl dithiobenzoate (M-DB) and 2-phenylprop-2-yl phenyl dithioacetate (P-PD) were used. The RAFT agents were prepared as described in literature.[12] The molecular structures of these compounds are depicted in Figure 4.2.
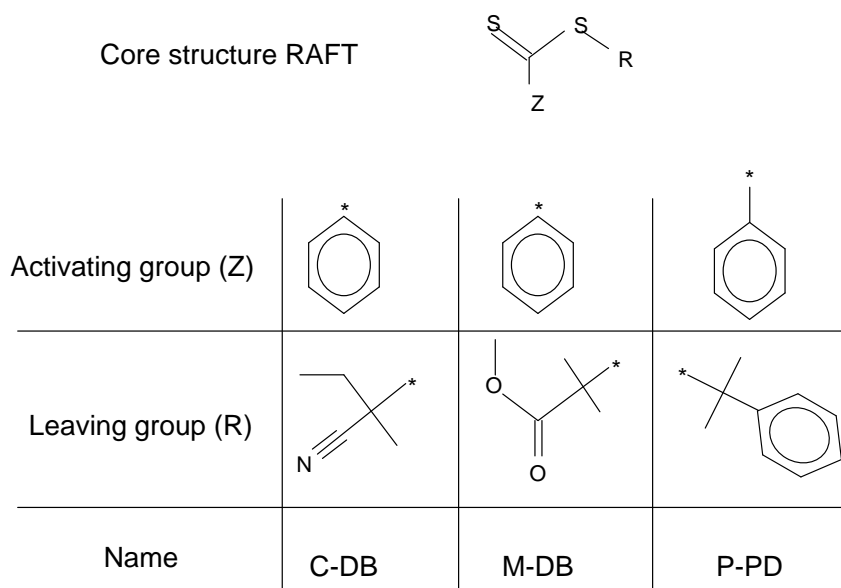

Figure 4.2:   Molecular structures of the investigated RAFT agents.

4.3.2 Sample preparation

The D263 glass substrates (5 × 5 cm) were cleaned by rubbing with a sodium hydroxide solution, flushed with demineralized water, rubbed with acetone, rubbed and flushed with ethanol and finally dried with nitrogen. Directly after cleaning the photopolymer

solution was spincoated on top of the glass substrates at 800 rpm with a Karl Suss RC8 spincoater. To remove the solvent the samples were dried at 80 °C for 20 minutes after which they were cooled to room temperature, resulting in dry films with a thickness of approximately 16 μm. The samples were exposed with an Omnicure S2000 UV light source (EXFO) having an intensity of 10 mW · cm^{-2} (λ = 320-390 nm). During exposure a rectangular lithographic mask (28 mm × 31 mm) that consisted of five parallel sectors (4 mm × 31 mm) was placed onto the sample. Each sector had a line grating with a periodicity of 40, 30, 20, 15 and 10 μm, respectively (dark and transparent areas of the same size). Unless stated otherwise only the results of the 40 μm periodicity are given. On top and perpendicular to the line mask a lithographic optical density (OD) mask was placed in order to change the intensity of the light that reaches the sample. The OD mask also consists of seven parallel sectors, absorbing 10, 49, 79, 89, 95, 98 and 99% of the light, respectively. After exposure the masks were removed and the sample was gradually heated to a temperature of 110 °C and kept for 10 minutes at this temperature. Finally, a flood exposure was applied for 5 minutes at a temperature of 110 °C. To study the effect of environmental oxygen during exposure, development and flood exposure, the samples were placed under a protective atmosphere by constant nitrogen blanketing using a custom build hot plate. This hot plate was built into an aluminum box that could be flushed with nitrogen and contained a quartz glass window through which the samples could be exposed to UV light.

4.3.3 Characterization

Confocal microscopy: The height of the photoembossed relief structures was investigated using a confocal microscope (Sensofar, PLμ2300) with a 50x objective.

Attenuated Total Reflection Infra-red (ATR-IR) spectroscopy: The IR measurements were performed on Excalibur FT-IR (FTS 3000 MX), which was equipped with a Specac Golden Gate diamond ATR. An Oriel light source housing (69054) which was equipped with a USHIO deep UV lamp (USH-200DP) was used for exposure of the sample. The samples were applied from solution and dried for 10 minutes at 80 °C after which they were cooled to 30 °C before the measurement was started. A continuous UV exposure (λ = 365 nm, I = 2.5 mW · cm^{-2}) was initiated 10 seconds after starting the experiment. After 10 seconds the exposure was stopped while the measurement was continued. The acrylate conversion was determined by measuring the absorbance at 1635 cm^{-1} and 1407 cm^{-1}. Only the results obtained at 1635 cm^{-1} are shown in the figures.

4.4   Results and discussion

4.4.1 Kinetics of light and dark reaction

The kinetics of a RAFT agent depends on the type of RAFT agent and the monomer system in which it is used. Therefore real-time ATR-IR measurements were performed to investigate the influence of three different RAFT agents on the polymerization kinetics. The acrylate conversion was measured under a nitrogen atmosphere both during a 10 second UV exposure and afterwards. The results are compared to a reference photopolymer without RAFT agent and the results are given in Figure 4.3. It can be observed that the initial acrylate conversion, during the exposure, was reduced by the addition of C-DB and M-DB. The presence of P-DB did not result in a significant change in kinetics. The rate of acrylate conversion is determined by the propagating radical concentration and is thus reduced by the transfer of these species to the RAFT agent. The radical remains at the RAFT agent until polymerization is reinitiated by fragmentation of R·. It can thus be expected that initially the contribution to the rate of polymerization via reinitiation is low. This will increase when the concentration of intermediate stabilized radicals increases as the reaction progresses. The difference in initial rate of polymerization between the different RAFT agents can be ascribed to the different activating groups. The phenyl group of C-DB and M-DB is known to be particularly good stabilizer for the intermediate radical, which resulted in a fast transfer to the intermediate stabilized species and thus retardation of the polymerization reaction.[9] The benzyl group of (P-PD) is often reported to give no retardation.[13,14]

After the UV exposure, it can be observed that the conversion of acrylate groups is continued. Propagating radicals react with monomer for minutes after the exposure until finally terminated or trapped within the growing polymer network. The presence of M-DB or P-PD did not influence the rate of polymerization, while C-DB appeared to give a small reduction. Since the photoinitiator is not activated and new propagating can be created as such, the contribution due to the reinitiation reaction via R· becomes significant. The benzylic radicals of P-PD have the propensity to add to polymer RAFT rather than to the monomer (thus to reinitiate), especially when used in high concentration.[9] The contribution via R· is thus low. Combined with the poor transfer of a propagating radical to the intermediate stabilized species it can thus be concluded that this RAFT agent was rather ineffective in the photopolymer. Both cyanobutyl (C-DB) and methoxycarbonyl propyl (M-BD) are more effective reinitiators.[9] The small difference in the rate of polymerization observed during the dark reaction could have occurred from a difference in electrophilicity, stability or steric effects.

It should be noted that although in principle also the chain equilibrium reaction contributes to the acrylate conversion it is expected that this reaction was (at least initially) low due to the relatively high concentration of RAFT.
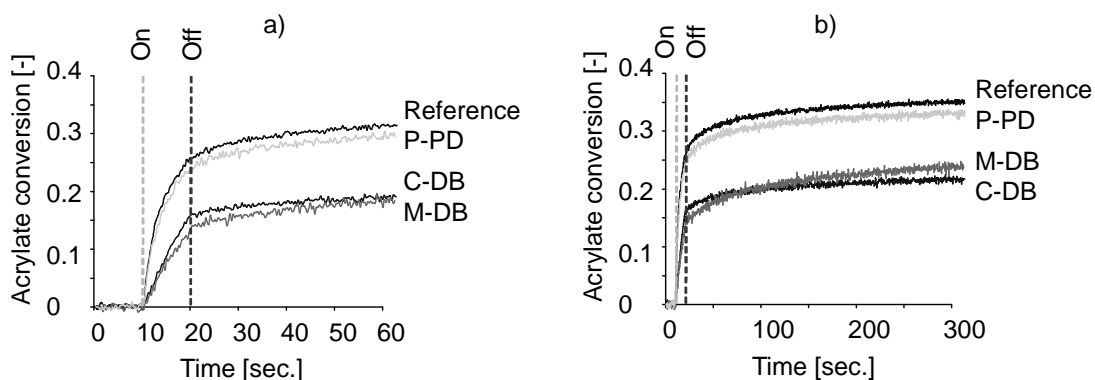

Figure 4.3:   Acrylate conversion upon a short (10 seconds) UV exposure of photopolymer layers containing different RAFT agents. The acrylate conversion was determined for (a) 60 seconds and (b) 300 seconds.

4.4.2 Aspect ratio

To investigate the effect of RAFT on the relief formation in photoembossing, different concentrations of C-DB were added to the photopolymer composition. The aspect ratio of relief structures obtained under inert processing conditions was determined by measuring the relief height via confocal microscopy. The results (Figure 4.4) show that the aspect ratio of the photoembossed relief structures increased upon the addition of the C-DB to the photopolymer. The increase is mainly ascribed to the transfer of propagating radicals and/or reactivation of mid-chain radicals (see also paragraph 3.3.1) by the RAFT agent. The mid-chain species are, although intrinsically still reactive, trapped within a crosslinked network. A crosslinked network not only makes the radicals inaccessible, but also restricts the diffusion of monomer. The RAFT agent enables the reactive species to escape from the traps. In addition the radicals are confined within a less dense network due to retardation of the polymerization reaction, despite the fact that the radical concentration is high. This in contrast with samples which are exposed with a lower dose which have also a lower conversion, but also a lower radical concentration, and therefore do not show the enhancement of the aspect ratio. Post-exposure polymerization during thermal development is therefore enhanced as well as by the diffusional mobility of the reactive species. Other effects that might affect the diffusion of monomer positively during the heating step, but are considered to be less dominant, are the reduction in kinetic chain length due to the chain transfer function and thus postponing gel point. Also, especially at high concentrations, the

RAFT agent may act to some extent as a plasticizer, thus reducing the modulus and glass transition temperature and enhancing diffusional monomer mobility.

It is also observed in Figure 4.4 that at too high C-DB concentrations the aspect ratio decreased. Based on the ATR-IR measurements it is likely to assume that at these concentrations a strong retardation of the polymerization reaction occurs. Since the conversion of monomer is one of the main contributions to a difference in chemical potential between the exposed and non-exposed areas this thus leads to a reduction in the aspect ratio of the relief structures. The effect can be postponed by choosing a higher exposure dose, increasing the concentration of the initially created reactive species.
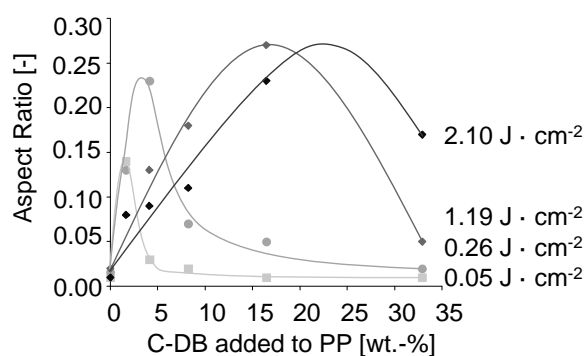

Figure 4.4: Aspect ratio of photoembossed relief structures of samples containing different concentrations of C-DB.

To investigate the influence of RAFT on the different periodic structures, the aspect ratio of relief structures with periodicities of 10, 15, 20, 30 and 40 μm were measured for a photopolymer containing the 16.5 wt.-% C-DB. The results are compared to a reference sample without C-DB (Figure 4.5). To avoid any confusion, it should be noted that the absolute values of aspect ratios are low compared the Figure 4.4. This results from the relatively high concentration of RAFT and low exposure dose used in these experiments. In Figure 4.5 it can be observed that at an exposure dose of $0.6 \text{ J} \cdot \text{cm}^{-2}$ the addition of C-DB increased the aspect ratio of relief structures of all periodicities. At a lower exposure dose of $0.2 \text{ J} \cdot \text{cm}^{-2}$ the aspect for a periodicity of <30μm was lowered by the addition of C-DB. This can be explained by considering that the diffusion of monomer is based, amongst others parameters, on a balance between surface tension and monomer conversion. Due to an enhanced surface to volume ratio (at the same aspect ratio), the effect of surface tension is larger on smaller periodicities. Although the addition of C-DB extents monomer diffusion, this is partially achieved by a reduction in monomer conversion due to retardation (Figure 4.3). It can be expected that at small

periodicities the positive effect of the extended diffusion was counterbalanced by a reduction in monomer conversion and the surface tension.

Second, it can be observed from Figure 4.5 that the maximum aspect ratio for a reference sample is obtained at a periodicity of 20 μm. The occurrence of a maximum is explained in terms of surface tension at small periodicities and limited monomer diffusion lengths at higher periodicity. For sample containing C-DB the maximum obtained aspect ratio shift to approximately 30 μm. This shift occurs due to an extension of the monomer diffusion lengths by a reduced network density.
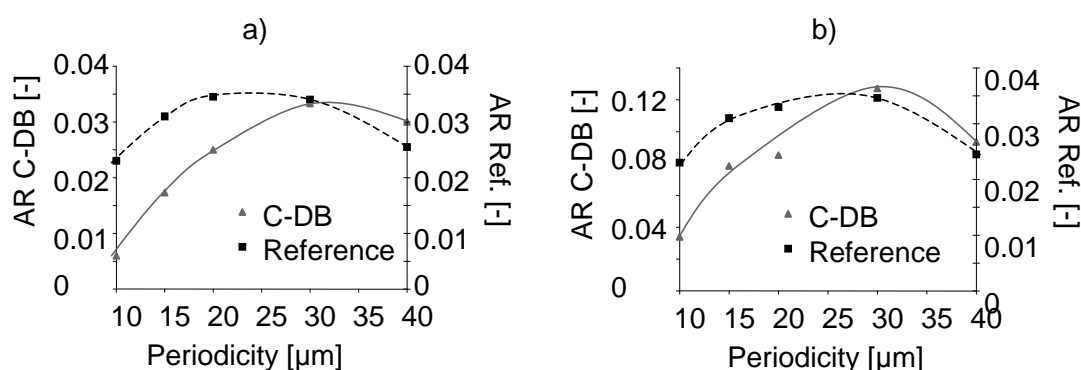

Figure 4.5:   Aspect ratio of photoembossed relief structures with different periodicity for in a reference sample and a sample containing 16.5 wt.-% of C-DB using an exposure dose of (a) $0.2 \, J \cdot cm^{-2}$ (b) $0.6 \, J \cdot cm^{-2}$.

In Figure 4.6 the results obtained from C-DB are compared to those obtained by M-DB, P-PD (2:1 wt/wt, RAFT:Initiator) and a reference sample. It can be observed that the maximum aspect ratio obtained by using P-PD was low. In fact, the obtained aspect ratio of 0.065 was only slightly higher than the maximum aspect ratio of 0.05 for a reference sample. This observation concurs with the ATR-IR data in Figure 4.3, which showed that P-PD does little interfere with the polymerization reaction. As also observed with the other two RAFT agents the effect of P-PD does depend on the exposure dose. At a higher exposure dose the difference with the aspect ratio of a reference sample became more pronounced. The amount of trapped mid-chain radicals increases with a high exposure dose and thus leading to more reinitiation by RAFT agent.
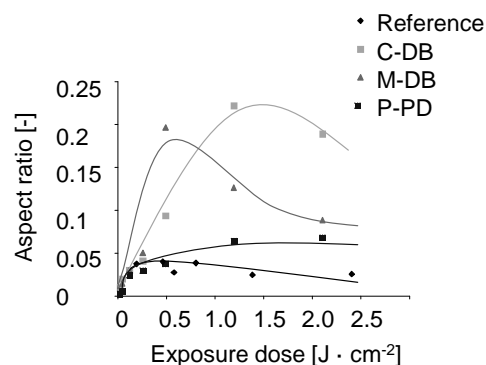
Figure 4.6: Aspect ratio of photoembossed relief structures of samples containing different RAFT agents.

The addition of M-DB resulted in a maximum aspect ratio which was approximately equal to the results obtained from C-DB. A lower exposure dose was however required. A possible explanation can be derived from the ATR-IR data, which showed that the methoxycarbonyl propyl leaving group of M-DB more easily reinitiates the polymerization than the cyanobutyl group of C-DB. To obtain the same monomer conversion, a lower initial radical concentration, as set by the exposure dose, is thus required for M-DB.

4.4.3 Retarders vs RAFT agents

It has been demonstrated that both retarders and RAFT agents can positively affect the performance of a photopolymer. Both systems are based on a transfer of propagating radicals to stabilized species and it is the subsequent reaction that differentiates the two compounds. RAFT agents reinitiate polymerization, while retarders (at least at room temperature) have the tendency to terminate the radical species. To demonstrate this difference, the reaction kinetics of a photopolymer containing a RAFT agent (M-DB) was measured during a short UV exposure and the subsequent dark reaction. In Figure 4.7 the results are compared to a photopolymer containing a retarder (*tert*-butyl hydroquinone, TBHQ) and a reference photopolymer without RAFT or TBHQ. M-DB and TBHQ were added to the photopolymer composition in equal molar concentration. Both compounds reduced the initial rate of acrylate conversion, however, when the exposure was stopped the acrylate conversion continued in the presence of M-DB, but was halted in the presence of TBHQ. This clearly shows that retarders, unlike RAFT molecules, are not capable of reinitiating the polymerization reaction at room temperature.
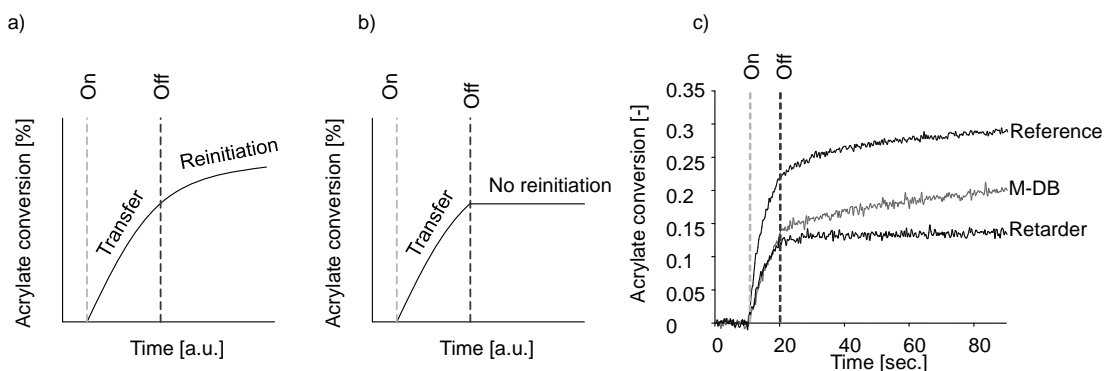
Figure 4.7: Schematic representation of the acrylate conversion for (a) a RAFT agent and (b) a retarder upon a short UV exposure and afterwards. (c) The measured acrylate conversion upon a short UV exposure and afterwards.

Another clear difference between the different compounds is that retarders were observed to be particularly useful under inert conditions. In the presence of oxygen a fast transfer and consequently termination of propagating radicals resulted in inhibition of the polymerization reaction. This did not result in a performance enhancement of the photopolymer (paragraph 3.3.2.). RAFT agents are less sensitive to the presence of environmental oxygen.[15] This was demonstrated by measuring the acrylate conversion with ATR-IR upon continuous exposure of a photopolymer containing M-DB under an air atmosphere. The results are compared to a measurement with the same photopolymer performed under an inert atmosphere in Figure 4.8. It is observed that oxygen had only little effect on the reaction kinetics in the presence of M-DB. Although usually for controlled living radical polymerizations the reaction compositions are thoroughly deoxygenated it is very well possible to obtain a well controlled polymerization in the presence of oxygen.[13] Peroxide groups formed by the radical initiated reaction with oxygen can even increase the rate of polymerization upon thermal decomposition.
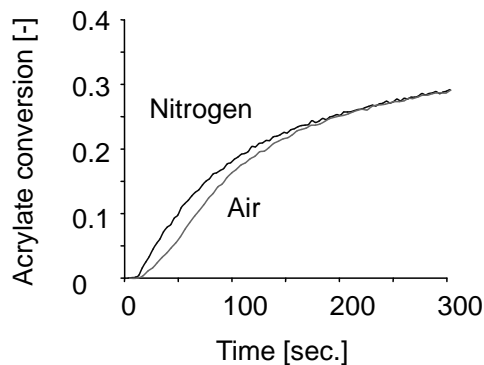

Figure 4.8 : Acrylate conversion upon continuous UV exposure (initiated after 10 seconds) under air for a reference photopolymer and a photopolymer containing 8.2wt.-% of M-DB.

When comparing the aspect ratios of samples which were photoembossed under an air atmosphere it was found that unlike retarders, RAFT agents can be used to increase the aspect ratio of the relief structures in the presence of oxygen (Figure 4.9). The maximum aspect ratio of 0.19 was slightly lower than that of structures made under inert conditions (0.22). This small reduction possibly results from additional radical termination by the presence of oxygen.

One particular drawback of RAFT agents is that most are colored as a result of the conjugated system between the dithioester moiety and the activating or leaving groups. Also alternative methods based on the reinitiated polymerization like atom transfer radical polymerization (ATRP) or stable free radical polymerization (SFRP) use molecules which are colored (e.g. cuprous halides or nitroxides). The presence of a color conflicts with the fact that photopolymers are often used in optical applications in the visible part of the spectrum such as diffraction gratings. In addition RAFT molecules are more expensive and often custom synthesized for a specific application.
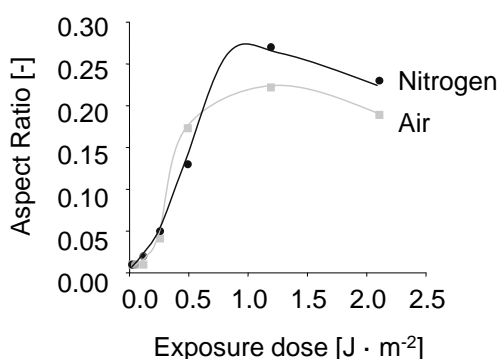

Figure 4.9: Aspect ratio of photoembossed relief structures of samples containing C-DB processed under inert and air conditions.

4.4.4 Comparison experimental and modeling results

The experimental results from this chapter show that a chain transfer reaction can improve the aspect ratio of photoembossed relief structures. The observed increase in aspect ratio suggests that these molecules not only react with propagating radicals, but also with trapped radicals. It was suggested in Chapter 2 that it would be possible for a small molecule (e.g. RAFT agent) to react with trapped radicals, even though the reaction with the larger monomer molecules is hindered. The fraction of trapped radicals which can react with the smaller chain transfer molecules was expressed by the parameter K_0. The model showed that only a small increase in aspect ratio (10%) is obtained by chain transfer, when K_0 is taken 0 (no reaction). By increasing the value of K_0, the aspect ratio increased up to a factor 2.4. The large increase in aspect ratio

observed in this chapter suggests that a significant fraction of the trapped radicals reacts with the chain transfer agent. This conclusion is supported by the lack of an ESR signal corresponding to trapped radicals in paragraph 3.3.1. Upon illumination of a reference photopolymer (without chain transfer molecules), the clear ESR signal of mid-chain radicals was observed. These radicals were found to be dominant species when propagating radicals are trapped in the polymer network. When TBHQ was added to the photopolymer, the ESR signal of the mid-chain was not observed, but instead the ESR signal of phenol radicals was observed. The signal of the phenol radicals was found to be less stable, which suggest that these radicals have at least some mobility.

4.5 Conclusion

It is the objective of this chapter to experimentally investigate the effect of compounds which reinitiate propagating radicals on the relief formation in photoembossing. This reaction is typically known as chain transfer. It was demonstrated by the addition of a RAFT agent that these molecules can improve the aspect ratio of photoembossed relief structures.

It was demonstrated that the kinetic effect of RAFT agents in a photopolymer depends on the leaving and activating group attached to the dithioester moiety. Stabilization of the intermediate stabilized radical species by a phenyl activating group (M-DB and C-DB) resulted in a fast transfer of propagating radicals to the RAFT agent and retardation of the polymerization reaction. Both methoxycarbonyl propyl (M-DB) and cyanobutyl (C-DB) leaving groups were shown to be able to reinitiate the polymerization reaction. As a result of the transfer reaction, the mobility of both the radicals and monomeric species in the exposed areas of the photopolymer were improved leading to higher relief structures. These observations concur with the expectation from the model in Chapter 2.

When comparing the results obtained with RAFT agents to retarders from Chapter 3 it was demonstrated that the main difference is that former is capable of reinitiating the polymerization reaction at room temperature and the latter is not. The main advantage of RAFT is its indifference towards an oxygen environment. The disadvantages of RAFT agents are their intrinsic color, which makes them less suitable for use in optical applications.

4.6 References

[1]   D.T. McCormicka, Z.W. Fordhama, J. Smitha, P.J. McMullana, S.F. Thamesa, C.A Guymon, *Polymer* **2003**, *44, 2751.*

[2]   M.J. Wisotsky, A.E. Kober, *J.Appl. Polym. Sci.* **1972**, *16*, 849.

[3]   G. Odian, *Principles of Polymeriztion*, 4th edition, Wiley Interscience, New Jersey, USA, **2004**,(255-264).

[4]   R. Hoogenboom, U.S. Schubert, W. Van Camp, F.E. Du Prez, *Macromolecules* **2005**, *38*, 7653.

[5]   E. L. Madruga, *Prog. Polym. Sci.* **2002**, *27*, 1879.

[6]   P. Liu, *e-Polymers* **2007**, *62*,1.

[7]   W. A. Braunecker, K. Matyjaszewski, *Prog. Polym. Sci. 32* **2007**, *32*, 93.

[8]   Arnaud Favier, Marie-Thérèse Charreyre, *Macromol. Rapid Commun.* **2006**, *27*, 653.

[9]   S. Perrier, P. Takolpuckdee, *J. Polym. Sci. Part A: Polym. Chem. A* **2005**, *43*, 5347.

[10]   G. Moad, J. Chiefari, Y.K. Chong, J. Krstina, R.T.A. Mayadunne, A. Postma, E. Rizzardo, S.H. Thang, *Polym. Int.* **2000**, *49*, 993.

[11]   Y. K. Chong, J. Krstina, T. P. T. Le, G. Moad, A. Postma, E. Rizzardo, S. H. Thang, *Macromol.* **2003**, *36,* 2256.

[12]   G. Bouhadir, N. Legrand, B. Quiclet-Sire, S.Z. Zard, *Tetrahedron Lett.* **1999**, *40*, 277.

[13]   Y. Luo, B. Liu, Z. Wang, J. Gao, B. Li, J. Polym. Sci. A. **2007**, *45*, 2304.

[14]   A. J. P. van Zyl, R. F. P. Bosch, J. B. McLeary, R. D. Sanderson, B. Klumperman, *Polymer* **2005**, *46*, 3607.

[15]   Z. Zhang, X. Zhu, J. Zhu, Z. Cheng, S. Zhu, *J. Polym. Sci. Part A* **2006**, *44*, 3343.

Chapter 5

Alternative photopolymers

The polymeric binder is added to conventional photopolymers to create a solid layer, which is convenient for processing (e.g. prevent dust uptake, allowing contact mask exposure). The polymeric binder itself is immobile and cannot contribute to the structure height. It thus limits the performance in terms of, for instance, maximum aspect ratio. A photopolymer which mainly consists of monomer could in theory result in much higher relief structures since more material could be displaced. To develop such a system, it is necessary to find monomers which are solid at room temperature but are mobile at an elevated temperature. Such characteristics can be expected from relatively large molecules, which form a glassy state at room temperature due to steric interactions, or small molecules, which form a glassy state due dipole-dipole interactions. A typical material which is solid at room temperature due to steric effects is SU-8 which is a multifunctional epoxide. This material is conventionally used as a negative photoresist for photolithography. It is demonstrated that surface relief structures can be developed into SU-8 at an optimal temperature of 155-190 °C. This temperature range is much higher than the glass transition temperature (31°C). Most likely this is caused by the large size of these molecules and the resulting lack of mobility. After optimization of the exposure dose it was found that structures of approximately 0.7 µm could be obtained in a 3 µm thick layer. Although this proves the concept, the actual value is still low. Higher structures (1.3 µm) were obtained by using EPON 164, which has less epoxide groups than SU-8. This reduces the network density in the exposed areas and enhances the diffusion of monomer. To investigate the use of monomers which become solid at room temperature due to dipole-dipole interactions tri(hexylacrylate) benzenetricarboxamide was synthesized. These molecules form a supramolecular polymer at room temperature by hydrogen bonding. At a temperature of 100 °C the rod-like aggregates collapse and a mobile isotropic phase is formed. These molecules are well suitable as a photopolymer since structures of 2.1 µm were obtained. This system outperforms all other photopolymers and demonstrates the potential of a photopolymer without polymeric binder.

5.1   Introduction

It has been the objective of the previous chapters (2-4) to increase the aspect ratio of photoembossed relief structures. Hereto, molecules which stabilize propagating radicals were added to a conventional photopolymer. This resulted in large improvement of the aspect ratio. To further enhance the systems performance, the fundamental limitation of the use of the immobile polymeric binder needs to be addressed. To create a solid dry film a significant amount, of up to 45 wt.-%, of polymeric binder is added to the low molecular weight reactive species.[1-3] The ratio between monomer and polymer determines the degree of solidification and the glass transition temperature of the photopolymer mixture.[4] If the glass transition of the photopolymer is below room temperature (e.g. by reducing the binder content) the sample becomes tacky which obstructs contact mask exposure and leads to increased dust uptake during processing. Also, as a result of the reduced viscosity of the photopolymer, partial development of the relief structures occurs already during or just after the exposure step, but before applying the development step. This premature surface relief development deforms the optical path when applying multiple exposure steps to create a complex relief structure. Although a polymeric binder is necessary to ensure easy processing and allow multiple exposure steps, the mobility of the polymeric binder is low, even at elevated temperatures, and it therefore does not contribute to the height of the surface relief structure.

In this chapter it is investigated whether a photopolymer without polymeric binder can be developed. Such a photopolymer should consist mainly of monomer and a photoinitiator. Of course the additives discussed in chapter 2-4 could also be used in this photopolymer provided that they are compatible with the type of polymerization. To avoid reducing the processability, it is necessary that the monomer/photoinitiator mixture is solid at room temperature. Most monomers are usually liquid at room temperature. However, some molecules are glassy at room temperature due their large size. A well known material which exhibits this characteristic is SU-8.[5,6] This material is conventionally used as a negative photoresist for photolithography. It consists of a monomer with eight epoxide groups (Figure 5.1a). The cationic polymerization of the epoxide groups is initiated by a protonic acid generated upon a photoreaction of a sulphonium salt. The solid nature of the material does not only allow easy processing, but also prevents diffusion of the protons and their reaction at room temperature. This ensures that an accurate latent image of a patterned exposure is obtained. After a patterned exposure the material is heated above the glass transition temperature to allow the exposed areas to crosslink. In photolithography, the non-exposed and thus non crosslinked areas are removed by dissolving in a proper solvent. The solid nature of the

material at room temperature and liquid behavior above the glass transition temperature make it an ideal candidate for an all monomer photopolymer for photoembossing.

It is also possible to use a monomer which consists of smaller molecules and solidifies at room temperature due to secondary interactions (e.g. hydrogen bonds). A suitable monomer could be tri(hexylacrylate) benzenetricarboxamide. The molecular structure of the hydrogen bonded reactive monomer is given in Figure 5.1b. These monomers form a supramolecular polymer at room temperature, but are highly mobile at elevated temperatures. A supramolecular polymer is a polymer consisting of repeating units that are held together by reversible non-covalent bonds (e.g. hydrogen bonds).[7] From literature it is known that C_3-symmetrical benzene tricarboxamides are disc-like molecules, which can form rod-like aggregates via amide hydrogen bonds.[8-11] The thus formed liquid-crystalline species are highly viscous at room temperature, but have increased mobility at elevated temperatures when hydrogen bonds are broken and the supramolecular phase changes into a liquid phase. Therefore, the use of this monomer obviates the need for a polymeric binder, while the reactive acrylate groups readily polymerize to form a covalently bonded network by exposure to UV light in the presence of a photoinitiator.[12] The existence of a solid state prior to polymerization, which can be easily broken up into a liquid state at elevated temperature, makes these molecules a second interesting candidate for replacing the polymer/monomer based photopolymers used in current photoembossing.
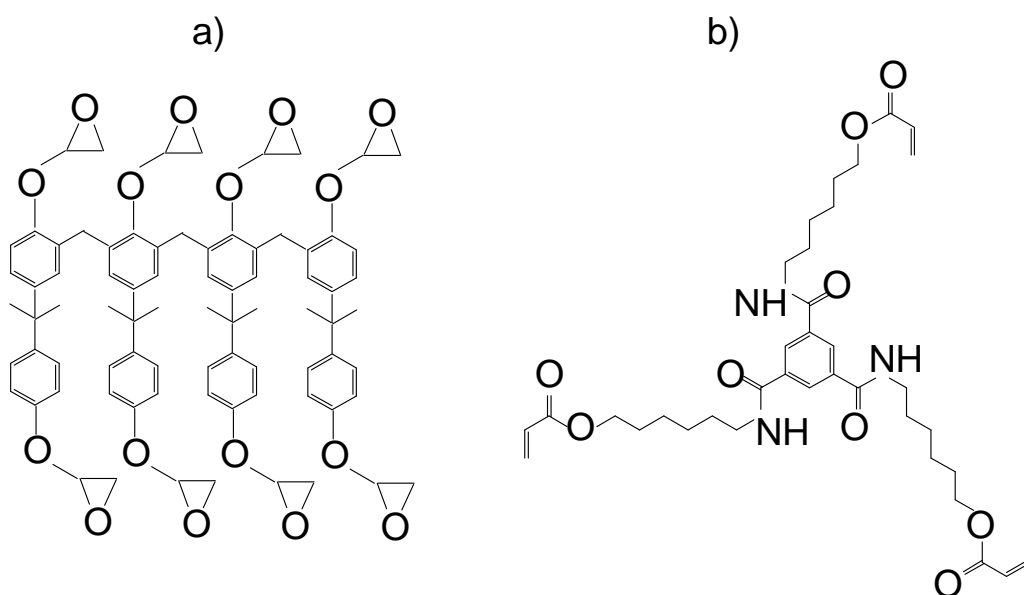

Figure 5.1: Chemical structure of (a) SU-8 and (b) tri(hexylacrylate) benzenetricarboxamide.

The two types of monomers are investigated by first determining the thermal phase behavior (paragraph 5.3.1) of solid films of these materials by differential scanning

calorimetry (DSC) and optical microscopy. In paragraph 5.3.2 and 5.3.3 the suitability as a photopolymer is assessed by measuring the aspect ratio of photoembossed relief structures with confocal microscopy and optimizing their performance for temperature and exposure dose. In paragraph 5.3.4 the systems are compared to each other and the conventional photopolymer.

5.2 Experimental section

5.2.1 Materials and coating procedure for SU-8

SU-8 2010 was purchased from MicroChem and diluted by using SU-8 thinner (MicroChem) to a solid content of 48 wt.-%. No photoinitiator was added to this mixture, since it is already present in SU-8 2010. The solution was spincoated on top of cleaned D263 glass substrates (5 × 5 cm). The substrates were cleaned by rubbing with a sodium hydroxide solution, flushed with demineralized water, rubbed with acetone, rubbed and flushed with ethanol and finally dried with nitrogen. Directly after cleaning the photopolymer solution was spincoated on top of the glass substrates at 2000 rpm with a Karl Suss RC8 spincoater. To remove the solvent the samples were dried for 1 minute at 65 °C and 2 minutes at 95 °C, after which they were cooled to room temperature. The resulting dry films had a thickness of approximately 3 μm.

5.2.2 Materials and coating procedure for hydrogen bonded reactive species

The hydrogen bonding reactive species (tri(hexylacrylate) benzene-tricarboxamides) were synthesized by reaction of benzene 1,3,5-tricarboxylic acid chloride and aminohexylacrylate, which was prepared as follows: to a 40 mL CH_2Cl_2 solution of aminohexanol (5.0 g, 43 mmol), di-*tert*-butyl dicarbonate (10g, 46 mmol) was added slowly. After 3 h of additional stirring, 7 mL of triethylamine was added and subsequently 4 mL of acryloyl chloride was added dropwise, while cooling in an ice bath. After stirring for 3 hours at room temperature the solution was filtered, and 100 mL of CH_2Cl_2 was added. The organic layer was washed with 1 M HCl and 1 M NaOH aqueous solutions and dried over $MgSO_4$. After removal of $MgSO_4$, solvents were evaporated to give the *N*-Boc-aminohexylacrylate as colorless oil. (9.5 g, 81 %). Aminohexylacrylate hydrochloride was obtained after reaction with 2 M HCl diethylether solution and was used for further reaction without purification. Aminohexylacrylate hydrochloride (1.5g, 7.2 mmol) and benzene 1,3,5-tricarboxylic acid chloride (0.50 g, 1.9 mmol) were dissolved in 10 mL of CH_3Cl. To the mixture, triethylamine (1.0 g, 10 mmol) was added dropwise, while cooling in an ice bath. Stirring for 30 minutes was followed by addition of 100 mL $CHCl_3$ and the product was

subjected to column chromatography with a chloroform/acetone gradient (CHCl$_3$ → CHCl$_3$/acetone 3:1 v/v): yield 0.55 g (43 %). ^{1}H NMR (400 MHz, CDCl$_3$): δ = 8.19 (s, 3H, Ph-H), 7.43 (t, 3H, -NH-), 6.4 − 5.8 (m, 9H, acrylate), 4.13 (t, 6H, CH_2CO), 3.38 (m, 6H, -CH_2NH-), 1.7 − 1.4 (m, 24H, other CH$_2$); ^{13}C NMR (100 MHz, CDCl$_3$): δ = 166.6, 135.6, 130.9, 128.7, 128.3, 64.6, 40.3, 29.5, 28.6, 26.7, 25.7. MALDI-TOF MS: Calculated: 669.36, found: 692.30 ([M+Na]$^+$)

To create a solid thin photopolymer film the hydrogen bonded reactive species were dissolved in chloroform in a 1:4 weight ratio. Different concentrations of photoinitiator (Irgacure 819 − Ciba Specialty Chemicals) were added to this mixture. Substrates were cleaned by rubbing with a sodium hydroxide solution, flushed with demineralized water, rubbed with acetone, rubbed and flushed with ethanol and finally dried with nitrogen. A solid film was created on the cleaned substrates (10 x 10 cm) by doctor blading the solution using an Erichsen Coatmaster 509MC-1 with a 20 μm spaced custom build blade. The custom build blade consisted of a rectangular stainless steel block with an outer circumference of 8 x 6 cm and an inner opening of 5 x 1.4 cm. The block contains a 20 μm gap at the bottom of 8 cm sides which connect the inner opening with the outer circumference. A film is created by placing a few drops of solution in the inner opening and moving the block with a constant speed of 25 mm · s^{-1} across the substrate. The obtained film was dried for 30 minutes at room temperature to remove any residual solvent. The thickness of the resulting solid film was approximately 3 μm.

5.2.3 Photoembossing procedure

The coated substrates were exposed using an EXFO OmniCure s-2000 light source (200W High Pressure Mercury Vapor) and a 40 μm periodic line mask with transparent/non transparent ratio of 0.5. To vary the intensity a linearly variable neutral density filter with the optical density ranging from 0.04 to 2 in seven steps was placed on top of the line mask during exposure. After the mask exposure step the samples were gradually heated to the developing temperature at which they were kept for a total of 20 minutes. In a final step the samples were flood exposed for 5 minutes with an intensity of 25 mW · cm^{-2} and cooled to room temperature.

5.2.4 Characterization and evaluation

Differential scanning calorimeter (DSC): The phase transition temperatures were determined with a TA Instruments Q1000 DSC. The thermal behavior of the dry coatings was assessed by mechanically removing the coatings after the solvent was evaporated. In the case of the hydrogen bonded reactive species, the tested coatings did not contain a photoinitiator. The presence of a photoinitiator causes severe polymerization during measurement and as a result no accurate data could be obtained.

The heating and cooling rates were kept constant at 10 ℃ · min^{-1}. The reported temperatures are the onset temperatures and the presented data is the data obtained from the second heating run.

Confocal microscopy: The height of the photoembossed relief structures was investigated using a confocal microscope (Sensofar, PLμ2300) with a 50x objective. In this chapter the height of the structures was used instead of the aspect ratio. This is done to avoid confusion with the previous chapters. The layer thicknesses of the samples in this chapter are, for processing reasons, significantly lower. The aspect ratio can thus not be simply compared with the results from the previous paragraphs.

Conventional microscopy: Optical microscope images were taken in transmission with a Leica CTR6000 equipped with a 50x objective. The samples were measured between crossed polarizers such that crystalline phases appear bright and amorphous phases appear black.

5.3   Results and discussion

5.3.1 Thermal phase behavior photopolymers

First, the thermal phase behavior of the material was investigated by using a DSC. The results for the SU-8 photopolymer are given in Figure 5.2. Here, it can be observed that the material has a glass transition temperature at approximately 31 °C. This value is slightly lower than the literature values which are around 50 °C.[13] Part of this deviation might be caused by using the onset temperature as the actual value of the glass transition temperature. The values for the midpoint (38 °C) or end (45 °C) in the step change are closer to the literature values. The slightly lower value of the glass transition temperature could also indicate the presence of minute amounts of residual solvent, which could act as a plasticizer and reduce the glass transition temperature. However, even SU-8 layers which were dried for 1 hour at 95 °C showed the same thermal behavior. It is thus unlikely that any residual solvent is present. It should be considered that the glass transition is a kinetic effect and depends on the heating/cooling rate. A faster heating will result in a higher glass transition temperature. Different measurement methods will thus result in slightly different values.
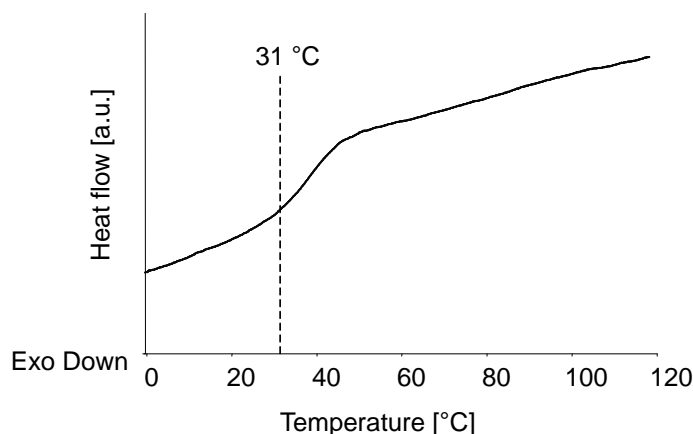
Figure 5.2: DSC curve of SU-8 photopolymer.

The results for the hydrogen bonded reactive species are given in Figure 5.3. The results show two phase transitions of which the first occurs at approximately 55 °C and the second at 100 °C. From the phase behavior reported on similar molecules, it is anticipated that the 55 °C transition is between two liquid crystalline mesophases M_1–M_2.[23] This is supported by polarization microscopy images of a thin supramolecular polymer film taken at different temperatures (Figure 5.4). The polarization microscopy images show that a thin supramolecular polymer layer is birefringent both below and above the 55 °C transition, but ceases to be birefringent above 100°C.
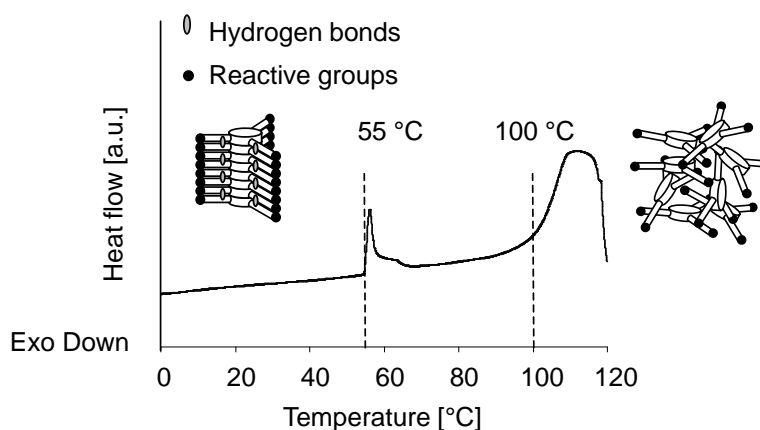

Figure 5.3: DSC curve of the hydrogen bonded reactive species.

During the transition at 55 °C the degree of order decreases. However, the macromolecular structure is at least still partially maintained by the hydrogen bonds. Hence both phases appear birefringent in the polarization microscopy images. During the second transition, the hydrogen bonds become highly dynamic and the system becomes mobile. Here the molecular order changes from M_2 to an isotropic phase (I),

which appears dark in the polarization microscopy images. The DSC results also show that at temperatures above the M_2 - I phase transition an exothermic process sets in. This process is most likely thermal polymerization of the material. From these results it is therefore expected that for surface relief development a temperature between 100-120 °C is most preferred. At these temperatures the reactive species are in a mobile phase and can easily diffuse. On the other hand, the temperature is low enough to avoid significant thermal polymerization, which would limit diffusion of the reactive species to the exposed areas during the photoembossing procedure.
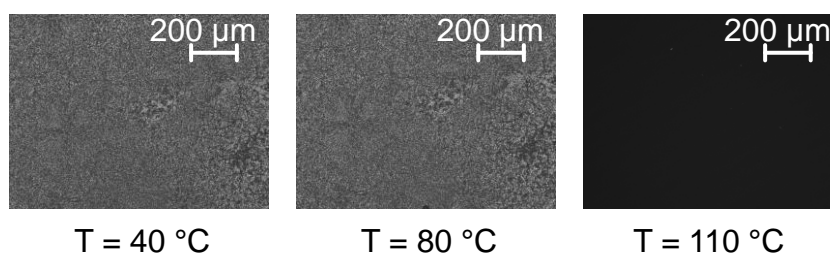

Figure 5.4:   Optical microscope images between crossed polarizers for 3 μm thick coating of hydrogen bonded reactive species at different temperatures.

5.3.2 Developing temperature

The DSC data has shown that in both photopolymers a phase transition occurs between a solid and mobile phase. It is not yet clear whether these transitions can be used to create relief structures by photoembossing. Therefore, first the effect of the developing temperature on the structure height was investigated. The SU-8 samples were exposed to an exposure dose of 60 mJ · cm^{-2}, which is common dose used for a 3 μm layer in photolithography.[14] The results are given in Figure 5.5. First of all it is observed that relief structures are formed upon heating (development). The height depends on the temperature and a maximum is obtained between 155-190 °C. This temperature is significantly higher than the glass transition temperature of the material as observed in Figure 5.2. The relatively large SU-8 monomers have low mobility just above the glass transition. With increasing temperature the mobility increases and higher structures are obtained. Based on these results a developing temperature of 175°C was used for further experimentations.
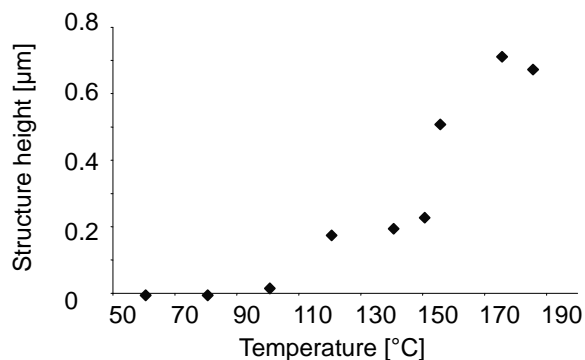
Figure 5.5: Influence of the developing temperature on the structure height when using the SU-8 photopolymer.

The results for the hydrogen bonded species are given in Figure 5.6. For these experiments a photopolymer mixture of supramolecular polymer (95 wt.-%) and initiator (5 wt.-%) was used. These samples were mask exposed using a $0.54 \text{ J} \cdot \text{cm}^{-2}$ exposure dose. The results show that structure development occurs at the onset of the M_2 - I phase transition, at 100 °C. Below this temperature no significant structure development was found to occur. This shows that the mobility of the monomer in the M_2 phase is still low and no large scale diffusion of reactive species can occur in this phase. At a temperature above 120 °C the height of the structures was found to decrease. This confirms that the significant thermal polymerization observed in the DSC measurements does indeed hinder the diffusion of the reactive species. Based on these results a developing temperature of 115 °C was used for further experimentation.
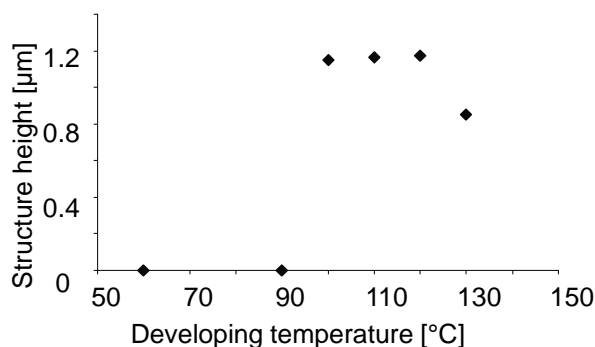

Figure 5.6: Influence of developing temperature on structure height on hydrogen bonded photopolymer.

5.3.3 Exposure dose

In the previous paragraphs it was demonstrated that both the SU-8 and the hydrogen bonded reactive species can be used as photopolymers. Also the optimal developing temperature was determined. In this paragraph the exposure dose is optimized to

determine the optimum conditions for relief formation in the two systems. In Figure 5.7 the structure height at different exposure doses is given for the SU-8 photopolymer. It is observed that at an optimal structure height is obtained by using an exposure dose between 30-100 mJ · cm^{-2}. This is approximately the same optimal exposure dose found for material in photolithography.[14]
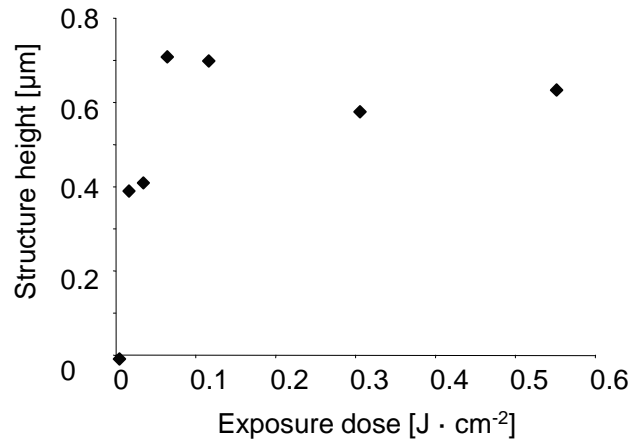

Figure 5.7:   Influence of exposure dose on structure height of SU-8 photopolymer.

In the case of SU-8, the concentration of initiator was not varied since an optimal concentration (at least for photolithography) was already present in the resin. For the hydrogen bonded species, also the optimal initiator concentration was determined. It can be observed from the results (Figure 5.8) that the height of the photoembossed relief structures is influenced by both the photoinitiator concentration and exposure dose. An optimal initiator concentration was found within the range of 5-9 wt.-% with an optimal exposure dose between 0.2 and 0.5 J · cm^{-2}. The results are similar to the optimization curves of the conventional polymer/monomer based photopolymer systems.[1-3] For these systems it has been proposed that that at low exposure dose or low initiator content only a small amount of the initiator is activated. This results in a low conversion by early termination of the reaction/diffusion process and consequently low structure heights. At a high exposure dose or high initiator content, monomer diffusion to the center of the developing structures is hindered by the densely crosslinked network that has formed due to the high monomer conversion. As a result, diffusing monomer accumulates at the edges of the developing structures and typical peaks appear at the contour of the final relief structure.[2]
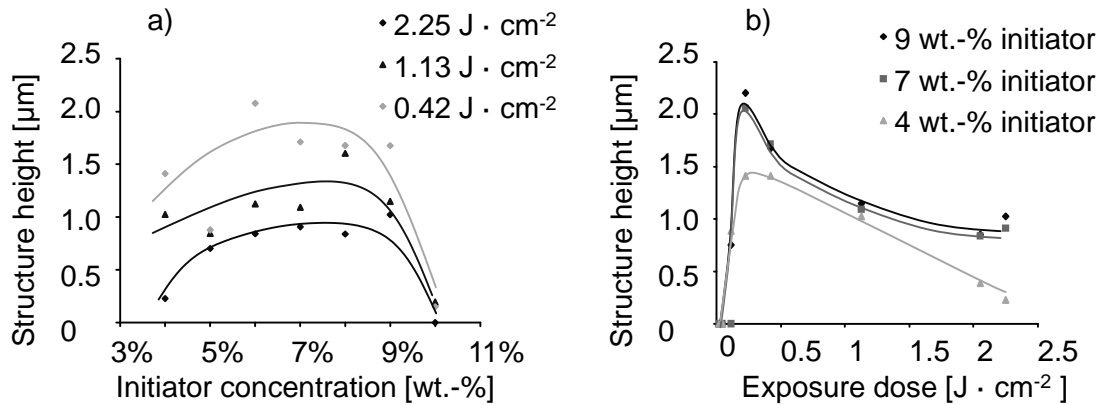
Figure 5.8: Influence of the photoinitiator concentration (a) and exposure dose (b) on the structure height of the hydrogen bonded photopolymer.

To investigate the appearance of peaks at contours of the relief structures, microscope images were taken of photoembossed relief structures positioned between crossed polarizers. The microscope images were compared to the corresponding height profiles as measured by the optical profilometer and the result are given in Figure 5.9. The images show that at the maximum structure height the sample were not birefringent. It can thus be concluded that after developing at 115 °C, and the final flood exposure at the same temperature, both the exposed and unexposed areas were fixed in the isotropic state. When the samples are overexposed, and thus the structure height is reduced and typical peaks appear at the edges of the structure, it is observed that the exposed areas were birefringent. This shows that in these areas the hydrogen bonded reactive species are polymerized into mesophase M_1 or M_2 before the mobile isotropic phase is reached during the heat development. This supports that the reduction in structure height, as well as the appearing of the peaks at the edges of the structures, at overexposed samples is indeed due to reduced mobility at the centre of the structures.
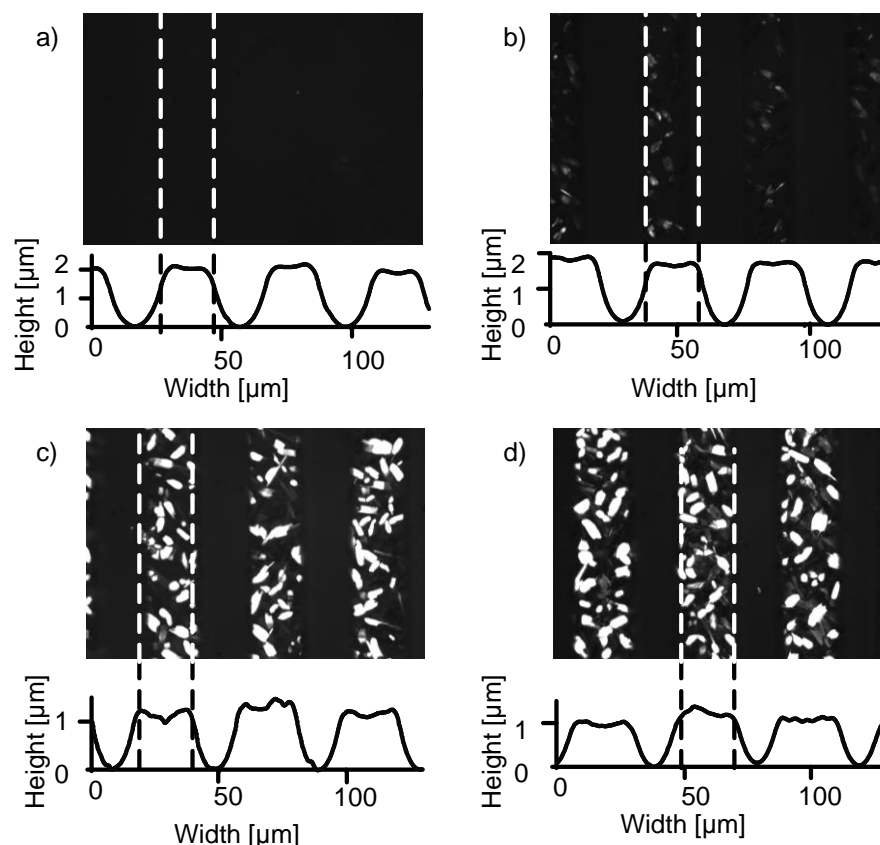
Figure 5.9: Optical microscope image between crossed polarizers and corresponding height profiles of surface relief structures containing 9 wt-% of photoinitiator and UV mask exposed to 0.23 (a), 0.42 (b), 1.13 (c), and 2.05 J · cm^{-2} (d).

5.3.4 Comparing photopolymers

From the results in the previous paragraph it can be concluded that photopolymers which basically consist of monomers can be successfully used for photoembossing. Especially in the case of the hydrogen bonded species high structures were obtained. It is remarkable that under optimal conditions the structure height can be tuned up to an observed relief height of 2.1 μm. Considering that the original layer thickness is approximately 3 μm it can be concluded that under optimized conditions a surface relief structure can be developed with a height equal to 70 % of the original layer thickness. To elucidate this effect, part of a photoembossed supramolecular thin film was mechanically removed from the substrate and a confocal microscope image was taken which shows the total film including the surface relief structure. The image (Figure 5.10) clearly show that structure height is large compared to the film thickness. The structure height (Figure 5.10b) is 2.1 μm measured from the top to the bottom of the structure and the remaining film thickness underneath is 1.9 μm (Figure 5.10c).
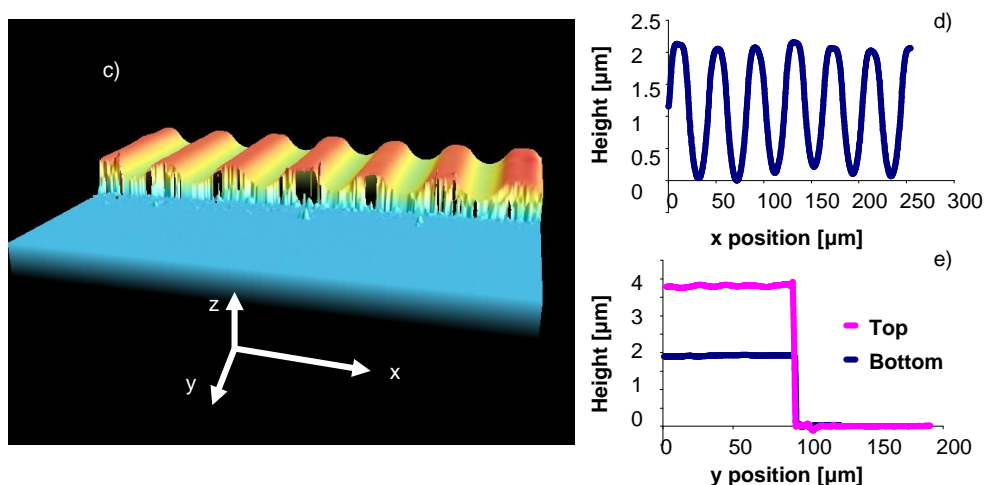
Figure 5.10: 3D confocal microscopy image (a) and a cross-sectional profile of a relief structure (b), and a cross-sectional profile (c) showing the remaining film thickness for a sample containing 6 wt.-% of initiator and mask exposed to $0.42\,J \cdot cm^{-2}$.

These results show a significant improvement over conventional photopolymers for photoembossing such as described in the previous chapters. Literature values reported on polymeric binder based photopolymers indicate that under similar conditions a maximum structure height of 800 nm can be expected.[1-3] These values are confirmed by measuring the height of relief structures obtained in a 3 μm layer thick reference photopolymer and a reference photopolymer with *tert*-butyl hydroquinone (TBHQ) (Chapter 3). The samples were processed under optimal conditions. The values in Table 5.1 clearly show that the reference samples, even with TBHQ, produces lower structures.

	Reference	Reference + TBHQ	Hydrogen bonded species
Processing atmosphere	Air	Nitrogen	Air
Max. structure Height [μm]	0.6	1.4	2.1

Table 5.1: Comparison structure height of 3 μm thick layer of different photopolymers.

Although it was not investigated, it can be expected that the addition of TBHQ to the hydrogen bonded species results in even higher surface reliefs. Both the conventional monomer/polymer and hydrogen bonded species photopolymers are based on acrylate chemistry. The new photopolymer is thus compatible with the chemistry of TBHQ. The extent of the improvement in relief height will, however, depend on other effects such as monomer functionality and the presence of a liquid-crystalline phase. These effects

will influence the trapping of radicals, the polymerization kinetics and thus the improvement by TBHQ.

The structure heights obtained by the SU-8 photopolymer resulted in lower structures than the hydrogen bonded species based photopolymer. It is believed that the main reason for this is the high number of functional groups present at monomer. These will form a densely crosslinked network which hinders monomer diffusion. It can thus be expected that similar molecules with less functional groups should result in higher structures. To test this hypothesis, a photopolymer based on Epon 164 (Hexion Specialty Chemicals) was developed. EPON 164 consists of SU-8 type of molecule with on average 4.1 epoxide groups. After optimization of the developing temperature and exposure dose it was found that a maximum structure height of 1.3 μm could be obtained. This is over twice as high as could be achieved with the SU-8 photopolymer. Less functional groups thus appear to have a positive effect on the relief development. Part of the improvement might also be attributed due to the smaller molecule size.
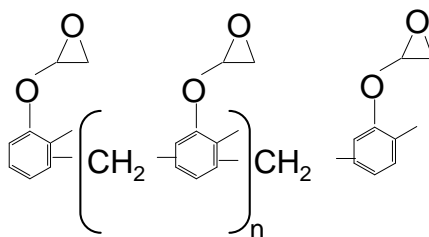

Figure 5.11:   Chemical structure of EPON 164.

5.4   Conclusion

In this chapter the possibilities of a photopolymer without polymeric binder were investigated. It was demonstrated that monomers which are solid at room temperature due to steric or dipole-dipole interactions can be used as photopolymers.

A typical monomer which is solid at room temperature due to steric effects is SU-8. This material consists of relatively large monomers which have a glass transition temperature of 31 °C. Using the photoembossing procedure, relief structures can be developed at an optimal temperature of 155-190 °C. This temperature is much higher than the glass transition temperature. Most likely this is caused by the large size of these molecules. As a result, high temperatures are required to create enough diffusional mobility. After optimization of the exposure dose it was found that structures of approximately 0.7 μm could be obtained in a 3 μm thick layer. Although this proves the concept, the actual value is still low. Higher structures (1.3 μm) were obtained by using EPON 164, which has less functional groups than SU-8. This reduces gel formation and the network density in the exposed areas and enhances the diffusion of monomer.

Tri(hexylacrylate) benzenetricarboxamide was used to investigate a photopolymer based on monomers which become solid at room temperature due to dipole-dipole interaction. These molecules form a supramolecular polymer at room temperature, and are highly mobile at elevated temperatures. The disc-like molecules can form rod-like aggregates via amide hydrogen bonds. Above a temperature of 100 °C, the rod-like aggregates collapse and an isotropic phase is formed. It is found that these molecules are well suitable as a photopolymer. The maximum structure height is obtained by using a developing temperature of approximately 100-120 °C. This range is determined by a lack of diffusional mobility when the molecules are in the mesophase (<100 °C) and thermal polymerization in the non-exposed areas at temperatures above 120 °C. By optimizing the photoinitiator content and exposure dose, structures were obtained of 2.1 µm. This system outperforms the conventional photopolymer as well as the photopolymers from chapter 2-4. It demonstrates the high performance which can be obtained by a photopolymer without polymeric binder.

5.5 References

[1] B-J de Gans, C. Sánchez, D. Kozodaev, D. Wouters, A. Alexeev, M. J. Escuti, C. W. M. Bastiaansen, D. J. Broer, U. S. Schubert, *J. Comb. Chem.* **2006,** *8,* 228.

[2] C. Sánchez, B.-J. de Gans, D. Kozodaev, D. Wouters, A. Alexeev, M. J. Escutti, C. Van Heesch, T. Bel, U. S. Schubert , C. W. M. Bastiaansen, D. J. Broer, *Adv. Mater.* **2005**, *17*, 2567.

[3] N. Adams, B-J. De Gans, D. Kozodaev, C. Sànchez, C. W. M. Bastiaansen, D. J. Broer, U. S. Schubert, *J. comb. Chem.* **2006**, *8*, 184.

[4] T. S. Chow, *Macromol.*, **1980**, *13*, 362.

[5] A. del Campo, C. Greiner, *J. Micromech. Microeng.* **2007**, *17***,** R81.

[6] E. Koukharenko, M. Kraft1, G. J. Ensell, N. Hollinshead, *J. Mater. Sci. Mater. Electron.*, **2005**, *16***,** 741.

[7] A. W. Bosman, L. Brunsveld, B.J.B. Folmer, R.P. Sijbesma, E.W. Meijer, *Macromol. Symp.* **2003**, *201*,143.

[8] Y. Matsunaga, N. Miyajima, Y. Nakayasu, S. Sakai, M. Yonenaga, *Bull. Chem. Soc. Jpn.* **1988**, *61*, 207.

[9] J. J. van Gorp, J. A. J. M. Vekemans, E. W. Meijer, *Mol. Cryst. Liq. Cryst.* **2003**, *397*, 191.

[10] M. P. Lightfoot, F. S. Mair, R. G. Pritchard, J. E. Warren, *Chem. Commun.* **1999**, 1945.

[11] M. Masuda, P. Jonkheijm, R. P. Sijbesma, E. W. J. Meijer, *Am. Chem. Soc.* **2003**, *125*, 15935.

[12] A. R. A. Palmans, J. A. J. M. Vekemans, H. Fischer, R. Hikmet, E. W. Meijer, *Chem. Eur. J.* **1997**, *3*, 300.

[13] R. Feng, R.J. Farris, *J. Micromech. Microeng.* **2003**, *13*, 80.

[14] www.microchem.com

Chapter 6

Applications for photoembossing

In this chapter several applications for photoembossing are demonstrated. These applications exploit the enhanced performance, which has been developed in the previous chapters, and the unique non-contact (i.e. heat) relief developing method of photoembossing. First, it is demonstrated that photoembossing can be used to create a microlens array. Current processing techniques for microlens arrays are mainly based on replication. The optical characteristics of the lenses are restricted to the mold design. In addition, post processing of the lenses is required to reduce the reflection losses and increase the quality. It is demonstrated that photoembossing can be used to create microlens arrays of which the optical characteristics can be easily controlled by tuning the processing parameters. The technique is shown to be particularly interesting since additional coatings (e.g. a solution processable antireflection coating) can be applied prior to the development of the microlens array when the film is still flat. This stimulates the formation of films with a homogeneous thickness distribution and obviates the use of further post processing steps. Secondly, a new in-situ method for sealing an array of pre-filled micro-cavities, such as encountered in electrophoretic displays, is presented. Photoembossing can be used to form a hermetic seal between the cover and the micro-cavity walls. The seal locations are defined by ultraviolet (UV) exposure through a photolithographic mask, forming a latent image overlapping with the locations of the cavity walls. During a thermal development step, while the cover is mounted on top of the micro-cavities, the seal evolves and makes firm contact with the cavity walls. This concept is demonstrated to be insensitive to small deviations in cavity height, flatness of the cover and thin fluid films remaining between the cover and the top of the cavity walls. In the past these aspects made it difficult to effectively seal large area devices. Finally, photoembossing can also compete with the currently used technologies based on its low material and processing costs. For example the technique can be used to create small protrusions which are used to increase the viewing angle in liquid crystal displays. These display components are currently manufactured via expensive lithographic techniques since replication techniques would damage the glass substrate or other components. Photoembossing simplifies the production process, but the remaining photopolymer layer in between the protrusions increases its power consumption. Other applications can be single use products such as replication mold or stamps.

6.1   Introduction

In the previous chapters several methods have been discussed to enhance the performance of photoembossing. These methods increase the aspect ratio of the surface relief structures such that features of several microns high can be obtained. In this chapter the improved aspect ratio is utilized to investigate new applications for photoembossing. It is especially the unique non-contact method of development by heat, which is an interesting feature. This allows relief structures to be developed when direct contact with etching fluid (photolithography) or a mold (replication) is not possible. This feature is exploited by creating microlens arrays with antireflection coatings in paragraph 6.2. In paragraph 6.3 it is demonstrated that the non-contact development can be used to in-situ seal an electrophoretic display. The technique of photoembossing is also characterized by low-cost and the ease of processing. Some possibilities where these properties can be exploited are briefly discussed in paragraph 6.4.

6.2   Antireflection coated microlens array

Microlens arrays are widely used as essential optical components for communication, imaging and sensing systems. Typical examples for their use are array based applications such as fiber optic array coupling and collimation, arrayed laser diode collimation, arrayed waveguide to fiber coupling and CCD camera arrays. In the display field they are for instance used in LCD based projectors, backlight homogenizers and 3D displays. Microlens arrays are often fabricated using replication techniques next to a variety of other processes like photoresist reflow, ion-milling, ink-jet printing and laser ablation.[1-5] These techniques are however complex and require several processing steps to obtain a well defined array of microlenses. In addition the shape and focal length of the lenses is often inherent to the manufacturing technique and cannot be altered by a simple modification of processing parameters. To increase the efficiency of the microlens array, the surface is usually coated with an antireflection coating. These layers can only be applied after manufacturing of the lenses themselves since contact with for example a replication mold would damage or remove the coating. Also it is difficult to use low cost, solution processable antireflection coatings since the relief of the microlenses causes uneven spreading of the coating and thus a variation in layer thickness.

   In this study it is investigated whether photoembossing can be used for creating an antireflection coated microlens array via a simple process. It is first investigated if photoembossing can be used to create a microlens array (without antireflection coating). The optical quality is assessed and the effect of the different processing parameters is evaluated. Next, it is attempted to apply a solution processable antireflection coating to the photopolymer layer prior to the development of the structures. The film is then still

flat which would stimulate the formation of films with a homogeneous thickness distribution by for instance spin coating. In addition no further post processing steps are required. In the case of photolithography and hot embossing such a coating, which is based on nano particles, would be removed or at least damaged by the etching fluids or embossing mold when applied before manufacturing of the microlenses.

6.2.1 Experimental

As a photopolymer, polybenzylmethacrylate (M_w 70 kg mol^{-1}; Scientific Polymer Products) was used as a polymeric binder, dipentaerythritol penta/hexa-acrylate (Sigma Aldrich) as a multifunctional monomer, *tert*-butyl hydroquinone (Sigma Aldrich) as a retarder and Irgacure 819 as a photoinitiator (CIBA Specialty Chemicals). As a solvent a 50/50 wt.-% mixture of ethoxypropylacetate (Avocado Research Chemicals) and propyleneglycol-methyletheracetate (Aldrich) was used. The photopolymer solution consisted of 23.5 wt.-% polymeric binder, 23.5 wt.-% monomer, 2.4 wt.-% photoinitiator, 3.6 wt.-% retarder and 47 wt.-% solvent. The photopolymer solution was spin-coated on a glass substrate at 800 rpm and dried for 20 minutes at 80 °C in order to remove residual solvent, resulting in dry films with a thickness of approximately 16 micron. OptoClear^{TM} (DSM) was applied as an antireflection coating on top of the dried photopolymer film by spincoating from solution at a speed of a 3000 rpm.[6] To avoid contact between the photopolymer and the alcohol based liquid medium, a barrier layer (±125 nm) consisting of polyvinylalcohol was deposited in between the two layers. The barrier layer was deposited on the photopolymer by spincoating a water based solution containing 5 wt.-% of polyvinylalcohol (Mw 31 - 50 kg mol^{-1}; Sigma Aldrich). After applying the barrier and the antireflection layer to the photopolymer the photoembossing procedure was performed (Figure 6.1).

The samples were exposed through a photolithographic mask with an EXFO OmniCure s-2000 light source (I = 10 mW · cm^{-2}). The photolithographic mask (1 x 1 cm) contained a hexagonal packing of 30 μm transparent holes that were separated from each other by a 30 μm spacing. After exposure the masks were removed and the samples were placed on a hotplate which was at a temperature of 110 °C. Finally, a flood exposure (I = 10 mW · cm^{-2}) was applied for 5 minutes while the sample was still at a temperature of 110 °C. To prevent oxygen inhibition during exposure, development and flood exposure, the samples were placed under a protective atmosphere by constant argon blanketing using a custom built aluminum box which contained a quartz glass window through which the samples could be exposed to UV light.

The resulting structure heights were measured with an optical profilometer (Sensofar Plμ 2300) using a 50x objective. The confocal measurements were performed with a an inverted Zeiss LSM 510 microscope equipped with a Plan Neofluar 10x/0.3

objective while using the halogen light source and a HeNe laser (543 nm) simultaneously.
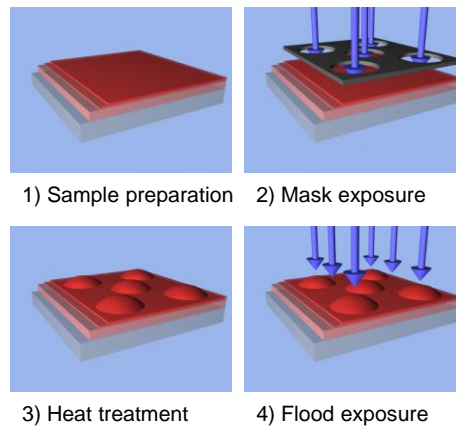

1) Sample preparation 2) Mask exposure

3) Heat treatment 4) Flood exposure

Figure 6.1:   Schematic representation of multi layer photoembossing. In this procedure, an additional coating (e.g. antireflection coating) is applied on top of a dried photopolymer layer before the patterned illuminated, heating and flood exposure step are applied.

The relative reflectance of a 1x1cm array of microlenses was measured using a UV-3100 UV-VIS-NIR spectrometer (Shimadzu) equipped with MCP-3100 external sample compartment. The samples were mounted at the back of the integrating sphere in the external sample compartment under an angle of 8-degree with respect to the incident sample beam. The reflection at the glass back surface of the samples was determined by measuring a flat glass substrate and the result was subtracted from the data obtained from microlens containing samples.

6.2.2 Results and discussion

It was first investigated if photoembossing could be used to create a microlens array (without antireflection coating). Since the shape (and thus the focal characteristics) of photoembossed relief structures is mainly controlled by three processing parameters; the exposure dose, developing temperature and developing time, we first investigated the effect of these parameters on the geometry of photoembossed microlenses. The microlens profile for different exposure doses is given in Figure 6.2. It is observed that compared to other reaction/diffusion processes, based on for example sold-gel hybrid materials, the exposure dose required to obtain a microlens with photoembossing is relatively low.[7,8] The height of obtained microlenses increased with increasing exposure dose. From conventional lenses it would be expected that an increase in height results, at constant lens diameter, in an increased curvature of the lens and consequently a reduction of the focal length. The curvature at the top of photoembossed microlenses

however did not increase with increasing height, but instead maximized at an exposure dose of 200 mJ $\cdot$ cm^{-2} (see Figure 6.2a). This maximum curvature can be explained by considering that during an exposure step, radicals are created in the exposed areas by activation of the photoinitiator in the photopolymer with UV light. Upon heating of the photopolymer these radicals locally initiate polymerization, creating a difference in monomer concentration between unexposed and exposed areas. As discussed in Chapter 2, it is the polymerization of monomer in the exposed areas that is the main driving forces for the diffusion of monomeric species to these areas.[12, 13] Although a high radical concentration increases the driving force for diffusion it also causes an increase in crosslink density in the exposed areas. As a result the diffusion of monomer to the centre of the developing microlenses is hindered. It is the balance between driving force and crosslink density that causes the curvature of the microlenses to reduce although the height still increases.
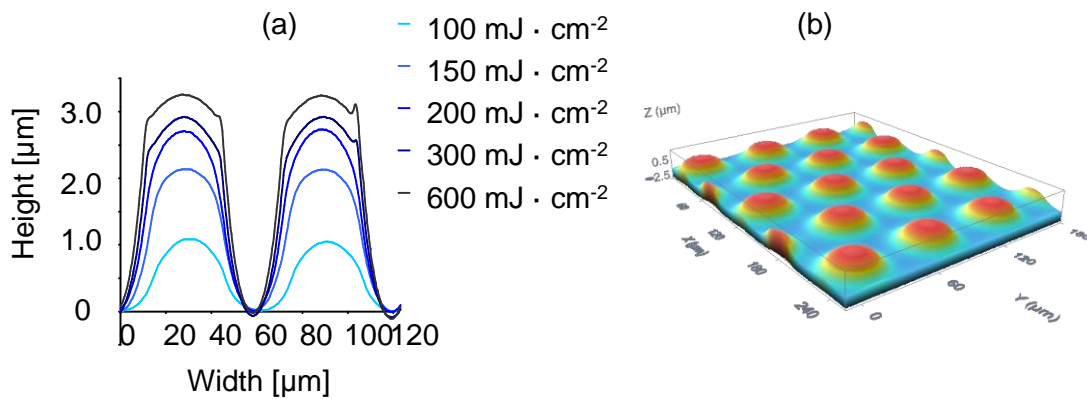

Figure 6.2:   (a) Shape of photoembossed microlenses for different exposure doses and (b) a 3D profile of a microlens array.

To confirm that the curvature of photoembossed microlenses indeed maximizes, the focal length of the obtained lenses was measured with confocal microscopy. The results, which are given in Figure 6.3a, show that at an exposure dose of 200 mJ $\cdot$ cm^{-2} a minimum focal length of 225 μm was obtained. A visual inspection of the focal plane, given in Figure 3b, showed a uniform distribution of the focal spots with a diameter of 8 μm, indicating good focusing characteristic. This observation concurs with confocal microscope measurements of the optical path of a collimated light source through the microlens array (Figure 6.4). Here, the red lines are from an additional laser light source which reflects from the front and back surfaces of the sample. It can be observed that the collimated light is focused in a repetitive and consistent manner by each single microlens within the array. For both an exposure dose higher and lower than 200 mJ $\cdot$ cm^{-2} in an increase in focal length of the microlenses was observed. An exposure dose above 200 mJ $\cdot$ cm^{-2} resulted however in increased optical aberrations at the focal spots

(Figure 6.4b). These aberrations most likely occurred because of the discontinuation in the shape of the microlenses which can be observed in Figure 6.2a. This discontinuation was a result of the difference in the diffusion mobility of the reactive species in the (crosslinked) exposed and non-exposed areas. The different curvature of the top (exposed) and bottom (non-exposed) part of the lenses caused these areas to have two different focusing characteristics, explaining the occurrence of optical aberrations when a relatively high exposure dose was used.
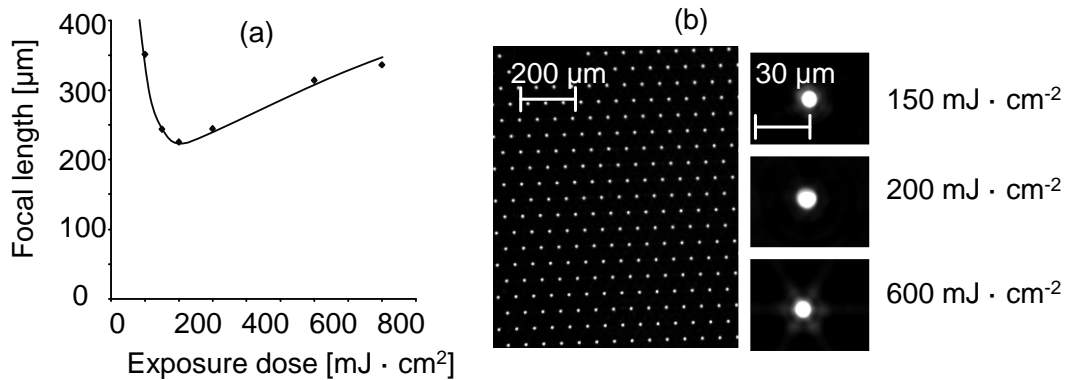

Figure 6.3: (a) The effect of the exposure dose on the focal length and (b) corresponding focal spots.

The effect of the developing time and temperature on the shape of a photoembossed microlens is given in respectively Figure 6.5a and b. It can be observed that in the initial stage of the developing step two small peaks were present at the edges of the exposed areas. These peaks grew in size and their position moved to the centre when the developing temperature and/or time were increased. Eventually the peaks overlapped, after 2-5 minutes at a temperature of 110 ºC, and a microlens was obtained of which the height increased only minimally with increasing time/temperature.

The time and temperature required for obtaining a microlens array are relatively fast compared to other reaction/diffusion techniques.[9] The observed phenomenon can be explained by considering that a heat treatment influences the mobility of reactive species in a polymeric matrix. Due to low mobility of reactive species during the initial stage of the development, both diffusion and polymerization are inhibited. As a result, only a small fraction of the reactive species is displaced over a small distance, causing the appearances of peaks at the edges of the exposed areas. When the mobility of the system is increased both polymerization and diffusion are enhanced and a larger fraction of reactive species diffuses over a longer distance. The diffusion of reactive species stops at the centre of the exposed areas.
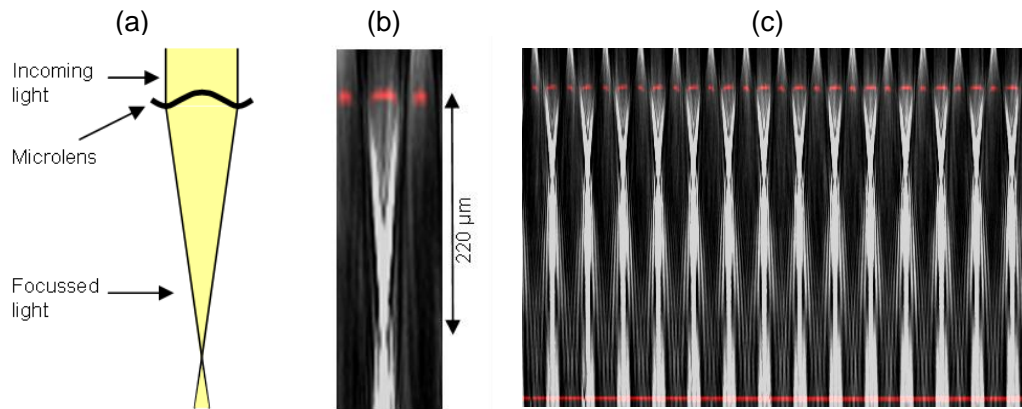
Figure 6.4: (a) Schematic representation and (b) confocal image of the optical path of a collimated light source through a single photoembossed microlens and (c) array of microlenses (exposure dose = 200 mJ · cm^{-2}, developing time is 300 seconds at a temperature of 110 °C).

One particularly interesting feature of photoembossing is that microlenses are developed in a non-contact process as opposed to for example hot-embossing or photolithography. To exploit this property and avoid post-processing of the microlenses we investigated the possibility of applying an antireflection coating to the array of microlenses by applying the coating on top of the photopolymer layer prior to the exposure and developing step. It is aimed that the antireflection coating deforms along with the developing relief structure during processing. For this experiment we used OptoClear^{TM} (DSM), which is based on a dispersion of nanoparticles, as a solution processable antireflection coating.
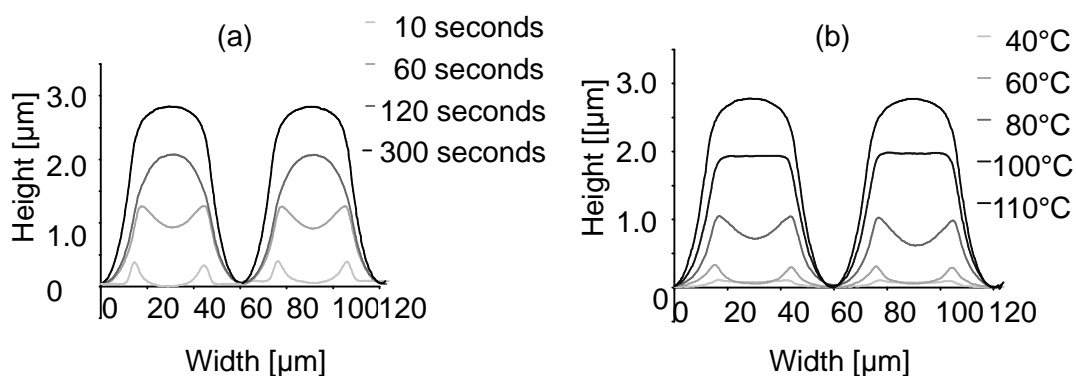

Figure 6.5: (a) Shape of photoembossed microlenses for different developing times and (b) developing temperatures.

The reflection losses of the front surface of a microlens array with and without an antireflection coating were measured and the results are given in Figure 6.6. The results

clearly show that a sample with antireflection coating had significantly less reflection losses than a sample without antireflection coating. The reference sample has a reflection of approximately 4.3% (at 500 nm), which is close to the expected value (R = 4.5%) based on the refractive index of the photopolymer (n = 1.55). When measuring the reflection of a sample containing a flat photopolymer layer (R = 4.5%) it is concluded that this small deviation is caused by the refraction of light through the microlens array.
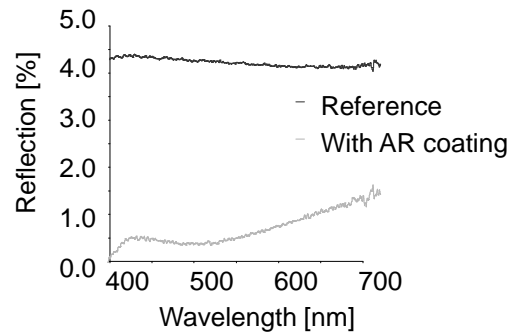

Figure 6.6:   Reflection from the surface of a photoembossed microlens array with and without antireflection coating.

On the sample with the antireflection coating the reflection is reduced to approximately 0.4%. It should be noted that also here the reflection is slightly lower than compared to a flat layer (R = 0.7%) due to refraction of light by the microlens array. From these results it can thus be concluded that the antireflection coating was successfully applied to the microlenses without any post-processing steps. Antireflection coatings like OptoClear^{TM} (DSM) are based on nano-particles which are applied from solution (Figure 6.7). In conventional replication techniques or resist reflow photolithography it is not possible to apply the nano-particles to the flat polymeric layer prior to the manufacturing of the array of microlenses. The particles would be damaged or completely removed upon contact with a mold or the etching fluids. In addition, when applying a coating from solution after development of surface structures will lead to an uneven layer thickness. Although the concept of applying additional coatings prior to development has been demonstrated here by means of an antireflection coating other coatings are possible. Such coatings can for example be anti-scratch coatings, antifogging coatings, semitransparent reflective coatings or diffractive gratings.[10]
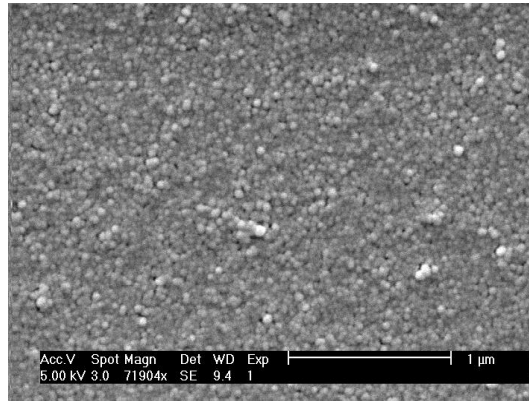
Figure 6.7:   SEM image of OptoClearTM (DSM) antireflection coating.

6.2.3 Conclusion

In conclusion we have shown that photoembossing can be used to create complex, multi-layer micro optical elements such as an antireflection coated microlens array. The base process was a coated solid thin film containing photoreactive components which after mild local exposure to UV light (dose $\leq$200 mJ · cm^{-2}) formed a surface relief structure by moderate heating (t = 120-300 seconds and T = 110 ℃). The total processing time is in the range of several minutes, which is significantly faster than other reaction/diffusion mechanisms requiring hours. The lens properties and quality in terms of the absence of aberrations can be controlled by the irradiation and processing conditions. An antireflection coating was applied to the photoreactive film prior to exposure and development step when the film was still flat. Upon deformation of the photoreactive film and developing of the microlens array the additional layers deforms conformably. Microlens arrays coated with high quality antireflections were obtained.

6.3   Sealing an electrophoretic display

Electrophoretic displays are becoming increasingly more important because of their low power consumption, ease of manufacturing and flexibility.[11,12] Unlike their liquid crystal counterparts, these non-emissive display devices exhibit superior readability over a wide range of viewing angles and ambient light conditions. An electrophoretic display is based on the (wavelength selective) scattering and/or absorption of ambient light by charged particles in colloidal suspensions. These charged particles are controlled by means of an electric field applied between drive electrodes. In a simple electrophoretic cell the fluid containing the charged particles is sandwiched between the transparent electrode surfaces of two parallel plates which are separated by spacers.[13] It is also possible to drive the electrophoretic ink via in-plane switching, by positioning the driving electrodes in the plane of only one of the plates. Independent on the mode of operation, it is preferred to restrict the undesired movement of the particles between

adjacent cells.[14] This can be done by partitioning of the space between the two plates into smaller cavities and equally distributing the colloidal suspension over these micro-cavities. However, the hermetic sealing of these cavities is, as also known from other devices comprising pre-filled cavities or channels, a challenging task.[15-17] Often these cavities are made by photolithography or hot-embossing during which, due to local differences in processing conditions, small deviations in the geometry of the single cavities in the array arise. The most challenging deviations are the resulting differences in cavity height. This is because a gap remaining between the top of the cavity walls and the cover can potentially result in the undesired movement of electrophoretic material between adjacent cells. Another contribution to leaking cavities results from the surface flatness of the cover and carrier plates.

Common methods used to seal micro-cavities are for example adhesive, fusion and anodic bonding.[15] These methods are less suitable for sealing a large scale array of fluid filled micro-cavities, since they do not sufficiently compensate for the above mentioned deviations. In addition, capillary action often creates a thin fluid film between the cover and cavity walls, which also prevents accurate sealing. Therefore several specific methods have been proposed to seal an electrophoretic display, each with its own merits and draw-backs. In one method a photopolymerizable substance is added to the electrophoretic ink, which is then positioned between two parallel plates. [18] Next, sealed micro-cavities are created by applying a patterned ultra violet (UV) exposure, causing the photopolymerizable monomer to polymerize in the exposed areas and diffuse away from the non exposed areas. It is however known from similar concepts, as for example encountered in the photo-enforced stratification of liquid crystal / monomer mixtures, that any photopolymerizable component remaining in the non-exposed areas, which are the pixels, influences the optical and electrical properties of the final device.[19] In another method a thermoplastic or thermoset precursor is dispersed into the colloidal suspension.[20] The precursor is immiscible with the ink and has lower specific density. After filling of the micro-cavities with the mixture of precursor and electrophoretic ink, the precursor phase separates from the electrophoretic ink and forms a thin layer on top of the fluid. This layer is then polymerized by heat or radiation to form a hermitic seal. Alternatively sealing can be accomplished by coating the electrophoretic ink with a solution containing the precursor. Because the formed seal is thin, additional mechanical strengthening is often applied. Furthermore precision filling of the array of micro-cavities is mandatory since the seal always develops on top of the ink. As a result the device can only be sealed effectively when no electrophoretic ink is present on top of the cavity walls.

In this study it is investigated if photoembossing can be used for sealing an array of pre-filled micro-cavities, such as encountered in an electrophoretic display. This technique allows an in-situ development of surface relief structures even if the

photopolymer is physically inaccessible by e.g. etching fluids or hot-embossing masters. It is this particular property of photoembossing that makes it an attractive technique for trying to seal a large sized array of pre-filled micro-cavities.

6.3.1 Materials and processing

Sample preparation

To demonstrate the sealing potential by photoembossing an in-plane switching electrophoretic device was manufactured. As can be seen in Figure 6.8, the device consists of an electrophoretic ink which is positioned between a bottom carrier and a cover plate. The electrophoretic ink comprised of a mixture of charged particles dispersed in a transparent paraffin solvent.

The bottom carrier comprised of a rigid glass substrate, interdigitated electrodes and an array of 100 x 200 micro-cavities. The micro-cavities were made of SU-8 photoresist via a standard photolithographic procedure. A single cavity in the array measured 180 x 180 x 10 μm in size and was separated from its nearest neighbors by means of a 20 μm wide cavity wall. The 120 μm spaced interdigitated drive electrodes were made of indium tin oxide (ITO) via conventional procedures.

The cover plate consisted of a rigid glass substrate coated with a photopolymer layer, applied via solution processing. The photopolymer solution consisted of 23.5 wt.-% polymeric binder, 23.5 wt.-% monomer, 3.6 wt.-% retarder, 2.4 wt.-% photoinitiator, and 47 wt.-% solvent. In this study polybenzylmethacrylate (M_w 70 kg mol^{-1}; Scientific Polymer Products) was used as a, polymeric binder, dipentaerythritol penta/hexa-acrylate (Sigma Aldrich) as a multifunctional monomer, *t*-butyl hydroquinone (Sigma Aldrich) as a retarder and Irgacure 819 (CIBA, Specialty Chemicals) as a photoinitiator. As a solvent a 50/50 wt.-% mixture of ethoxypropylacetate (Avocado Research Chemicals) and propyleneglycol-methyletheracetate (Aldrich) was used. The thus prepared photopolymer solution was spin-coated at 1000 rpm onto a series of glass substrates, and subsequently hot-plate dried for 10 minutes at 80 °C. Afterwards the cover plates were allowed to cool to room temperature. The final film thickness was approximately 14 μm. No photopolymer layer was applied to the rigid glass cover of the reference samples.
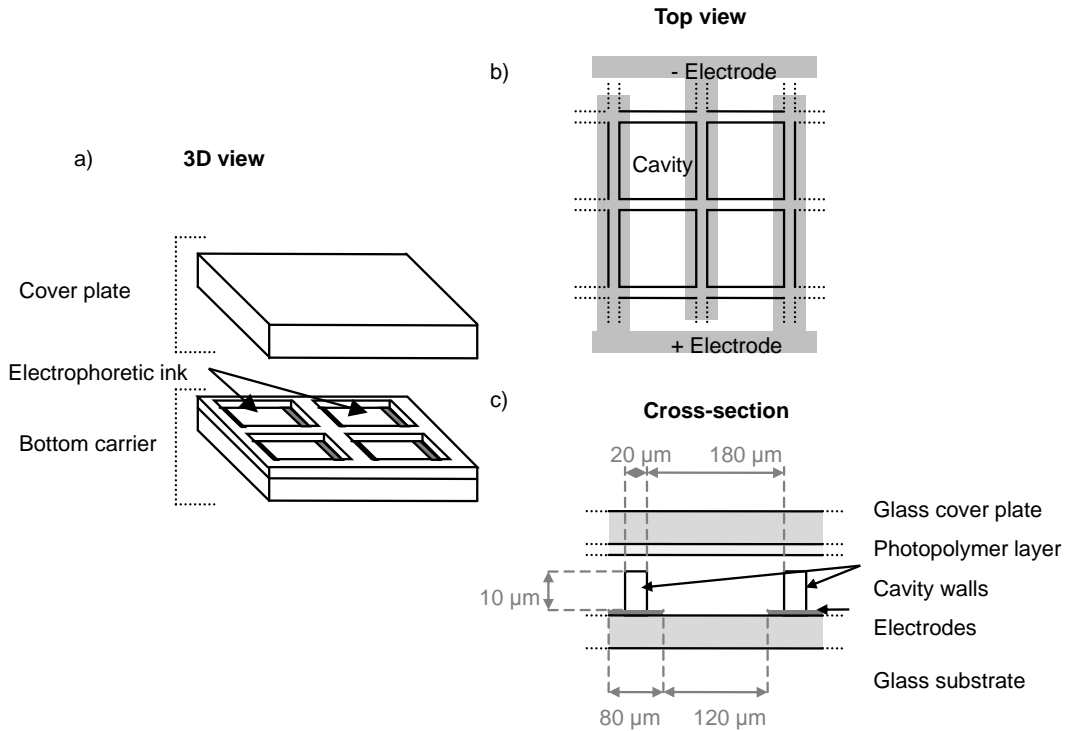
Figure 6.8:   (a) Schematic representation of the device design showing the build-up of 4 cavities in the electrophoretic display, (b) showing the position of the electrodes and the micro-cavities and (c) a cross-sectional profile of a single cavity.

Filling and sealing

The micro-cavities on the bottom carrier were overfilled with electrophoretic ink by using a 25 μL micropipette. Next the cover plate was placed on top, with the photopolymer layer facing the bottom carrier.

 The electrophoretic ink filled cavities were sealed using a photoembossing procedure. This procedure consisted of a mask-exposure, a heat development and a flood-exposure step. A schematic representation of the procedure is given in Figure 6.9. After device assembly, the samples were exposed ($E = 0.6 \text{ J} \cdot \text{cm}^{-2}$, $\lambda = 365$ nm) through a photolithographic mask that was positioned on top of the cover plate. During exposure a latent image of the cavity walls was formed into the photopolymer layer. This latent image was developed into a surface relief structure by heating the sample for 10 minutes at 80 °C. Finally, a flood-exposure was applied ($E = 5 \text{ J} \cdot \text{cm}^{-2}$, $\lambda = 365$ nm) to polymerize the remaining monomer.
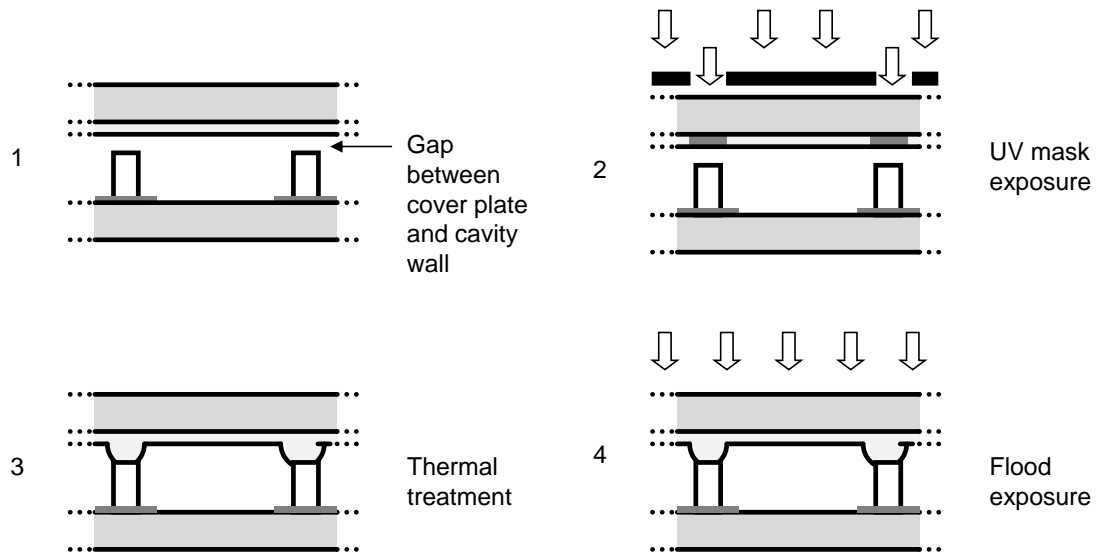
Figure 6.9: Schematic representation of the sealing method.

Sample evaluation

The quality of the obtained photo-embossed seals was evaluated at the top the cavity walls by means of an optical microscope (Leica) equipped with a red-green-blue (RGB) charge coupled device (CCD) camera (Qimaging) while driving the electrophoretic ink (see Figure 6.11f). The obtained raw RGB channel data was processed by a home-made Labview™ program. This software allows observing the optical transmission over a long period of time.

After completion of the electro-optical evaluation the cover glasses were mechanically removed, and the shape of the relief seal at the cover was investigated by using a scanning electron microscope (SEM) (Philips, XL40 FEG) and an optical profilometer (Veeco, Wyko).

6.3.2 Results and discussion

In contrast to any previously reported photoembossing studies, the photopolymer layers in this study are in contact with a fluid (i.e. the electrophoretic ink) during development of the surface relief structures.[13-15] Therefore we first investigated the effect of fluid on the development of the surface relief structures by using only the glass covers coated with the photopolymer layer. The photopolymer layers were exposed under a nitrogen atmosphere through the same photolithographic mask used in the sealing experiments. After the patterned exposure a drop of pure paraffin oil, which is similar to the dispersing medium of the electrophoretic ink, was applied to photopolymer surfaces. After the thermal development and flood exposure, the paraffin oil was removed from the samples by rinsing with heptane. The height of the obtained relief structures was

compared to samples developed in the absence of the paraffin oil. The results (Figure 6.10) show that, independent of the used exposure dose, the height of the relief structures that during development were in contact with the paraffin oil is approximately 30% higher. It is believed that the observed effect can be explained by considering that the development of the relief structures is based on a balance between diffusion and surface/interfacial tension (γ).[16,17] When applying a layer of paraffin oil to the photopolymer layer the interfacial tension is estimated to be lowered from ± 35 mN $\cdot$ m^{-1} in ambient environment to ± 17 mN $\cdot$ m^{-1}. This suggests that upon reduction of the interfacial tension the height of the relief structures is enhanced. It is expected that this effect also occurs when the photoembossing procedure is used to seal an array of liquid-filled micro-cavities, since upon contact between the cover and the liquid-filled micro-cavities a thin fluid is formed on top of the cavity walls due to surface tension effects. Conventional sealing methods often disfavor from fluid contact, however photoembossing can clearly benefit.
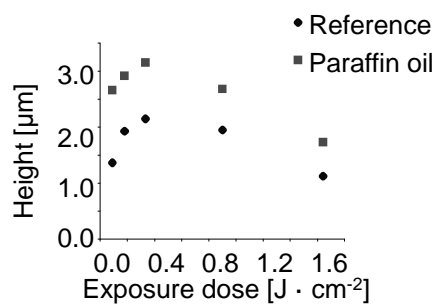

Figure 6.10:   The height photoembossed relief structures that were developed in contact with paraffin oil and a reference sample that was developed under (inert) ambient conditions.

Next, sealed and non-sealed electrophoretic devices were prepared and evaluated by applying a direct current (DC) voltage of 6 Volts between the drive electrodes. Since neighboring pixels have mirror images of the drive electrodes, this resulted in collecting of the electrophoretic ink at both sides of every alternate cavity wall. A microscope image of a typical reference sample with a cover plate which was not coated with photopolymer is given in Figure 6.11a. Here it can be observed that electrophoretic ink has also been collected at the top of the cavity walls. This clearly shows that the sample was not well sealed, resulting in some uncontrolled movement of the ink between adjacent cavities (see Figure 6.11b). A microscope image of a typical sample with a cover plate that was coated with the photopolymer and has been treated with the photoembossing procedure is given in Figure 6.11c. Here it is observed that the top of the cavity wall is clearly visible and only a few dark spots remain. This result suggests that at least most of the gap between the top of the cavity wall and the cover plate is sealed (see Figure 6.11d). From the optical transmission traces, as shown in Figure

6.11e, this is indeed confirmed. In case the micro-cavity was not sealed, the transmission measured at the top of the cavity wall was reduced significantly by the presence of the electrophoretic ink. The photoembossed samples showed no decrease in transmission indicating that the samples were indeed sealed. It is found that measuring the optical absorption traces, is particularly useful method since even very small gaps between the cavity wall and the cover plate can be easily detected while this cannot be observed by eye. For comparison Figure 6.11e also shows an optical transmission trace for a partition in which the gap is relatively small. Although this sample is initially suggested to be sealed, the transmission shows that the signal slowly declines to about 0.9, indeed confirming undesired ink movement. When investigating the dark spots in the sealed sample with the optical trace measurements it was found that the transmission of the dark spots does not change during driving of the electrophoretic ink. This suggests that the dark spots consist of electrophoretic ink that has become trapped between the partition and the cover glass during development of the seal.
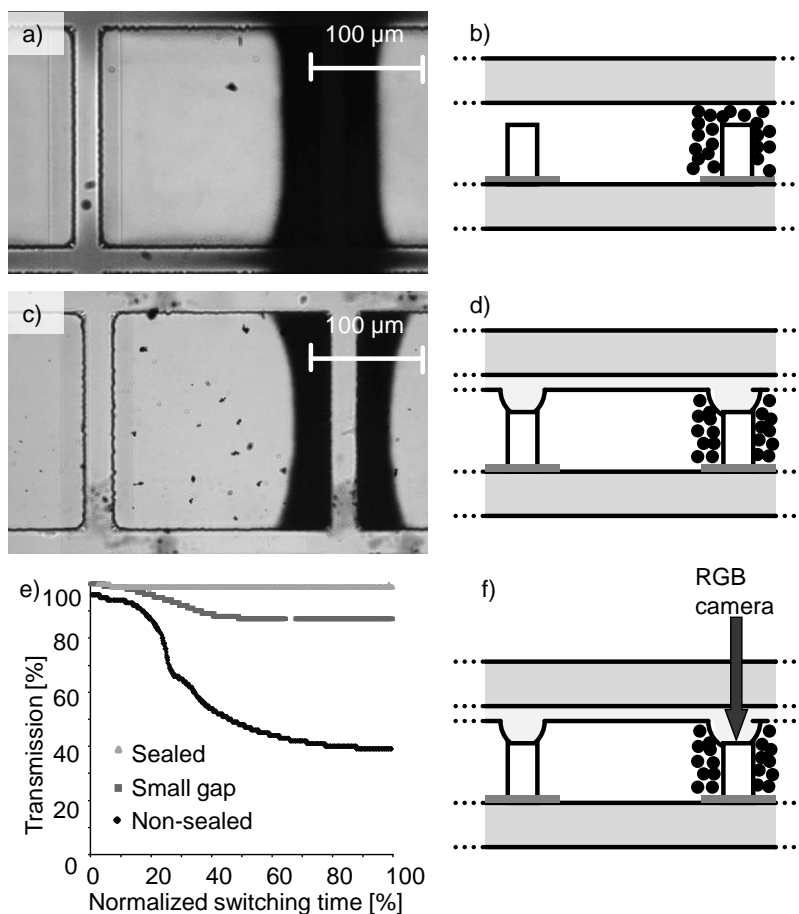

Figure 6.11: Optical microscope image and the corresponding schematic representation of the cross-sectional profile of a non-sealed reference sample (a, b) and a sample sealed by photoembossing (c, d). Sealing was confirmed by measuring the optical transmission at the top of the cavity wall (e, f).

To investigate the shape of the developed seal, SEM images were taken after mechanically removing the cover plate. The SEM images are given in Figure 6.12a and b. In both figures small-sized particles can be observed to remain at the surface after evaporation of the suspending liquid of the electrophoretic ink. The SEM images clearly show that the contours of the tops of the cavity walls have become embedded into the seal. This observation, in addition to the optical data, supports the observation that the cavities were indeed fully sealed. Upon closing the fluid filled gap between the top of the cavity walls and the cover plate, the seal does not develop itself any further, but instead proceeds to develop in the regions around the cavity wall. As a consequence, objects (e.g. defects) which are smaller than the size of the gap between the tops of cavity walls and cover glass, but not larger than the width of the cavity walls, can be embedded into the seal, and do not prevent the relief structures from effectively sealing the array of micro-cavities, as well as the peripheral edge of the device.
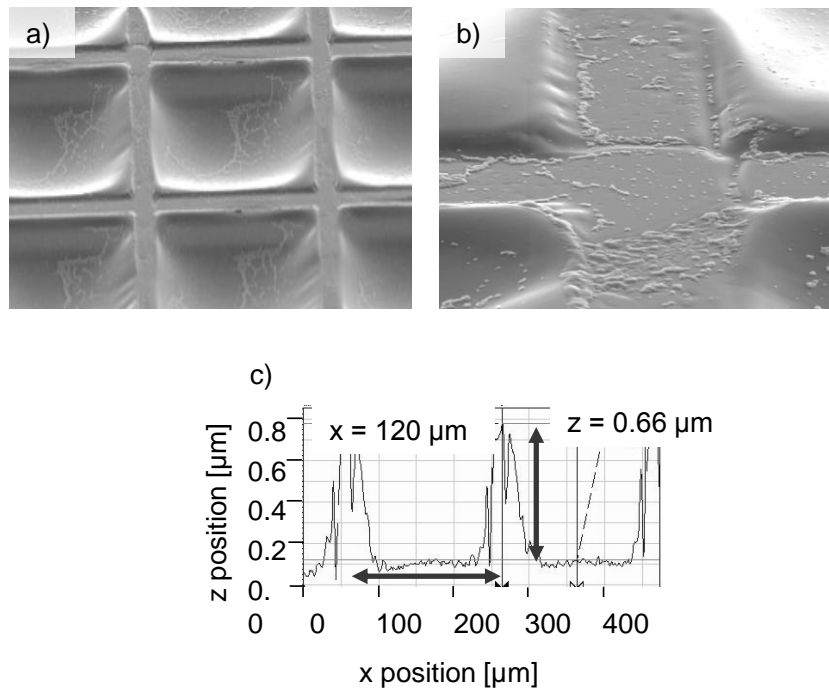
Figure 6.12: An SEM image of a mechanically removed seal at the cover plate (a) and a close-up of the imprint of the partition wall in the photopolymer (b). The height and shape of the developed seal as determined by using an optical profilometer (c).

The SEM images also show a concave shape of the areas which are not exposed during the mask exposure step. This shape is due to the diffusion-based mechanism of photoembossing. Via interferometry, see Figure 6.12c, it was determined that the difference in height between the centre of the cavity and the top of the developed seal is about 0.66 μm. Because the formation of the seal geometry is based on diffusion, its

height is limited. The maximum observed height, in the case of a 14 μm thick photopolymer layer, was approximately 2.6 μm. This was found to be sufficient for the sealing of the electrophoretic display samples since the average gap between the array of micro-cavities and cover plate was in general no more than 2 μm. However, it is well known that the maximum relief height obtained by photoembossing depends on the layer thickness of the applied photopolymer layer.[13,14] It is therefore possible to overcome larger gaps sizes by simply applying a thicker photopolymer layer to the rigid glass cover.

6.3.3 Conclusion

In this study we have demonstrated that photoembossing can be used as a method to in-situ seal an array of pre-filled micro-cavities. It is shown that this technique can bridge gaps up to 2.6 μm between the cover and the cavity wall. It can be expected that the sealing of larger gaps is possible via simply increasing the layer thickness of the applied photopolymer layer. The imprint of the partition in the developed seal and optical transmission traces clearly show that the samples were well sealed. It was also shown that the contact between the photopolymer layer and fluid can have a positive effect on the development of the seals. Despite the fact that the closure of micro-cavities of electrophoretic displays has been chosen as a practical demonstration of photo-embossed micro-sealing, the technology can be applied much wider than that. Examples are biosensor arrays, lab-on-a chip devices and miniaturized gas handling devices.

6.4   Miscellaneous applications

The technique of photoembossing can be used for a wide range of applications. As shown in the previous paragraphs, the non-contact development allows creating structures in case contact with an etching fluid or replication mold is not possible. Other particularly interesting features of the technique are the low costs and the ease of processing. An example were this particular property might be useful is in multi-domain vertically aligned liquid crystal displays (MDVA-LCD). An LCD is based on controlling the polarization of light by applying an electric field on a cavity filled with liquid crystals. The cavity is located between two perpendicular oriented polarizers (Figure 6.13). If the polarization of the incident light is not altered by the liquid crystals, all the light is blocked by the polarizers and the cavity appears dark. The liquid crystals used in displays are rod like molecules which can self organize in a certain orientation. In a MDVA-LCD this orientation is vertical in the absence of an electric field. In this state the liquid crystal molecules do not affect the polarization of the light and the cavity appears dark. When applying an electric field the orientation of the molecules switches to horizontal. The liquid crystals now cause the incident light to change its polarization

such that it is transmitted and the cavity appears bright. This type of display has very large viewing angle (>180°) and fast response time (±10 ms) compared to other type of displays such as in-plane switching (IPS) or super twisted nematic (STN). Part of this high performance can be attributed to small protrusions located within each cavity. These protrusions subdivide the cavity such that each subdivision orients the light in a different direction. This increases the viewing angle, but at the expense of a reduction in brightness. The protrusions are manufactured by using photolithography since replication would damage the delicate glass substrate and other components from which the display is build.
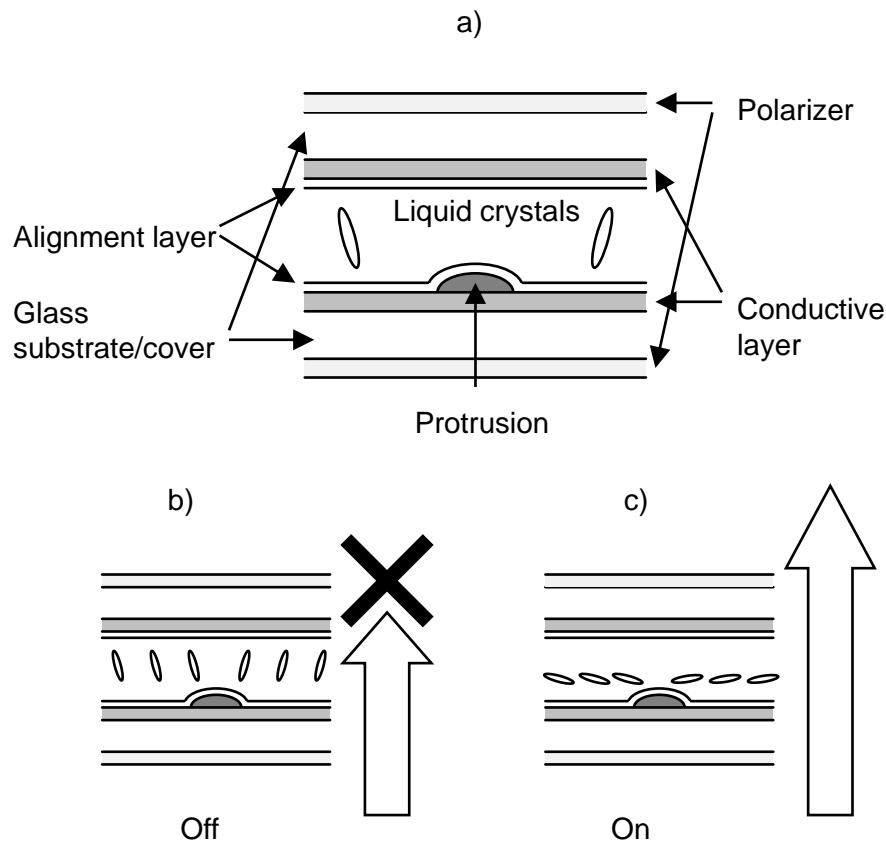

Figure 6.13: (a) Schematic presentation of a cross-section of a MDVA-LVCD. In the off-state (b) incident light is blocked by the two polar. By switching the liquid crystals the light is transmitted (c).

Since photolithography is quite expensive and time consuming it is interesting to use photoembossing to create those protrusions. It is especially the distance between two protrusions (80 μm) which will be challenging from a photoembossing point of view. Results (Figure 6.14) obtained by using a photopolymer as described in paragraph 6.3.2 shows that the distance of 80 μm can be easily overcome. The height of the photoembossed protrusions is approximately equal to the commercial lithographically

obtained protrusions (±1.5 μm). The drawback of photoembossing becomes also visible from Figure 6.14. Unlike photolithography, a layer of photopolymer remains in the areas between the protrusions. As a result, the distance between the two conductive layers is increased and a higher driving voltage is required to retain the electric field. This leads to increased power consumption. To successfully use photoembossing for this application it is thus required to develop a photopolymer which does not leave any "residue" in between the protrusions. Also the simultaneous development of other components, such as spacers, might simplify the display manufacturing process and make photoembossing an attractive technique.
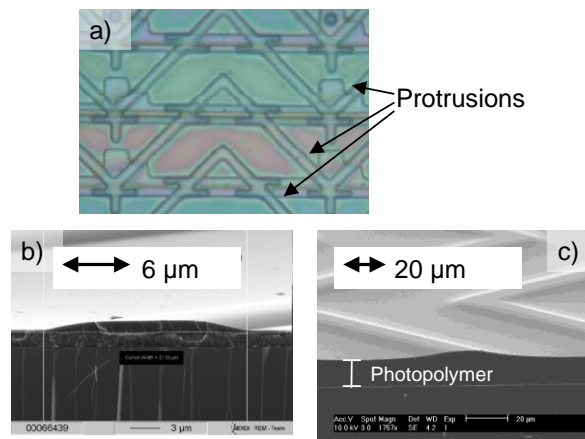

Figure 6.14: Microscope image (a) of an MDVA-LVD display which shows the fishbone like protrusions. An SEM image of a cross-sectional profile of a photolithographically manufactured (b) and a photoembossed (c) protrusion.

The photoembossing process can also be used to replace expensive processes for the manufacturing of single use components such as replication mold or stamps. For example the technique can be used to create disposable molds for the manufacturing of glass diffraction gratings via the sol-gel SiVARA® process (Figure 6.15a). Another option is to use the technique to create a microcontact printing stamp. These stamps usually are usually created in a rubbery material (e.g. polydimethylsilane) via replication from a master. The master is expensive since its production comprises lithographic processing steps. With photoembossing, a stamp can be manufactured directly without master. An additional coating of a polydimethylsilane / polystyrene (PDMS-PS) blockcopolymer is applied on top of the photopolymer layer prior to the thermal development step. Upon development, the PMDS-PS layer deforms into the desired shape and the obtained relief can be used as stamp for microcontact printing (Figure 6.15b, c and d).
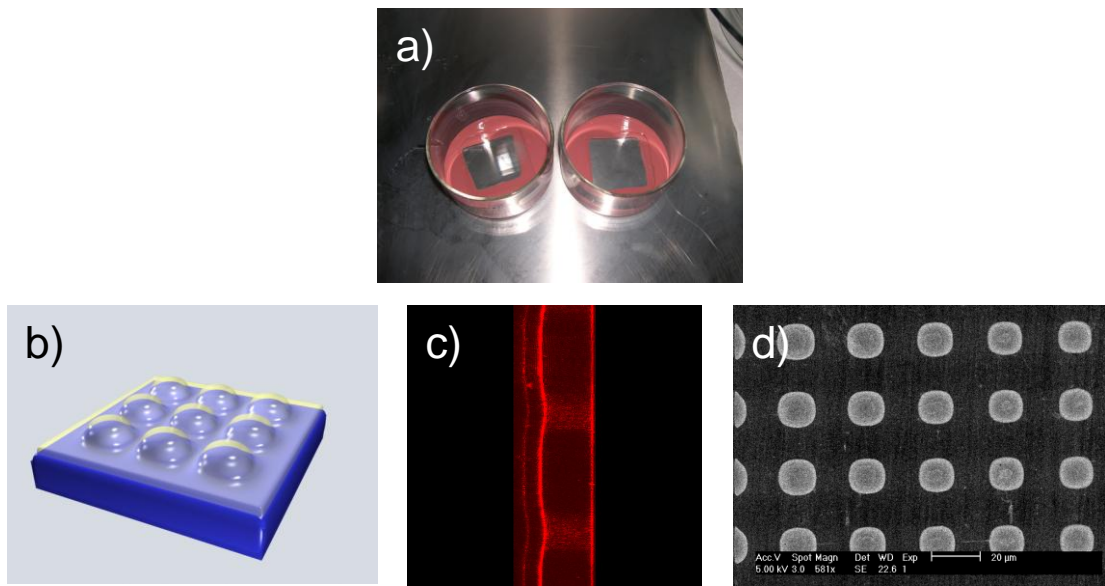
Figure 6.15: (a) Preparation of photoembossed gratings for sol-gel replication via the SiVARA® process. (b) Schematic presentation and (c) a confocal microscope image of a photoembossed microcontact printing stamp. (d) SEM image of a gold coated substrate which is patterned by using the photoembossed microcontact printing stamp.

6.5 Conclusion

In this chapter several potential applications for photoembossing have been investigated. It is especially the non-contact method of development which is used for some unique possibilities.

It is demonstrated that photoembossing can be used to create a microlens array. The optical characteristics of the lenses can be altered by changing the processing parameter. A particularly interesting feature is that additional coatings, such as a solution processable antireflection coating, can be applied prior to the development of the microlens array when the film is still flat. This stimulates the formation of films with a homogeneous thickness distribution and obviates the use of further post processing steps.

Another application it the in-situ sealing of an array of pre-filled micro-cavities, such as encountered in electrophoretic displays. Photoembossing can be used to form a hermetic seal between the cover and the micro-cavity walls. The seal locations are defined by ultraviolet (UV) exposure through a photolithographic mask, forming a latent image overlapping with the locations of the cavity walls. During a thermal development step, while the cover is mounted on top of the micro-cavities, the seal evolves and makes firm contact with the cavity walls. This concept is insensitive to small deviations in cavity height, flatness of the cover and thin fluid films remaining

between the cover and the top of the cavity walls. In the past these aspects made it difficult to effectively seal large area devices.

Other interesting features of photoembossing are the low material/processing costs and the ease of processing. These features can for example give photoembossing a competitive edge when used to create small protrusions, which are used in increase the viewing angle in liquid crystal displays. These display components are currently manufactured via expensive lithographic techniques since replication techniques would damage the glass substrate or other components. Photoembossing simplifies the production process, but the remaining photopolymer layer in between the protrusions increases its power consumption. Photoembossing can also be used to create single use products such as replication mold or stamps.

6.6   References

[1]   F. T. O'Neill, J. T. Sheridan, *Optik (Jena)* **2002**, *113*, 391.

[2]   R. Danzebrink, M. A. Aegerter, *Thin Solid Films* **1999**, *351*, 115.

[3]   C.-Y. Chang, S.-Y. Yang, M.-H. Chu, *J. Micromech. Microeng.* **2007,** *84*, 355.

[4]   S. Mihailov, S. Lazare, *Appl. Opt.* **1993**, *32*, 6211.

[5]   Y.-Q. Fu, N. Kok, A. Bryan, *Microelec. Engineering* **2000**, *54*, 211.

[6]   J. Thies, E. Currie, G. Meijers, J. Southwell, C. Chawla, *Digest of Technical Papers - Society for Information Display International Symposium* **2004**, *35,* 1174.

[7]   T. J. Trout, J. J. Schmieg, W .J. Gambogi, A.M. Weber, *Adv. Matter.* **1998**, *10*, 1219.

[8]   D. J. Kang, J. Jeong, and B. Bae, *Optics Express* **2006**, *14*, 8347.

[9]   F. T. O'Neil, I. C. Rowsome, A. J. Carr, S. M. Daniels, M. R. Gleeson, J.V. Kelly, J. R. Lawrence, J. T. Sheridan, *Proc. of SPIE* **2005**, *5827*, 445.

[10]   P. Vukusic, J. R. Sambles, C. R. Lawrence, *Nature* **2000**, *404*, 457.

[11]   T. Z. Kosc, *Optics & Photonics News* **2005**, *16,* 18.

[12]   B. Comiskey, J.D. Albert, H. Yoshizawa, J. Jacobson, *Nature* **1998**, *394* 253.

[13]   A. L. Dalisa, *IEEE Trans. Elec. Dev.* **1977**, *24*, 827.

[14]   M. A. Hopper, V. Novotny, *IEEE Trans. Elec. Dev.* **1979**, *26*, 1148.

[15]   J. Kentsch, S. Breisch, M. Stelzle, *J. Micromech. Microeng.* **2006,***16*, 802.

[16]   H. Nguyen, J. Bejhed, J. Kohler, G. Thornell, *J. Micromech. Microeng.* **2006**, *16,* 2369.

[17]   Y. Song, C. S. S. R. Kumar, J. Hormes, *J. Micromech. Microeng.* 2004, **14** 932-940.

[18]   L. J. M. Schlangen, R. Penterman, D. J. Broer, *Electrophoretic display devices and a method for manufacturing such a device,* **2004**, WO2004111716.

[19]   R. Penterman, *Photo-enforced stratification of liquid crystal / monomer mixtures*, Technische Universiteit Eindhoven, Eindhoven, The Netherlands, **2005**, Chapter 4.

[20]   R. C. Liang, M. Chan-Park, S.C-J. Tseng, Z. G. Wu, H-M. Zang, *Electrophoretic display*, **2000**, WO01/67170.

Chapter 7

Biosensor

Diffuse to structure, structure to diffuse

With photoembossing relief structures are made via diffusion of molecules to pre-specified locations. The opposite, relief structures inducing the diffusion of molecules, is also possible. This effect is used in molecular diagnostics (MDx) devices or biosensors. These devices are used to detect biomolecular species (analyte) such as DNA/RNA or proteins in a sample fluid. Conventionally biosensors consist of flat substrates on which capture probes have been printed in an array. Depending on the type of device, the sample fluid is pumped many times through or over these substrates to ensure that most of the analyte can bind to the capture probes. To detect the bonding of analyte, fluorescently labeled proteins or DNA fragments are used to bind to the reacted sites. Currently, the analysis is performed by using either a flow-over or a flow-through concept. The former concept is based on a solid substrate on which the capture probes are located in wells which can be positioned in microfluidic channels. This system requires small volumes of sample fluid, but has only a low sensitivity due to a lack of specific surface area. The flow-through device is based on a porous substrate. This type of system requires a larger volume of sample fluid, but has a higher sensitivity due to large specific surface area. In this chapter a new type of biosensor is designed, manufactured and evaluated. This device is based on a microfluidic channel in which locally porous membranes are located on which the capture probes can be printed. This system requires small sample volumes since it is based on a microfluidic channel and has a high sensitivity due to the large specific surface area of the membranes. The biosensor is manufactured by using photolithography and can in principle be sealed by using photoembossing (Chapter 6). Since the binding of analyte in a microfluidic system is diffusion limited, also a method is discussed to enhance the sensitivity even further by using static micromixers.

7.1   Introduction

In previous chapters it has been discussed how the diffusion of molecules can be used to create relief structures. The opposite, relief structures inducing the diffusion of molecules, is also possible. This effect is used in molecular diagnostics (MDx) devices or biosensors. Biosensors are built around substrates that contain patterns of capture probes which are capable to bind with biomolecular species (analyte), such as DNA/RNA fragments or certain specific proteins (Figure 7.1).[1] To sense whether specific binding has occurred the substrates are commonly brought into contact with DNA fragments or proteins with a fluorescent label. These molecules only bind to the reacted sites. The presence of the analyte can then be detected by means of a CCD camera if the fluorescent probes are excited to emit light. Also various other methods have been developed, or are under development, to sense whether the specific binding has occurred. Popular are optical methods, e.g. based on fluorescence, refractive index changes, spectral changes, but also changes in localized magnetic or dielectric behavior are being used.[2-5]
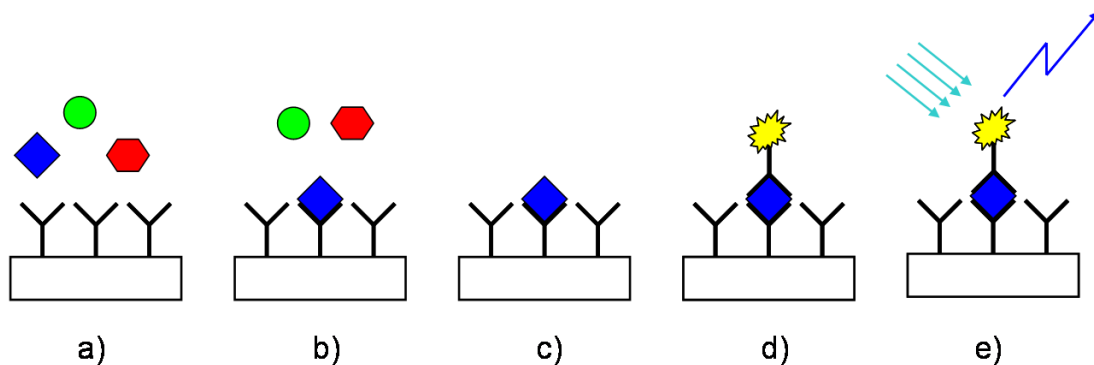

Figure 7.1:   Example of a sandwich assay and detection by a fluorescent probe.

In principle there are two biosensor designs. The first design is based on the so-called "flow-over" principle.[6,7] Here, a substrate is provided with an array of spots of different capture probes via e.g. inkjet printing. The capture probes are printed in preformed wells on the substrate. To bind the analyte, the sample fluid is pumped over the spots containing the capture probes. The advantage of this design is that pumping of the fluid is quite simple due to a low pressure drop over the sample. In addition the size of the spots is determined by the size of the wells in which the capture probes are printed. The spots are thus small and well-defined. In principle the printed spots can be placed in series such that the analyte hits every spotted area. In practice this often is not the case as flow in microfluidic devices normally is laminar such that transport from the target molecules to the capturing probes should occur by diffusion. This results in long contact times if the channel depth is large in comparison to the sizes of the molecules

(1-20nm).[8] A particular disadvantage of this system is its low sensitivity. The flat (or rounded) surfaces on which the capture probes are printed provide a small specific surface area and limit the number of capture probes per projected area. The more capture probes in a projected areas, the higher the fluorescent signal and the more sensitive the device.

In order to enhance the sensitivity of the analysis, bringing detection limits into the pico-molar range or better, "flow-trough" principles are used. In a flow-through device the sample fluid is pumped through a microporous substrate containing spots of immobilized capture probes. The high specific surface area of the microporous substrate cause a large number of specifically bonded capture probes on the detection spots, resulting in a high sensitivity for the detection of bonded molecules. A drawback is that the capture areas are placed parallel and that therefore a specific targeted area misses many analyte molecules as they pass outside the targeted area. In order to solve this, the analyte is pumped through the spotted membrane several times. Examples of products that are on the market is the Pamgene biosensor, based on etched pores in an aluminum oxide membrane (Figure 7.2), and the Nytran membrane, based on a phase separated nylon scaffold (Figure 7.3).[9,10]
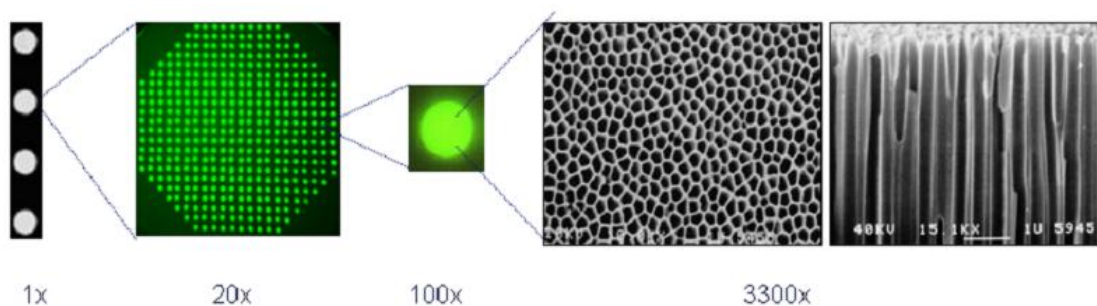

1x   20x   100x   3300x

Figure 7.2:   The Pamgene membrane in different enlargements. At the left a strip is shown, more or less in its real dimensions, showing four areas that are printed with a micro array. Then at an enlargement of 20x one can see the array of spots containing the various capture probes. At the right side the nanoporous membrane is shown in top view and in cross-section. The inner surface of the membrane pores are coated with the capture probes.

Both the flow-over and the flow-through biosensors exhibit their own merits and demerits. The flow-over devices, when built-in in a microchannel, require only small volumes of sample fluid, but their sensitivity is low as well the capture probability of the analyte in fast assay. The flow-through devices are providing a higher signal-to-noise ratio but larger volumes of analyte are needed as well as that the analyte has to be pumped through the membrane to enhance the sensitivity for low concentrations of target molecules. It is the objective of this chapter to design (paragraph 7.2), manufacture (paragraph 7.3) and evaluate (paragraph 7.4) the layout of a new type of biosensor which can overcome the problems encountered with conventional devices.
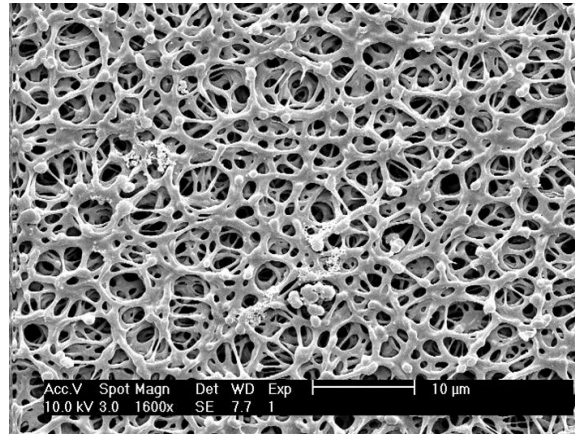
Figure 7.3:   SEM image of Nytran membrane.

7.2   Design new sensor

7.2.1 Basic layout LIFE sensor

To overcome the disadvantages of the conventional biosensors, a new type of biosensor is designed. This new biosensor is based on small membranes localized in a microfluidic channel (Figure 7.4). The microfluidic channel is used to transport the sample fluid in a lateral motion to in-series connected detection spots. It thus requires small sample volumes. The detection spots consist of membranes with a large specific surface area, which provides a large signal. The concept thus uses the benefits of both the conventional flow-over and flow-through devices.

The membranes consist of a collection of vertical sheets (called "elements") which are placed parallel to the flow direction of the microfluidic channel. This design gives the membranes a large internal surface area, providing a large signal, on a small projected surface area, providing high intensity and large resolution. In addition, the gap between the elements is monodisperse. Compared to a random gap size, the pressure drop over the membranes is relatively small. This allows the placement of a large number of membranes in series without the need of using large pressures to transport the sample fluid through the channel. By placing the elements in the membranes close to each other the average diffusion distance of analyte to reach the capture probes at the surfaces of the elements is relatively small, which translates itself in short assay times.

The surface of the elements is covered with capture probes such as oligo DNA, RNA or antibodies. They can be applied by the conventionally used technique of inkjet printing. Conveniently, the printed drops are confined within the membranes by the capillary action induced by the large surface of the localized membranes. This prevents contamination of the open channels with capture probes which would give background signal and lower the S/N ratio.

Overall it can be concluded that this new design combines the necessity of only small sample volumes, fast measuring protocols and high signal-to-noise of the detection signals. The concept is called the Lateral Immoassay Flow-through Elements sensor or LIFE sensor.
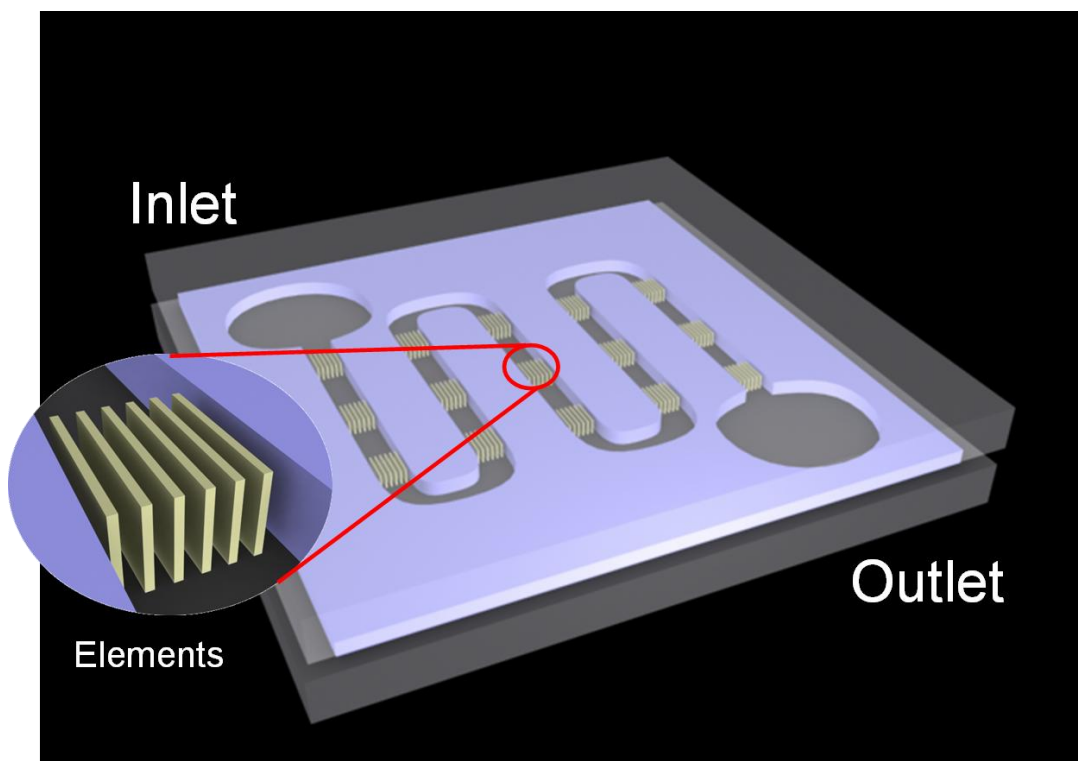

Figure 7.4: Schematic picture of the LIFE sensor containing the microfluidic channel and the localized membranes. Each membrane consists of parallel placed elements.

7.2.2 Micromixers

Although the LIFE sensor already provides a large improvement over the existing devices there is still a problem to solve. In a typical microfluidic channel, the dimensions and flow rates are such that Reynolds numbers are low, resulting in a laminar flow. Transport towards the walls of the elements, and consequently also the binding of analyte, is therefore diffusion-limited. The length scales between the elements are too large for rapid diffusion and too small for the application of active mixers. An active mixer is a unit which causes mixing of two or more components by movement (often triggered by external stimuli) of the unit itself.[11] Because mixing is induced by the active movement of the unit, these type of mixers are ideal where mixing is desired over a small length scale (e.g. inside a microreactor or a small length micro channel). However, the implementation of an active mixer between the membranes is impossible due to the high aspect ratio, height of channel divided by the width of the channel, of the microfluidic channel between the elements. To solve this problem, static

micromixers can be used to reduce the assay time or alternatively increase the sensitivity of the device. A static mixer commonly consists of a multitude of microstructures that are placed on the top and/or bottom of a microfluidic channel.[12] The structures are placed in such a way that the components inside the channel mix after moving a certain distance along the length of the channel. These types of mixers can only mix efficiently if the height of the channel is sufficiently small compared to the height of the microstructures itself. Unfortunately, the large aspect ratio of the microfluidic channel between the elements in the membranes makes it impossible to use conventional static micromixers. Therefore, a method has to be developed to place micromixers on the walls (instead of the bottom/top) of thee high aspect ratio microfluidic channels between the elements (Figure 7.5). In addition these micromixers could provide additional surface area to which capture proves can be bound.
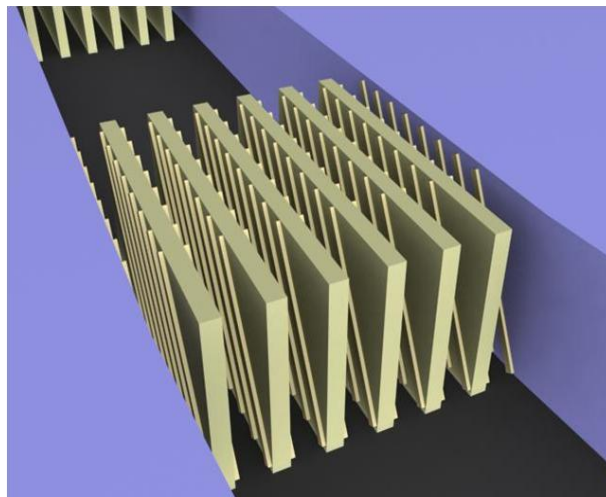

Figure 7.5:   Schematic representation of micromixers placed on the walls of the elements in the localized membranes.

7.3   Manufacturing

7.3.1 Processing techniques

The LIFE sensor can be made by using conventional photolithographic techniques. With these techniques, a photoreactive resin (photoresist) is applied to a substrate. Via an exposure through a mask which contains a negative image of the channels and membranes, a latent image is created into the photoresist. The illuminated areas are polymerized by heating and the non-illuminated are subsequently removed by dissolving into a proper solvent. By this simple photolithographic approach the complete sensor template (i.e. microfluidic channel and the membranes) can be made in a single procedure.
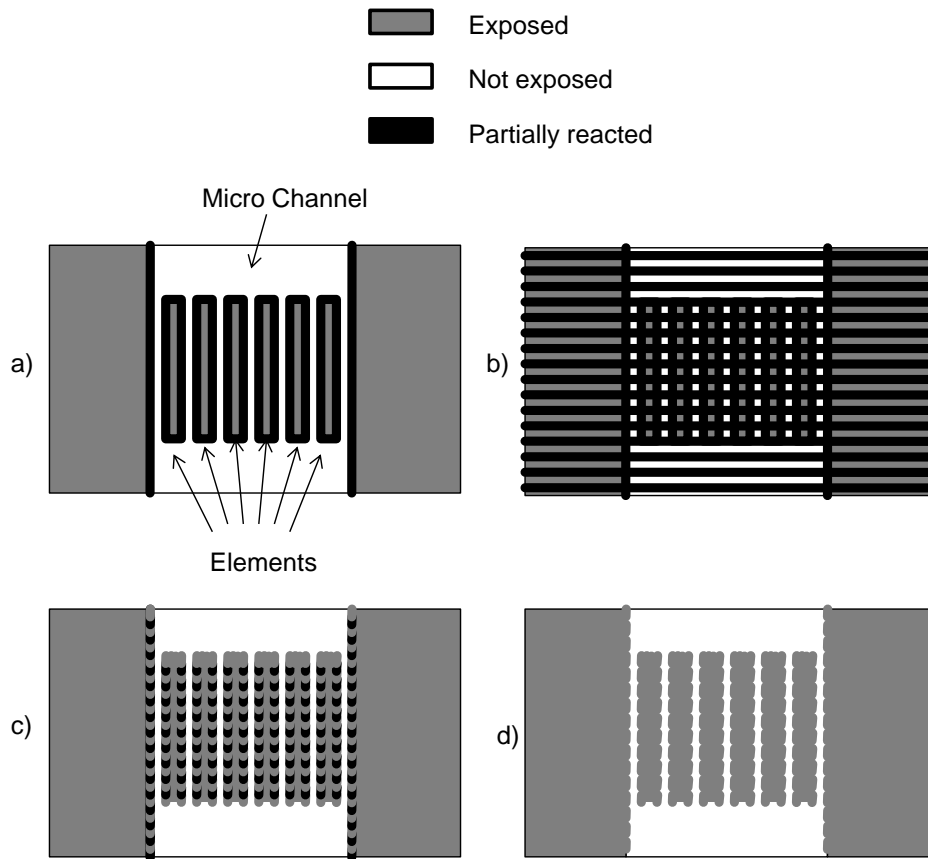
Figure 7.6: Schematic representation of manufacturing of micromixers. After creating a latent image of the microfluidic channel and the membranes.

To efficiently induce mixing, conventional micromixers aim to stretch and fold the fluid. This can be done by for example placing a herringbone texture in staggered confirmation on the bottom of a microfluidic channel.[12] It is, however, extremely difficult to create this exact pattern at the walls of the elements. Instead much simpler micromixers (as depicted in Figure 7.5) can be made by using holography. These mixers are expected to be less effective, but will still induce a rotating motion of the fluid and thus increase contact time between analyte and capture probes. With holography a single laser beam is split into two identical beams. These coherent beams are focused on the same spot and their interference pattern creates a sinusoidal intensity profile. This intensity profile can be used to create relief features in photoresist via standard photolithography. To make the micromixers, this intensity profile is focused under an angle on a layer of photoresist in which a latent image of the LIFE sensor is already present (Figure 7.6). To make sure that the holographic exposure results in relief features which are only at the walls and do not block the microfluidic channels, an under exposure is applied. A photoresist contains a buffer which created a threshold value for the exposure dose. Below the threshold value, the buffer prevents

polymerization and the areas can still be removed by dissolving into a proper solvent. Above the threshold value, the effect of the buffer is overcome and the illuminated areas are polymerized and cannot be dissolved. The threshold value thus ensures that it is possible to create very small or high aspect ratio relief features. By using an under-exposure for the holographic illumination step, most of the intensity profile is ineffective and does not result in structure formation. Hence, no structures are formed inside the microfluidic channels. However, the areas close to the edges of the latent image of the microchannels contain less buffer due to diffusion of activated photoinitiators and diffraction at the edges of the photolithographic mask. The reduced buffer content in these areas, which eventually form the walls of the microfluidic channels, locally lowers the threshold value. The holographic exposure dose in these areas is sufficient to create relief features. It should be noted that this technique does not only produce a surface texture at the vertical walls of the elements, but also the vertical walls and the bottom of the microchannel. These textures are unlikely to affect the flow in the microchannel, since the size is too small compared to the dimension of the channel.

7.3.2 Procedures

The LIFE sensor consisted of a thick (50 μm) layer of SU-8 in which the microfluidic channel and membranes were created and a thin SU-8 layer to promote adhesion to the glass substrate. First the adhesion layer was applied to the glass substrates by spincoating a layer of SU8-2010 (MicroChem) on cleaned glass substrates. The D263 glass substrates (5×5 cm) were cleaned by rubbing with a sodium hydroxide solution, flushed with demineralized water, rubbed with acetone, rubbed and flushed with ethanol and finally dried with nitrogen. Directly after cleaning the SU-8 2010 was spincoated on top of the glass substrates at 2000 rpm with a Karl Suss RC8 spincoater. A pre-bake step (2 minutes at 65 ˚C and 10 minutes at 95 ˚C) ensured that all solvent was evaporated and that the SU8 was in the glassy state. The samples were flood exposed for 60 seconds with an Omnicure S2000 UV light source (EXFO) having an intensity of 10 mW $\cdot$ cm^{-2}. After the exposures, a postbaking step was performed by heating the samples to 65 ˚C for 1 minute, 95 ˚C for 2 minutes to induce polymerization of the photoresist.

Next, a thick layer of SU-8 was applied to the substrates containing the SU-8 adhesion layer. SU-8 2100 was spincoated on top of the adhesion layer at 2000 rpm with a Karl Suss RC8 spincoater. A pre-bake step (45 minutes at 65 ˚C and 90 minutes at 95 ˚C) ensured that all solvent was evaporated and that the SU8 was in the glassy state. The samples were exposed through a photolithographic mask which contained a negative image of desired pattern. The pattern was a single microfluidic channel (4 cm x

50 µm) which contained 5 membranes (50 x 50 µm). To allow fluid to enter and exit the microfluidic channel, a 1x1 cm area was positioned at each end of the microfluidic channel as an inlet/outlet. Each membrane consisted of 12 elements (50 x 2.5 µm) with a periodicity of 5µm. The exposure was performed for 1.8 seconds by using a UV laser from SpectraPhysics ($\lambda = 351$ nm, Beamlok 2085S) having an intensity of 26 mW · cm^{-2}. After the exposure step, a post baking step was performed by heating the samples to 65 ˚C for 5 minute and 95 ˚C for 10 minutes. Afterwards the non-crosslinked areas were washed away with SU8-developer (mr-Dev 600, MicroChem), followed by rinsing with isopropanol.

To create the micromixers, an additional step was included into the process. In this case a holographic exposure is applied to the 50 µm thick layer of SU-8 which already contained a latent image of the microfluidic channel and membranes. The holographic exposure was applied before the postbaking step by using a UV laser from SpectraPhysics ($\lambda = 351$ nm, Beamlok 2085S) with an intensity of 26 mW · cm^{-2} for 0.6 seconds. The angle between the bisector of the two laser beams and the normal of substrate was 40˚. After the holographic exposure the samples were processed as described before.

The final device was sealed by using 1mm thick slab of polydimethylsiloxane (PDMS) and a polymethylmethacrylate (PMMA) cover plate. Both contained holes to fit tubing above the inlet and outlet areas of the microfluidic channel (Figure 7.7).
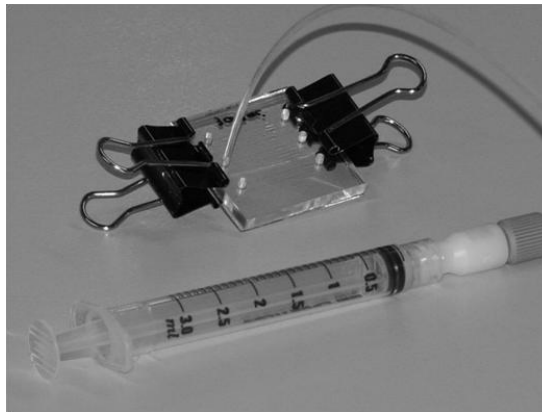

Figure 7.7:   Photograph of a LIFE sensor.

7.3.3 Characterization

Scanning Electron Miscopy (SEM): SEM images were taken with an XL30 ESEM from Philips. The samples were coated with a thin gold layer by vapor deposition. The images were taken perpendicular to the sample.

Optical microscopy: Optical microscopy was used to check if the device was sealed. Hereto, water containing a small amount of red dye (Rhodamine B) was inserted into the inlet area of the microfluidic channel. The dyed water was moved through the channel via two methods. First, the water was pumped by using a syringe; an under/over pressure was applied at the outlet/inlet of the channel. Second, the water was moved by capillary force; after plasma etching the SU-8 surface. During the movement of the dyed water, the sample was investigated by using 5x objective.

7.4 Evaluation

First, the membranes (without micromixers) were evaluated by using SEM. The results are given in Figure 7.8. The images show that by using photolithography it was possible to create high aspect ratio elements (2x50x50 μm). The elements were easily grouped together into a membrane and several membranes were placed into a microfluidic channel. The membrane increased the specific surface area locally from 7500 μm^2 (walls and bottom) to 66250 μm^2. This could potentially result in a signal enhancement by a factor 8.8 compared to a flat substrate.
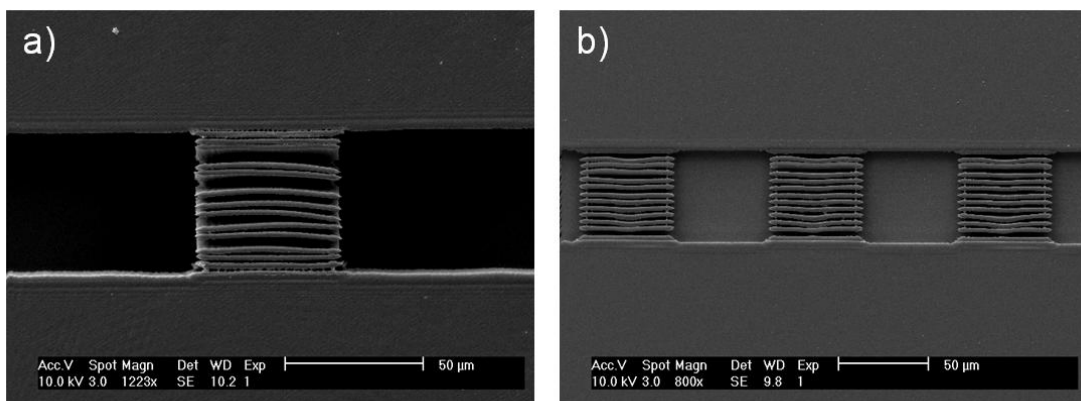
Figure 7.8: SEM images of the membranes in the microfluidic channel. Each membrane consists of 12 elements, which are each 2 x 50 x50 μm in size.

Next, the membranes with micromixers were evaluated by using SEM. The results are given in Figure 7.9. The images show that by using holography it was possible to create relief structures at the walls of the elements. These structures were approximately 100 nm high and increase the specific surface area to ±70000 μm^2. Although the mixing (or rotating) of fluid cannot be deduced from the SEM images, the structures look promising.

From both Figure 7.8 and Figure 7.9 it also becomes clear that the elements are delicate and careful handling of the device is required. Bending of the elements was observed to results in slight variation of the spacing between the elements. This effect

was caused by the high aspect ratio the elements which makes them susceptible to breaking or bending. This problem was observed during manufacturing of the devices, but is expected to be less problematic once the devices are sealed.
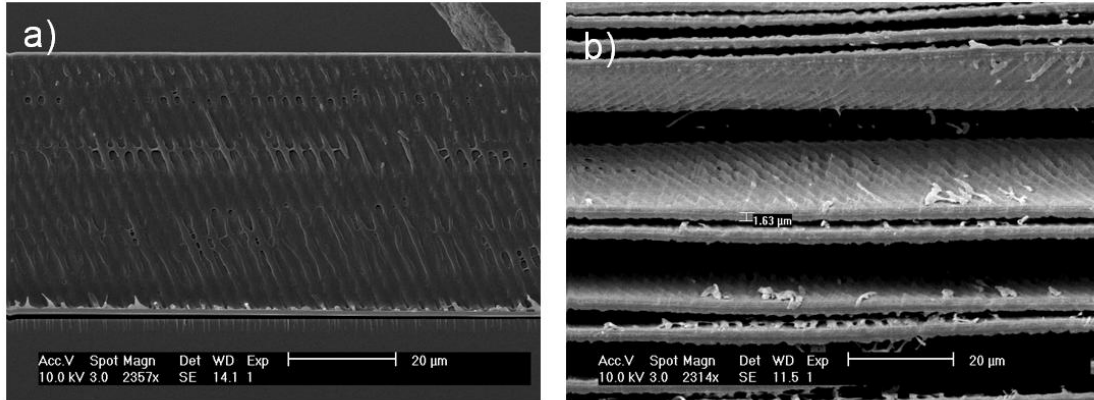
Figure 7.9:   SEM images of (a) the side view of micromixers on an element and (b) the top view of micromixers on several elements.

Next, the samples (without micromixers) were sealed by using a PDMS slab (1mm) and PMMA cover plate (1mm). It was checked if fluid could be moved through the channel by using over-pressure, under-pressure or capillary force. The seal was checked for leakages by using red dyed water. Small leaks could be easily detected by this method (Figure 7.10). It was found that the PDMS layer locally detached from the SU-8 surface (and thus leaking) when an overpressure was applied at the inlet. This could be overcome by using permanent sealing method (e.g. photoembossing), however this is not convenient during the test phase of the sensor.

Figure 7.10:   Optical microscope images of a sealed (a) and non-sealed (b) sample.

It was found that samples were well sealed when the fluid was pumped by applying a vacuum at the outlet (under pressure) of the device. More convenient, the device could also be filled by using capillary force. Filling by c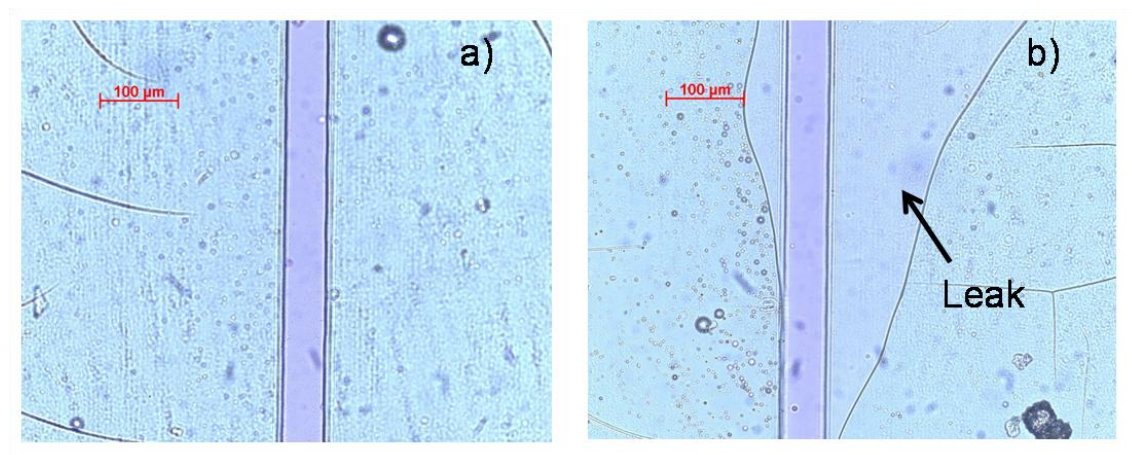apillary force is interesting since it could potentially eliminate external pumping of the sensor. The velocity of the water inside the channel depends on the hydrophilicity of the channel. An untreated SU-8 surface is hydrophobic, which resulted in slow filling of the microchannel. However, when the channel was made hydrophilic by for example plasma etching, fast velocities were obtained. This is elucidated in Figure 7.11. Microscope images of water moving through a plasma etched microchannel containing 5 membranes clearly showed that fast movement was possible. The initial speed of the water was approximately 11 mm · s^{-1}, where after the membranes this was reduced to 0.8 mm · s^{-1}. The reduction in velocity occurs from the pressure drop over the membranes. The fluid speed in the channel can thus be controlled by the hydrophilicity of the surface. By using alternate region of different hydrophilicity it might even be possible to move the fluid in a stepwise motion.

Figure 7.11:   Fluid movement by capillary force through a microfluidic channel including 5 membranes.

7.5   Conclusion

A new type of biosensor was designed, manufactured and evaluated. This biosensor was based on a microfluidic channel which locally contained membranes. The concept combined the advantages of conventional flow-over and flow-through devices. Only small sample volumes were required due to in-series connection of membranes by the microfluidic channel. The design of the membranes, which consisted of vertically elements, ensured a large signal on a small projected surface area. In addition micromixers were placed on the walls of the elements to increase the contact time between analyte and the capture probes.

The microfluidic channel and membranes were manufactured by using mask photolithography. With this technique, a photoreactive resin (photoresist) was applied to a substrate. A latent image, which was projected into the resin via a mask exposure, was developed into relief structures by dissolving the non illuminated areas. The micromixers were created by applying an additional holographic exposure prior to the latent image of the microchannel and the membranes.

It was observed that by using photolithography it was possible to create the microfluidic channel and the membranes containing the high aspect ratio elements (2x50x50 µm). The membrane increased the specific surface area locally from 7500 μm^2 (walls and bottom) to 66250 μm^2. The successful addition of the micromixers at the walls of the elements increased the specific surface area to approximately 70000 μm^2. Whether the mixers induce mixing has not been proven yet. The elements (with or without mixers) were observed to be delicate and careful handling of the device was required. This problem occurred during manufacturing of the devices, but is expected to be less problematic once the device is sealed. It was demonstrated that an effective seal could be obtained with a PDMS slap and PMMA cover plate. Sealed samples were easily filled with fluid by using capillary force or a vacuum at the outlet. Especially capillary force was interesting since this would eliminate the use of an external pump.

7.6   References

[1]   M. Schena, *Protein Microarrays*, (Eds. M Schena), Jones and Bartlett Publishers, Sudbury, USA, **2005**, Ch.1.

[2]   M. Megens, M. Prins, *J. Magn. Magn. Mater.* **2005**, *293*, 702.

[3]   Y. Huang, H. Liu, K. Li, Y. Chen, Q. Zhang X. Wu, *Sensors and Actuators A* **2008**, *148*, 329.

[4]   E. Özkumur, J. W. Needham, D. A. Bergstein, R. Gonzalez, M. Cabodi, J. M. Gershoni, B. B. Goldberg, M. S. Ünlü, *PNAS* **2008**, *105*, 7988.

[5]   J. Kim, A. Babajanyan, A. Hovsepyan, K. Lee, B. Friedman, *Rev. Sci. Instrum.* **2008**, *79*, 086107.

[6]   L. C. Taylor, D. R. Walt, *Analytical Biochemistry* **2000**, *278*, 132.

[7]   W. Kusnezow, T. Pulli, O. Witt, J. D. Hoheisel, *Protein Microarrays*, (Eds. M Schena), Jones and Bartlett Publishers, Sudbury, USA, **2005**, Ch.14.

[8]   S. Papadopoulos, K. D. Jürgens, G. Gros, *Biophys. J.* **2000**, *79*, 2084.

[9]   www.pamgene.com

[10] www.whatman.com

[11] V. V. Khatavkar, P. D. Anderson, J. M. J. den Toonder, H. E. H. Meijer, *Phys. Fluids* **2007**, *19*, 083605.

[12] A. D. Stroock, S. K. W. Dertinger, A. Ajdari, I. Mezić, H. A. Stone, G. M. Whitesides, *Science* **2002**, *25*, 647.

Technology assessment

Micro sized polymeric relief structures are currently widely used on an industrial scale in a range of applications. Typical examples of their use are in liquid crystal displays (LCD), digital video discs (DVD) or video projection systems. These surface relief structures are mainly manufactured by using replication and photolithography. Due to its simplicity, replication via structured masters or molds is the most frequently used technique to create micro sized relief structures. Thousands or even millions of replications can be produced by using a single mold and the processing times are usually within the order of seconds or minutes. This makes replication a fast and cost effective technique when large quantities of the same product are required. Photolithography is, although more expensive and time consuming, particularly useful for creating very small sized (±30 nm) and high aspect relief structures. Both techniques are well developed and it cannot be expected that a new processing technique will easily replace these manufacturing methods. One of the main problems is that most companies have already invested in processing equipment and are not willing to reinvest for a new process.

In some existing markets, however, photoembossing might be interesting. The low material/processing costs and the ease of processing make the technique suitable for creating small quantities of single use products such as replication mold or stamps. Alternatively some display components can be manufactured at lower costs (see also Chapter 6). Currently, these components are manufactured via expensive lithographic techniques since replication techniques would damage the glass substrate or other components. Photoembossing simplifies the production process, but the remaining photopolymer layer in between the protrusions increases its power consumption. Although future photopolymers might induce higher modulations and thus lower the layer thickness in between the protrusion, this application is currently a step too far for photoembossing.

With the ongoing trend of miniaturization also new markets for polymeric relief structures arise. A typical technology area which has gained large global interest over the last few years is in biomedics. Here, relief structures are used as scaffolds for tissue engineering or in sensors to detect biochemical species. Also in the area of microelectromechanical systems (MEMS) there is an increasing demand for new type of relief structures to be used in for example the automotive industry or electronics. It is especially in these new markets that novel technologies are required that can be used to

create on large scale new types of relief structures, which cannot be made with photolithography or replications.

For these new markets, photoembossing is an attractive technology. The technique is characterized by its ease of processing. The process consists of only two steps (i.e. patterned exposure and heating), which can be performed within a total processing time of 1 or 2 minutes. Photoembossing is also very efficient. Instead of removing material from the substrate, as in photolithography, the technique is based on moving material on the substrate. Furthermore, novel complex textures can be created by applying multiple exposures before development. Hereby benefiting from the fact that the surface remains relatively flat until the temperature is raised, thus not altering the optical path of the second exposure. A unique feature of the process is the non-contact (i.e. by heat) development of the relief structures. Unlike the conventional patterning techniques, photoembossing does not require contact with molds or solvents.

The range of potential application for photoembossing was originally limited due to the low aspect ratio of the relief structures which could be obtained. In the past, the technique was originally proposed for the formation of diffusive reflectors in reflective displays. These diffuse reflectors can redirect ambient light efficiently to a viewer. The structures needed for this application are relatively shallow and relatively easy to realize. By improving the aspect ratio, as presented in this thesis, the range of potential applications has been widely broadened (see also Chapter 6 and 7). For example, it has been demonstrated that photoembossing can be used to create a microlens array. The optical characteristics of the lenses can be altered by changing the processing parameter. A solution processable antireflection coating was applied prior to the development of the microlens array when the film is still flat. This stimulates the formation of films with a homogeneous thickness distribution and obviates the use of further post processing steps. Another application is the in-situ sealing of an array of pre-filled micro-cavities, such as encountered in electrophoretic displays. Photoembossing can be used to form a hermetic seal between the cover and the micro-cavity walls. The concept was found to insensitive to small deviations in cavity height, flatness of the cover and thin fluid films remaining between the cover and the top of the cavity walls. In the past these aspects made it difficult to effectively seal large area devices.

Overall it can conclude that photoembossing is an attractive technique for creating relief structures. It is unlikely that the technique can replace (at least in most applications) the current manufacturing method of replication and photolithography. However, the ease of processing, complex relief textures, efficient use of material and the non-contact method of development make photoembossing attractive for newly developing markets in which novel manufacturing techniques/textures are required. Especially the increase in performance, as demonstrated in this thesis, widens the scope of possibilities.

Samenvatting

In verschillende technologieën worden micro-oppervlaktestructuren in polymeren gebruikt. Voorbeelden hiervan zijn te vinden in optische dataopslag, beeldschermen, microfluidics en coatings. Met het doorzetten van de huidige trend om alles te minutiarizeren is het voor de handliggend dat micro-oppervlaktestructuren een steeds belangrijkere rol zullen gaan vervullen. Hiervoor zullen technieken ontwikkeld moeten worden om nieuwe structuren in massaproductie te kunnen maken. Vanwege de eenvoud van het proces heeft photoembossing de potentie om een dergelijke techniek te zijn.

Het basismateriaal bij photoembossing is een dunne film welke bestaat uit een mengsel van een polymeer, een monomeer en een fotoinitiator. Dit mengsel wordt ook wel het fotopolymeer genoemd. Een latent beeld van het gewenste oppervlaktereliëf wordt in het fotopolymeer aangebracht door het lokaal met ultraviolet (UV) licht te belichten. Daardoor wordt de fotoninitiator geactiveerd en ontstaan er radicalen in de belichte gebieden. Het oppervlaktereliëf ontstaat door het fotopolymeer te verwarmen tot boven de glastransitietemperatuur van het mengsel. Hierdoor verhoogt de mobiliteit van het systeem en wordt de radical geïnitieerde polymerisatie doorgezet. Door het lokale verschil in compositie ontstaat diffusie van het monomeer naar de belichte gebieden. De diffusie zorgt voor de groei van oppervlaktestructuren in de belichte gebieden. De maximale aspect ratio (hoogte van de structuur gedeeld door de breedte) die momenteel met deze techniek gehaald kan worden is echter laag. Dit beperkt het aantal applicaties waar de techniek potentieel gebruikt zou kunnen worden. In dit proefschrift worden verschillende methodes gepresenteerd om de aspect ratio van de oppervlaktestructuren te verbeteren. Tevens worden nieuwe applicaties voor deze unieke techniek gedemonstreerd.

Allereerst, is het ontstaan van de oppervlaktestructuren onderzocht door middel van een numeriek model. Dit model omschrijft de diffusie van het monomeer als gevolg van een lokale verandering in het chemisch potentiaal, wat ontstaat door de polymerisatiereactie in de belichte gebieden. Het effect van componenten die interfereren met de polymerisatiereactie (zoals bv. zuurstof) is meegenomen in het model. Het model laat zien dat terminatie van de radicalen, met name door trapping, een belangrijke factor is in het ontwikkelingsproces van het reliëf. Moleculen die de terminatie van radicalen bevorderen (zoals bv. zuurstof) hebben dan ook een negatief effect op de hoogte van het reliëf. Moleculen die de polymerisatiereactie herinitiëren na reactie met de radicalen (zoals bv. chain transfer agents) hebben een positief effect op

de structuurgroei. De transfer/reinitiatie reactie zorgt voor ophoping van gestabiliseerde radicalen. Deze radicalen dienen als "latente initiatoren" die tijdens de verwarmingstap de polymerisatiereactie kunnen voortzetten.

Door aan het fotopolymeer moleculen toe te voegen die de terminatie van radical bevorderen (inhibitors/retarders) en die de polymerisatiereactie reinitiëren (chain transfer) zijn de modelresultaten experimenteel onderzocht. Aangetoond is dat een inhibitiereactie een negatief effect heeft op de structuurgroei. Retardatie daar en tegen zorgt voor verbetering van de aspect ratio tot een factor 7. Onderzoek naar het type radicaal, de stabiliteit van de radicalen en het kinetisch effect op de reactie toont aan dat deze verbetering toegeschreven kan worden aan chain transfer reacties. Het effect van de chain transfer reactie is nader onderzocht door het toevoegen van reversibele addition-fragmentation (RAFT) agents. Ook deze moleculen verbeterden de structuurhoogte van het reliëf tot een factor 7. De RAFT agents hebben het voordeel dat ze ongevoelig zijn voor de aanwezigheid van zuurstof in de omgeving, wat ideaal is voor industriële applicaties. Helaas, maakt hun intrinsieke kleur ze minder geschikt voor optische toepassingen.

Om de structuurhoogte verder te verbeteren zijn er nieuwe fotopolymeren ontwikkeld. Anders dan met de conventionele systemen bevatten deze fotopolymeren geen grote hoeveelheid polymeer. Conventioneel bestaat het fotopolymeer tot wel 50 wt.-% aan polymeer om het materiaal na aanbrengen een vaste toestand te geven. Echter het polymeer kan niet diffunderen en draagt daardoor niet bij aan de uiteindelijke structuurhoogte. De nieuw ontwikkelde systemen bestaan uit mobiele monomeren die bij kamertemperatuur in een vaste staat verkeren door sterische of dipool-dipool interacties. Aangetoond is dat in deze nieuwe fotopolymeren relatief hoge structuren gemaakt kunnen worden.

De verbeterde performance en warmte geïnitieerde reliëfontwikkeling maken het mogelijk om photoembossing te gebruiken voor unieke applicaties. Aangetoond wordt dat de techniek gebruikt kan worden om een array van microlenzen met een antireflectie coating te maken. De optische eigenschappen van de lenzen kunnen eenvoudig aangepast worden door de procesparameters te veranderen. Photoembossing kan ook gebruikt worden om in-situ een array van gevulde microbakjes (zoals bv. in een electroforetische display) hermetisch te sluiten. Het concept is ongevoelig voor kleine afwijkingen in de hoogte van de wanden van de bakjes, vlakheid van het dekglas en dunne vloeistoflaagjes die achterblijven tussen het dekglas en wanden van de bakjes. Een andere eigenschap van photoembossing is dat zowel de materiaal- als productiekosten laag zijn. De techniek kan hierdoor gebruikt worden om een reliëf voor het verbeteren van de kijkhoek van displays, wegwerpbare replicatiemallen of stempels te maken.

Bij photoembossing wordt een reliëfstructuur gemaakt door diffusie van moleculen naar van te voren bepaalde gebieden. Het omgekeerde, reliëfstructuren die de diffusie van moleculen induceren, is ook mogelijk. Dit effect wordt gebruikt in biosensoren. Deze apparaten detecteren briomoleculaire stoffen, zoals bv DNA/RNA of proteïnen, in vloeistoffen. De huidige systemen hebben ofwel kleine volumes aan monstervloeistof nodig ofwel een hoge gevoeligheid. In dit proefschrift wordt een nieuw type sensor, welke een klein monstervolume combineert met een hoge gevoeligheid, ontworpen, gemaakt en geëvalueerd. Het apparaat is gebaseerd op een microfluidic kanaal waarin een lokaal poreus membraan is aangebracht. De sensor kan in principe hermetisch afgesloten worden door middel van photoembossing.

Samengevat is er aangetoond dat het mogelijk is om reliëfstructuren met een hoge aspect ratio te krijgen door middel van photoembossing. De verbeterde performance kan gebruikt worden voor een aantal nieuwe applicaties en opent een scala aan andere mogelijke toepassing.

Acknowledgements

This project would not have been possible without the help of many colleagues, friends and family whom have supported me during my PhD. I would like to thank all of them. Some people, however, I would like to acknowledge in particular.

First of all, I would like to thank my promoter Dick Broer and Co-promoter Cees Bastiaansen whom have given me the opportunity to work in their group. Dick, it was a pleasure working with you and I enjoyed our discussions on the many topics that have passed during those 4 years. Cees, you have given me many opportunities of which I am truly grateful. Both of you have been of great inspiration to me.

At the beginning of my PhD, I had the opportunity to work together with Carlos Sanchez. It is partially your work which forms the strong foundation of this project. Thank you for the helping me on the way and also for the discussions we had during your frequent visits back to Eindhoven. The initial phase of the project would also not have been so swift without the help of Pit Teunissen. You showed me how to create those relief structures in the lab. It has been a great pleasure to work with you on the topic, but also to have you as a room and carpool mate.

It was very motivating to know that the project was not just academic work, but that it was also was driven by applications from Philips Research. The sealing of an electrophoretic display would not have been possible without the help of Marc van Delden. It was a pleasure working with you and hope you have that 914 restored soon; summer is coming. My thanks also go to Chamindie Punyadeera and Ron van Lieshout for introducing me to the world of biochemistry in the biosensor project. Who would have thought that something like a "sheep-anti-mouse" is not some kind of mousetrap but a protein.

With quite a few of these projects I have had the pleasure to work together with An Prenen and Joost Valeton. An, thanks for the pleasant work on the biosensor project, photoembossing model and many side projects. Joost, I enjoy our work together in NeoDec and I am looking forward to make it a huge success. I would like to thank you both and wish you the best for the final few months of your PhD projects. Also many thanks to my other colleagues of the PICT group: Anastasia Harris, Blanca Serrano Ramon, Carmen Luengo-Gonzales, Casper van Oosten, Charlotte Kjellander, Chris van Heesch, David Trimbach, Helena Plasschaert, Katherina Pacheco Morillo, Ken Harris, Maud Kastelijn, Michael Debije, Nick Wakefield, Nico Verloop, Paul Verbunt, Shabnam Zaker Hamidi, Shufen Tsoi, Thijs Meijer, Soney Varghese, Thijs de Jong and

Xiaoran Li. Also the people from the group of SKT are acknowledged and especially Pauline Schmit and Anne Spoelstra for optical measurements.

Some of the work was also performed in collaboration with other research groups. I would like to thank Ulrich Schubert, Jolke Perelaer, Rint Sijbesma, Itsuro Tomatsu, Rene Janssen and from the University of Cologne I would like to thank Klaus Meerholtz and Matthias de la Rosa. During my PhD I also had the pleasure of working together with two students from the University of Mainz. Florian Wolf greatly contributed to the experimental research in Chapter 3 and Michael Matecki on the work in Chapter 5. I would also like to thank Robert Vrancken (Validus Technologies) and Halim Kusumaatmaja (Max Planck Institute of Colloids and interfaces) for a side project which was started together on the topic of surface tension.

Half way my PhD I was introduced, by Bart Kranz, into the world of entrepreneurship and he encouraged me to start a company. This decision has led to a rollercoaster of experiences from which I have learned a lot. I would also like to thank Ben Slager, Rob van den Akker and Peter de Leeuw for working together and being patient with somebody who up to now could not focus his attention full time on the entrepreneurial activities. All of you: Thanks and I am looking forward to continue our projects with full effort!

Finally, I would like to thank my family (in law) for their support during these sometimes hectic and always busy times. It is especially, and without any doubt, due to the patience, support, understanding and love of my beloved wife Linda Hermans that the PhD is finally finished. Now this is finished I am looking forward to spending more time with you. Linda: Thank you!

Curriculum vitae

Ko Hermans was born in Venlo at the 8th of June 1980. After finishing secondary school in 1998 (Philips van Horne Scholengemeenschap), he studied chemical engineering at the Fontys Hogeschool in Eindhoven. After obtaining his bachelor degree in 2001, he continued his study on chemical engineering at the University of Technology in Eindhoven. In 2004, he received his Master's degree on the topic of "Luminescent Solar Concentrators". This work was performed in the group of Polymers for Information and Communications Technology with Prof. Dr. Dick Broer and Dr. Cees Bastiaansen.

Directly after obtaining his Master's degree, Ko continued to work on his PhD project in the same group. During his PhD, he co-founded the company Growfoil B.V., which focuses on the development and production of foil for enhancing the growth of crops in greenhouses. In 2008, Ko also co-founded the company NeoDec B.V.. NeoDec B.V. focuses on the development and production of printing inks for creating conductive tracks on plastic substrates.

Patents and refereed publications

Ko Hermans, Florian K. Wolf, Jolke Perelaer, Rene A. J. Janssen, Ulrich S. Schubert, Cees W. M. Bastiaansen, Dirk J. Broer, *High aspect ratio surface relief structures by photoembossing,* Applied Physics Letters (2007), 91(17), 174103/1-174103/3

Jolke Perelaer, Ko Hermans, Cees W. M. Bastiaansen, Dirk J. Broer, Ulrich S. Schubert, *Surface Relief Structures in Photo-Embossed Gratings with Increased Aspect Ratio by Addition of Reversible Addition-Fragmentation Chain Transfer (RAFT) Agent,* Advanced Materials (2008), 91(17), 174103-1/3

Ko Hermans, Itsuro Tomatsu, Michael Matecki, Rint P. Sijbesma, Cees W. M. Bastiaansen and Dirk J. Broer, *Highly Efficient Surface Relief Formation via Photoembossing of a Supramolecular Polymer*, Macromolecular Chemistry & Physics (2008), 209(20), 2094-2099

Ko Hermans, Marc van Delden, Cees W. M. Bastiaansen, Dirk J. Broer, *An in-situ sealing method for liquid filled micro-cavities based on photoembossing*, Journal of Micromechanical and Microengineering (2008), 18(9), 095022

Ko Hermans, Shabnam Zaker Hamidi, Anne B. Spoelstra, Cees W. M. Bastiaansen, Dirk J. Broer, *Rapid, direction fabrication of anti-reflection coated microlens arrays by photoembossing*, Applied Optics (2008), 47(35), 6512-6517

Ko Hermans, Cornelius Wilhelmus Maria Bastiaansen, Dirk Broer, Jolke Perelaer, *Process for preparing a polymeric relief structure*, WO2008025508

Chamindie Punyadeera, Dirk Broer, Ron van Lieshout, Ko Hermans, An M. Prenen, Cees Bastiaansen, *Flow-Through Biosensor*, WO2008139389

Jolke Perelaer, Ko Hermans, Cees W. M. Bastiaansen, Dirk J. Broer, *Process for preparing a polymeric relief structure*, WO2008151915

An M. Prenen, Ko Hermans, Cees Bastiaansen, Dirk Broer, Ron van Lieshout, Chamindie Punyadeera, *Membranes suited for immobilizing biomolecules*, patent filed (2007)

Ko Hermans, Itsuro Tomatsu, Rintje Pieter Sijbesma, Cornelius Wilhelmus Maria Bastiaansen, Dirk Jan Broer, *Process for preparing a polymeric relief structure*, patent filed (2008)

Ko Hermans, An M. Prenen, Cees Bastiaansen, Dirk Broer, Ron van Lieshout, Chamindie Punyadeera, *Diagnostic device*, patent filed (2008)

Patents and refereed publications not related to this thesis

R. J. Vrancken, H.Kusumaatmaja, K. Hermans, C. W. M. Bastiaansen, D. J. Broer, O Pierre Louis, J. Yeomans, *Reversible transition from Wenzel to Cassie-Baxter states on corrugated superhydrophobic surfaces*, submitted.

Paul P. C. Verbunt, Anthony Kaiser, Ko Hermans, C. W. M. Bastiaansen, Dick Broer, and Michael G. Debije, *Improved waveguide emission using dye molecules planarly aligned by liquid crystals*, submitted.

Joost J. P. Valeton, Ko Hermans, Cees W. M. Bastiaansen, Dirk, J. Broer, Jolke Perelaer, Ulrich S. Schubert, Gregory P. Crawford, Patrick J. Smith, *Conductive silver features obtained at room temperature using spin-coating and inkjet printing*, in preparation 2009

Joost J. P. Valeton, Ko Hermans, Patrick J. Smith, *Process for manufacturing conductive tracks*, patent filed (2007)

Ko Hermans, Ben Slager, *Greenhouse for enhanced plant growth*, patent filed (2008)

Ko Hermans, Ben Slager, *Greenhouse for enhanced plant growth*, patent filed (2008)